LEIBNIZ-INSTITUT FÜR ARBEITSFORSCHUNG AN DER TU DORTMUND

fakultät für chemie und chemische biologie

Development of an in vitro test battery for a test system to predict human drug-induced liver injury

Dissertation

zur Erlangung des akademischen Grades des Doktors der Naturwissenschaften (Dr. rer. nat.) an der Fakultät für Chemie und Chemische Biologie der Technischen Universität Dortmund

vorgelegt von

Tim Brecklinghaus (M. Sc.)

1. Gutachter: Prof. Dr. Jan G. Hengstler
2. Gutachter: Prof. Dr. Jörg Rahnenführer

Veröffentlicht als Dissertationsschift zur Erlangung des akademischen Grades des Doktors der Naturwissenschaften (Dr. rer. nat.) an der Fakultät für Chemie und chemische Biologie der TU Dortmund.

Promotionsort und Jahr: Dortmund, 2021

Tag der mündlichen Prüfung: 22.12.2021

Eidesstattliche Versicherung (Affidavit)

Name, Vorname
(Surname, first name)

Matrikel-Nr.
(Enrolment number)

Belehrung:

Wer vorsätzlich gegen eine die Täuschung über Prüfungsleistungen betreffende Regelung einer Hochschulprüfungsordnung verstößt, handelt ordnungswidrig. Die Ordnungswidrigkeit kann mit einer Geldbuße von bis zu 50.000,00 € geahndet werden. Zuständige Verwaltungsbehörde für die Verfolgung und Ahndung von Ordnungswidrigkeiten ist der Kanzler/die Kanzlerin der Technischen Universität Dortmund. Im Falle eines mehrfachen oder sonstigen schwerwiegenden Täuschungsversuches kann der Prüfling zudem exmatrikuliert werden, § 63 Abs. 5 Hochschulgesetz NRW.

Die Abgabe einer falschen Versicherung an Eides statt ist strafbar.

Wer vorsätzlich eine falsche Versicherung an Eides statt abgibt, kann mit einer Freiheitsstrafe bis zu drei Jahren oder mit Geldstrafe bestraft werden, § 156 StGB. Die fahrlässige Abgabe einer falschen Versicherung an Eides statt kann mit einer Freiheitsstrafe bis zu einem Jahr oder Geldstrafe bestraft werden, § 161 StGB.

Die oben stehende Belehrung habe ich zur Kenntnis genommen:

Official notification:

Any person who intentionally breaches any regulation of university examination regulations relating to deception in examination performance is acting improperly. This offence can be punished with a fine of up to EUR 50,000.00. The competent administrative authority for the pursuit and prosecution of offences of this type is the chancellor of the TU Dortmund University. In the case of multiple or other serious attempts at deception, the candidate can also be unenrolled, Section 63, paragraph 5 of the Universities Act of North Rhine-Westphalia.

The submission of a false affidavit is punishable.

Any person who intentionally submits a false affidavit can be punished with a prison sentence of up to three years or a fine, Section 156 of the Criminal Code. The negligent submission of a false affidavit can be punished with a prison sentence of up to one year or a fine, Section 161 of the Criminal Code.

I have taken note of the above official notification.

Ort, Datum
(Place, date)

Unterschrift
(Signature)

Titel der Dissertation:
(Title of the thesis):

Ich versichere hiermit an Eides statt, dass ich die vorliegende Dissertation mit dem Titel selbstständig und ohne unzulässige fremde Hilfe angefertigt habe. Ich habe keine anderen als die angegebenen Quellen und Hilfsmittel benutzt sowie wörtliche und sinngemäße Zitate kenntlich gemacht.
Die Arbeit hat in gegenwärtiger oder in einer anderen Fassung weder der TU Dortmund noch einer anderen Hochschule im Zusammenhang mit einer staatlichen oder akademischen Prüfung vorgelegen.

I hereby swear that I have completed the present dissertation independently and without inadmissible external support. I have not used any sources or tools other than those indicated and have identified literal and analogous quotations.

The thesis in its current version or another version has not been presented to the TU Dortmund University or another university in connection with a state or academic examination.*

*Please be aware that solely the German version of the affidavit ("Eidesstattliche Versicherung") for the PhD thesis is the official and legally binding version.

Ort, Datum
(Place, date)

Unterschrift
(Signature)

Table of contents

Table of contents

Table of contents

Summary

Drug-induced liver injury (DILI) is a major concern for patients, pharmaceutical companies, as well as clinicians due to its poor predictability. Recently, we have developed an in vitro/in silico test system for the prediction of human DILI in relation to oral doses and blood concentrations. It is based on the determination of effective concentrations (EC) in vitro using a cytotoxicity test (CTB assay) with primary human hepatocytes (PHH) and comparison to in vivo concentrations determined in silico by physiologically based pharmacokinetic modeling. Additionally, two indices, the toxicity separation index (TSI) and the toxicity estimation index (TEI) were introduced for the quantitative evaluation of a test system and its input parameters.

In this PhD-thesis, I studied whether extending the in vitro test battery, so far consisting only of the cytotoxicity test, by additional functional readouts would lead to improved performance and thus allow a more accurate prediction. In total, three different approaches that address putative DILI-relevant mechanisms were explored. For this purpose, test compounds with known hepatotoxicity status (for specific human doses) and well-established pharmacokinetics were considered.

In the first approach, the influence of a bile acid mix on the cytotoxicity of test compounds in cultivated primary human hepatocytes was investigated. Therefore, PHH were incubated with or without bile acids in combination with a test compound, followed by the CTB assay. The bile acid mix consisted of physiological ratios of the most abundant human bile acids at a cholestatic sum concentration of 0.5 mM, which corresponds to 50% of the EC_{10} (cytotoxicity) of the mix. Cytotoxicity of in total 18 test compounds with and without the addition of the bile acid mix was measured. Considering the EC_{10} median from at least three different human donors, the initial TSI of 0.79 decreased slightly to 0.77 and the TEI of 0.73 to 0.69 with the addition of bile acids. Also, a combination of both assays only resulted in a TSI and TEI of 0.80 and 0.76, respectively. In summary, increased and decreased susceptibility to both hepatotoxic and non-hepatotoxic substances was observed with the addition of bile acids, which did not improve the indices and therefore the assay was not included in the in vitro test battery.

Next, an assay was evaluated that measures the inhibition of bile acid export carriers. For this purpose, PHH were incubated with a test compound and 5-chloromethylfluorescein diacetate (CMFDA). Subsequently, the intra- and extracellular fluorescence of the CMFDA-derived 5-CMF, which is a substrate of known bile acid transporters such as BSEP and MRP2, was measured. Totally 36 compounds were tested by the CMFDA assay and compared to the cytotoxicity test. Substantially lower EC_{10} values were obtained using the CMFDA assay for several known BSEP and/or MRP2

inhibitors. When combining both assays, using the lower EC_{10} value of the two tests, the TSI was increased to 0.89 and TEI to 0.83 compared to the CTB assay alone (TSI and TEI 0.77 and 0.69, respectively). In conclusion, the CMFDA assay is able to detect bile acid export carrier inhibition in PHH and integration into the in vitro test battery improves the differentiation of hepatotoxic and non-hepatotoxic compounds.

In a third approach the AdipoRed assay was established. Intracellular lipid accumulation in HepG2 cells was investigated for a total of 60 compounds. For this purpose, HepG2 cells were artificially fattened by the addition of free fatty acids and simultaneous incubation with a test compound. Staining of the cells with AdipoRed and subsequent measurement and analysis showed that with addition of the AdipoRed assay, both TSI (0.74 → 0.80) and TEI (0.67 → 0.81) were improved compared to the cytotoxicity assay in primary human hepatocytes alone. In conclusion, it was shown that the addition of the AdipoRed assay improved both indices.

In summary, three assays were developed for the in vitro test battery of a test system to predict drug-induced liver injury. Quantitative analysis revealed that two of the three assays lead to improved separation of hepatotoxic and non-hepatotoxic compounds, as well as improved estimation of in vivo relevant blood concentrations. These improvements allow more accurate prediction of DILI by the test system.

Zusammenfassung

Arzneimittelbedingte Leberschäden sind aufgrund ihrer schlechten Vorhersagbarkeit ein großes Problem für Patienten, Pharmaunternehmen und Kliniker. Vor kurzem haben wir ein in vitro/in silico Testsystem für die Vorhersage von arzneimittelbedingten Leberschäden im Menschen in Bezug zu oralen Dosen und Blutkonzentrationen entwickelt. Es basiert auf der Bestimmung effektiver Konzentrationen (EC) in vitro, unter Verwendung eines Zytotoxizitätstests (CTB-Test) mit primären menschlichen Hepatozyten (PHH) und dem Vergleich mit in vivo Konzentrationen, die in silico durch physiologisch basierter pharmakokinetischer Modellierung bestimmt werden. Zusätzlich wurden zwei Maßzahlen, der „Toxicity separation index“ (TSI) und der „Toxicity estimation index“ (TEI), für die quantitative Bewertung eines Testsystems und seiner Eingabeparameter eingeführt.

In dieser Dissertation habe ich untersucht, ob die Erweiterung der in vitro Testbatterie, die bisher nur aus dem Zytotoxizitätstest besteht, durch zusätzliche funktionelle Messungen zu einer Verbesserung führt und somit eine genauere Vorhersage ermöglicht. Insgesamt wurden drei verschiedene Ansätze getestet, die mutmaßlich relevante Mechanismen für arzneimittelbedingte Leberschäden angehen. Zu diesem Zweck wurden Prüfsubstanzen mit erwiesener Hepatotoxizität (für bestimmte humane Dosen) und gut bekannter Pharmakokinetik verwendet.

Im ersten Ansatz wurde der Einfluss einer Gallensäuremischung auf die Zytotoxizität von Testsubstanzen in kultivierten primären menschlichen Hepatozyten untersucht. Dazu wurden PHH mit oder ohne Gallensäuren in Kombination mit einer Testsubstanz inkubiert und anschließend der CTB-Test durchgeführt. Die Gallensäuremischung bestand aus physiologischen Verhältnissen, der am häufigsten vorkommenden menschlichen Gallensäuren in einer cholestatischen Gesamtkonzentration von 0,5 mM, welche 50 % der EC_{10} (Zytotoxizität) der Gallensäuremischung entspricht. Von insgesamt 18 Prüfsubstanzen wurde die Zytotoxizität mit und ohne Zugabe der Gallensäuremischung gemessen. Unter Berücksichtigung des EC_{10}-Medians von mindestens drei verschiedenen menschlichen Spendern sank der ursprüngliche TSI mit dem Zusatz von Gallensäuren leicht von 0,79 auf 0,77 und der TEI von 0,73 auf 0,69. Auch eine Kombination aus beiden Tests ergab nur einen TSI und TEI von 0,80 bzw. 0,76. Zusammenfassend lässt sich sagen, dass durch den Zusatz von Gallensäuren eine erhöhte bzw. verringerte Anfälligkeit sowohl gegenüber hepatotoxischen als auch gegenüber nicht-hepatotoxischen Substanzen beobachtet wurde. Da dies jedoch nicht zu einer Verbesserung der Maßzahlen führte, wurde der Test nicht in die in vitro Testbatterie aufgenommen.

Als nächstes wurde ein Test evaluiert, der die Hemmung von Gallensäuretransportern misst. Zu diesem Zweck wurden PHH mit einer Testsubstanz und 5-Chloromethylfluorescein-Diacetat (CMFDA)

inkubiert. Anschließend wurde die intra- und extrazelluläre Fluoreszenz des von CMFDA abgeleiteten 5-CMF, welches ein Substrat bekannter Gallensäuretransporter wie BSEP und MRP2 ist, gemessen. Insgesamt wurde der CMFDA-Test auf 36 Substanzen angewendet und mit dem Zytotoxizitätstest verglichen. Für mehrere bekannte BSEP- und/oder MRP2-Inhibitoren wurden mit dem CMFDA-Test wesentlich niedrigere EC_{10}-Werte ermittelt. Im Vergleich zu dem CTB-Test alleine (TSI und TEI 0,77 bzw. 0,69) wurde bei der Kombination beider Tests unter Verwendung des niedrigeren EC_{10}-Wertes beider Tests der TSI auf 0,89 und der TEI auf 0,83 erhöht. Zusammenfassend lässt sich sagen, dass der CMFDA-Test in der Lage ist, die Hemmung des Gallensäureexports in PHH nachzuweisen, und dass die Integration in die in vitro-Testbatterie die Trennung zwischen hepatotoxischen und nicht-hepatotoxischen Substanzen verbessert.

In einem dritten Ansatz wurde der AdipoRed-Test etabliert. Hierbei wurde die intrazelluläre Fettakkumulation in HepG2-Zellen wurde für insgesamt 60 Testsubstanzen untersucht. Zu diesem Zweck wurden HepG2-Zellen durch Zugabe von freien Fettsäuren und gleichzeitiger Inkubation mit einer Testsubstanz künstlich verfettet. Die Färbung der Zellen mit AdipoRed und anschließender Messung und Analyse zeigte, dass im Vergleich zum Zytotoxizitätstest in primären menschlichen Hepatozyten durch Zusatz des AdipoRed-Tests sowohl der TSI (0,74 → 0,80) als auch der TEI (0,67 → 0,81) verbessert wurden.

Zusammengefasst wurden drei Tests für die in vitro Testbatterie eines Testsystems zur Vorhersage von arzneimittelbedingter Leberschäden im Menschen entwickelt. Die quantitative Analyse ergab, dass zwei der drei Tests zu einer verbesserten Trennung von hepatotoxischen und nicht-hepatotoxischen Testsubstanzen sowie zu einer verbesserten Schätzung der in vivo relevanten Blutkonzentrationen führen. Diese Verbesserungen ermöglichen eine genauere Vorhersage von arzneimittelbedingten Leberschäden im Menschen durch das Testsystem.

Abbreviations

%	Percent
×	Fold
°C	Degree Celsius
µg	Microgram
µL	Microliter
µm	Micometer
µM	Micromol per liter
2D	Two-dimensional
3D	Three-dimensional
4pLL	Four-parameter log-logistic
5-CMF	5-Chloromethylfluorescein
AIC	Akaike Information Criterion
ALP	Alkaline phosphatase
ALT	Alanine aminotransferase
AMIO	Amiodarone
APAP	Acetaminophen
AR	AdipoRed
ASP	Aspirin
ATP	Adenosine triphosphate
ATRO	Atropine
AVS	Atorvastatin
BAM	Bile acid mix
BC	Brain-Cousens
BCRP	Breast cancer resistance protein
BOS	Bosentan
BPR	Buspirone
BSA	Bovine serum albumin
BSEP	Bile salt export pump

Abbreviations

BSO	DL-buthionine-sulfoximine
BZB	Benzbromarone
BZT	Benztropine
CBZ	Carbamazepine
CDCA	Chenodeoxycholic acid
CHL	Chlorpheniramine
CLFI	Clofibrate
CLON	Clonidine
C_{max}	Peak concentration
CMFDA	5-Chloromethylfluorescein diacetate
CO_2	Carbon dioxide
COD	Codeine
CSA	Cyclosporin A
CTB	CellTiter-Blue
d	Day
DCA	Deoxycholic acid
DFN	Diclofenac
DIGI	Digoxin
DILI	Drug-induced liver injury
DMEM	Dulbecco's modified eagles medium
DMSO	Dimethyl sulfoxide
dNTP	Deoxynucleotide triphosphate
DPH	Diphenhydramine
EC	Effective concentration
EC_x	Concentration at which an effect size increase or decrease of x% occurs
EDTA	Ethylene diamine tetra acetic acid
ETC	Entacapone
EtOH	Ethanol
FBS	Fetal bovine serum
FFA	Free fatty acids

g	Gram
GCA	Glycocholic acid
GCDCA	Glycochenodeoxycholic acid
GDCA	Glycodeoxycholic acid
GLC	Glucose
GoF	Goodness of fit
GSH	Glutathione
GSSG	Oxidized glutathione
h	Hour
H_20	Water
HYZ	Hydroxyzine
IBU	Ibuprofen
IC	Inhibitory concentration
IC_x	Concentration at which an inhibition size decrease of x% occurs
IfADo	Leibniz Research Centre for Working Environment and Human Factors
INDO	Indomethacin
ISS	Isosorbide dinitrate
ITS	Insulin transferrin selenite supplement
KC	Ketoconazole
KCl	Potassium chloride
kg	Kilogram
KH_2PO_4	Potassium dihydrogen phosphate
L	Liter
Log	Logarithm
MCP-Mod	Multiple comparison procedure and modeling
MDR	Multidrug resistance gene product
MEL	Melatonin
mg	Milligram
mL	Milliliter
ML	Monolayer

Abbreviations

mm	Millimeter
mM	Millimol per liter
MRP	Multidrug resistance-associated protein
MTX	Methotrexate
N/A	Not applicable
Na_2HPO_4	Disodium hydrogen phosphate
NAC	N-acetylcysteine
NaCl	Sodium chloride
NaOH	Sodium hydroxide
NDP	Nifedipine
nm	Nanometer
NPC	Non-parenchymal cell
NPV	Negative predictive value
NTCP	Na+-taurocholate cotransporting polypeptide
OATP	Organic anion transporting polypeptide
OST	Organic solute transporter
OXC	Oxycodone
OXM	Oxymorphone
p	Probability
PBPK	Physiologically based pharmacokinetic modeling
PBS	Phosphate buffered saline
PCR	Polymerase chain reaction
PDX	Pyridoxine
pH	Potentia hydrogenii
PHH	Primary human hepatocytes
PIN	Pindolol
PIO	Pioglitazone
PMZ	Promethazine
PPL	Propranolol
PPV	Positive predictive value

PRI	Primidone
PRIMA	Primaquine
PRX	Perhexiline
PZB	Pazopanib
QSAR	Quantitative structure-activity relationship
RGZ	Rosiglitazone
RIF	Rifampicin
ROS	Rosuvastatin
rpm	Revolutions per minute
RT-qPCR	Quantitative real time PCR
SC	Sandwich culture
SIM	Simvastatin
SOP	Standard operating procedure
SPB	Sodium phenylbutyrate
STAVU	Stavudine
SXS	Sitaxentan
tBHQ	tert-Butylhydroquinone
TC	Tetracycline
TEI	Toxicity estimation index
THE	Theophylline
TOLC	Tolcapone
TPL	Triprolidine
TROG	Troglitazone
TSI	Toxicity separation index
TSN	Triclosan
TTD	Tolterodine
U	Units
VITC	Vitamin C
VPA	Valproic acid
w	With

Abbreviations

w/o	Without
ZAL	Zaleplon

1 Introduction

1.1 The liver and drug-induced liver injury

The liver is the central metabolic organ in humans and is involved in essential tasks of the energy metabolism and detoxification. It is connected to the gastrointestinal tract via the hepatic portal vein, through which nutrient-rich blood is transported for further processing [1], [2]. Glucose absorbed from the blood can be stored in the liver in form of glycogen (glycogenesis) and released again if required (glycogenolysis) [3]. In addition, glucose can be synthesized from non-carbohydrate precursors like pyruvate (gluconeogenesis). Furthermore, lipids can be taken up or newly synthesized in the liver (de novo lipogenesis). Triglyceride synthesis and lipid droplet formation together with lipid consumption, including fatty acid degradation (lipolysis), β-oxidation, and the secretion of very-low-density lipoproteins are further important elements for the regulation of the energy homeostasis [4]–[6]. Other functions include regulating blood volume and filtration, supporting the immune system, and producing and secreting bile, proteins, and coagulation factors [2], [7]–[9].

As the main detoxification organ, the liver is involved in the inactivation of toxins and xenobiotics and the excretion of exogenous and endogenous compounds [10]. Many toxic compounds are well soluble in fat and poorly soluble in water, and have to be processed by the liver before they can be excreted. These reactions can be divided into three phases, which can occur consecutively or independently, depending on the compound [11]. In phase I, toxins are converted into less harmful compounds through oxidation, reduction, and hydrolysis reactions mediated mainly by enzymes of the cytochrome P450 enzyme group [12], [13]. During these processes, reactive metabolites and free radicals can be formed, which are neutralized by antioxidants like glutathione (GSH). In the second phase, chemicals are bound by conjugation to functional groups such as cysteine. These reactions are mainly performed by transferases like UDP-glucuronosyltransferases, sulfotransferases, N-acetyltransferases, glutathione S-transferases, and methyltransferases [14]. Consequently, these compounds become less harmful and more soluble in water, allowing them to be excreted from the body through the kidneys via urine [10], [11], [15], [16]. Excretion of compounds via transport enzymes of the ATP-binding cassette and solute carrier transporter superfamilies is referred to as the third phase [17]. A majority of the biotransformation takes place in the liver, especially in the hepatocytes. However, several of the involved enzymes are also expressed in extrahepatic tissue [18]. The function as a detoxification organ often results in liver drug concentrations multiple times higher than the blood concentration and in combination with the described processes, this leads to a particular susceptibility of the liver to drug-induced injuries [19], [20].

Drug-induced liver injury (DILI) is the leading cause for severe liver disease in Western countries and poses a major challenge for the pharmaceutical industry, physicians, and patients because the current in vivo and in vitro methods do not allow an accurate prediction of the risk [21]. Up to 50% of the cases of acute liver failure in Western countries are due to DILI and, in addition, it is the major reason for drug failure or withdrawal of drugs from the market [21]–[23]. Reliable data on the incidence of DILI are difficult to gather, but studies in Western countries expect that there are approximately 14 to 19 cases of drug-induced liver injury per 100,000 patients, with liver-related death rates ranging from 1 to 5.8% [24]–[28]. Paracetamol toxicity is of particular relevance, as it accounts for between 40 and 70% of all DILI cases in Western countries [29].

1.2 Mechanisms of DILI

DILI can be divided into two different toxicity types; intrinsic and idiosyncratic toxicity [30]–[32]. Intrinsic toxicity is dose-dependent and usually predictable when certain doses or exposure limits are exceeded. Idiosyncratic toxicity is difficult to predict, limited dose-dependent, and usually involves an immune response. Compared to intrinsic toxicity, which usually occurs after a few days, idiosyncratic toxicity often takes weeks or months to manifest. To identify DILI in the clinic, liver function tests are performed that determine the increase, decrease, and or ratio of specific liver enzymes such as alanine aminotransferase (ALT) and alkaline phosphatase (ALP). Based on these measurements, a distinction is made between hepatocellular (more severe, elevated ALT levels) and cholestatic (elevated ALP levels) damage. A mixed phenotype is characterized by increased total bilirubin levels in combination with increased ALT levels. The underlying mechanisms which result in the clinical assessment of DILI are diverse and often a drug induces not one but several [33], [34].

At the cellular level, DILI can occur through a variety of chemical reactions and interactions of the parent drug or its metabolites. These include alterations in mitochondrial functions leading to adenosine triphosphate (ATP) depletion and impaired ß-oxidation with subsequent lipid accumulation, generation of reactive oxygen species and GSH depletion, activation of immune responses, the release of inflammatory cytokines, and inhibition of transporters and other important enzymes [31], [35]–[37]. Many of these processes are reproducible and measurable with in vitro systems. The detection of these mechanisms in vitro is an attempt to identify markers for hepatotoxic compounds and thus to predict in vivo hepatotoxicity. Approaches include measuring GSH and ATP depletion, alteration of mitochondrial membrane potential, inhibition of liver-specific transporters, abnormal lipid accumulation, or altered gene expression [38].

This thesis largely deals with the inhibition of bile acid transport, so this mechanism will be explained in more detail. Bile acids (BA) are synthesized from cholesterol in hepatocytes, this process accounts for a large part of cholesterol breakdown in the liver [39]. As a major component of bile, bile acids are essential for the lipid metabolism by breaking down lipids and thus making them accessible for lipases [40], [41]. In addition, bile acids are essential for the transport and absorption of fat-soluble vitamins [42]. After synthesis and conjugation, bile acids are transported into the bile canaliculi by the bile salt export pump (BSEP) and the multidrug resistance-associated protein 2 (MRP2) [43] (**Figure 1**). In addition to bile acids, organic anions and glutathione conjugates are also transported via MPR2. Other canalicular transporters are the multidrug resistance gene products 1 and 3 (MDR1 and 3) and the breast cancer resistance protein (BCRP), through which organic cations, phospholipids, and sulfated organic anions are exported, respectively. Bile acids enter the gastrointestinal tract via the canalicular network. Up to 95% of them can be recycled from the intestine by transport through the portal vein and subsequent uptake by the Na+-taurocholate cotransporting polypeptide (NTCP) and organic anion transporting polypeptide (OATP) into the hepatocytes [44]. In addition to the canalicular route, bile acids can also be exported to a certain degree via the MRP3, MRP4, and the organic solute transporter (OSTα/β), but this acts more as a compensatory mechanism when the intracellular bile acid concentration is too high [45], [46] (**Figure 1**).

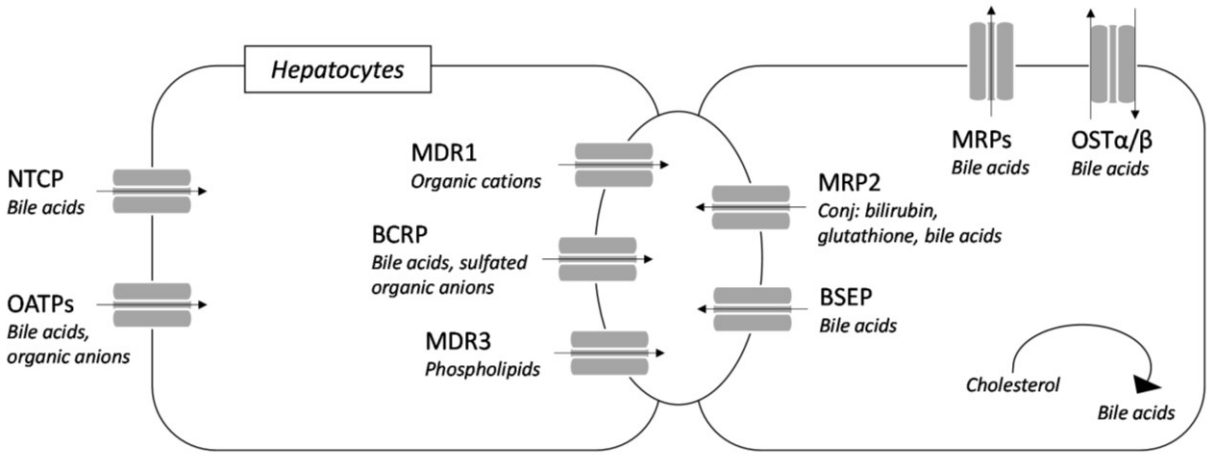

Figure 1: Transporters in human hepatocytes. NTCP: Na+-taurocholate cotransporting polypeptide, OATP: organic anion transporting polypeptide, MDR: multidrug resistance gene product, BCRP: breast cancer resistance protein, MRP: multidrug resistance-associated protein, BSEP: bile salt export pump, OST: organic solute transporter. (Adapted from [47]).

Bile acid accumulation, also called cholestasis, can occur through direct inhibition of the bile acid transporters, particularly BSEP and MRP2, or indirectly by the presence of an exogenous substrate of these transporters. In addition, impaired functions of the endoplasmic reticulum or the mitochondria

can influence the bile acid concentration, for example, if ATP-dependent transport is no longer possible due to ATP depletion [48], [49]. Furthermore, genetic predispositions and mutations can also lead to a malfunction of these transporters and thus to a disturbed bile acid balance [50], [51]. If the bile acid concentration reaches certain thresholds it becomes cytotoxic and can finally lead to cell death.

Some hepatotoxic drugs currently on the market, as well as withdrawn ones, are known inhibitors of bile acid transporters and can lead to cholestasis in vivo. Studies have shown that inhibition of bile acid transport often occurs at concentrations that are not yet cytotoxic in vitro, suggesting that this might be a potential marker for the risk assessment on the hepatotoxicity of drugs [52], [53].

1.3 Current test systems; advantages and limitations

Contrary to public perception, in vitro models are already used in many areas of drug development and contribute to bringing safe and effective medicines on the market. Nevertheless and despite all efforts to develop alternatives, under current law, drugs must undergo toxicity studies in animals, particularly in mice and rats, before they can be approved [54], [55]. However, these toxicity studies are not optimal, as translatability is often not given due to species differences [56]. In addition, the time and costs involved are immense, and ethical reasons oppose animal testing [57], [58].

To avoid species differences in the development of alternative non-animal test systems, a major focus is placed on the use of human cells, especially hepatocytes, which make up around 80% of the liver tissue volume [59]. There are different cell systems available, for example, pluripotent stem cells, which can be differentiated into hepatic cell-like cells, hepatocellular carcinoma cell lines, which were isolated from tumor tissue, or primary human hepatocytes (PHH), which are isolated from human livers that are no longer considered for transplantation. Each of these cell systems has advantages and disadvantages [60], [61]. Pluripotent stem cells require complex differentiation protocols and ultimately gain only partial functions compared to primary human hepatocytes, but they can be cultivated and allow patient-specific applications [62], [63]. Liver carcinoma cell lines such as HepG2 have the advantage of being easy to handle and cost-effective. However, they also lack liver-specific functions in metabolism and transport, which are crucial for detoxification processes [64], [65]. Primary human hepatocytes are the gold standard as they possess most liver-specific functions like phase I and II metabolism, expression of import and export carrier, and the formation of bile canaliculi-like structures under specific culture conditions [60]. However, they are limited in availability and dedifferentiate rapidly under standard cultivation conditions. In addition, they show large donor-donor

differences, which reflect the individuality of patients, but complicates the generation of reliable and reproducible data [60], [66]–[68].

Various cultivation techniques are used with hepatocytes in vitro to simulate the in vivo situation of the liver and to obtain liver-specific functions and properties [60]. This is done, for example, by cultivating cells between extracellular matrixes or as spheroids which allow longer cultivation periods, the formation of bile canaliculi-like structures, and the activity and maintenance of liver-specific functions [69]–[72]. In addition, there are approaches to cultivate liver cells together with non-parenchymal cells as well as genetic engineering approaches [73]–[75]. Despite these many possibilities and great advances, robust in vitro test systems for the prediction of drug-induced liver toxicity have not yet been developed. Among others, the following three test systems have been developed and introduced in the last years. All of these utilized primary human hepatocytes as their cell system.

Khetani et al., 2012: Primary human hepatocytes were cultured in a micro pattern surrounded by 3T3-J2 murine embryonic fibroblasts for 14 days and received four repeated drug administrations in total. Afterward, ATP and GSH levels were measured and statistical analysis resulted in 65.7% sensitivity and 90% specificity [76].

Proctor et al., 2017: Primary human hepatocytes cultured in a two-dimensional (2D) format on a collagen monolayer or in a three-dimensional (3D) format as spheroids. ATP levels were measured and statistical analysis resulted in 40.6% and 59.4% sensitivity and 97.6% and 80.5% specificity for the 2D and 3D configuration, respectively [77].

Xu et al., 2008: Primary human hepatocytes were cultured on a collagen layer with subsequent matrigel overlay. Mitochondrial damage, oxidative stress, intracellular glutathione, and cell nuclei were stained and analyzed. The approach yielded 60% sensitivity and 100% specificity [78].

Although these test systems achieved a high specificity, they lack the sensitivity to detect potentially harmful compounds. In addition, these approaches only aim to classify a compound as hepatotoxic or non-hepatotoxic, whereby it is also of interest at what concentration a compound shows an increased risk of hepatotoxicity. To address this issue, a novel test system was developed by us and collaboration partners to determine the risk of hepatotoxicity in relation to in vitro toxicity and the oral dose [79].

1.4 Test system applied and further developed in the present study

We propose the following three steps for the prediction of human hepatotoxicity:

(1) determination of the lowest compound concentrations positive in an in vitro test relevant for in vivo hepatotoxicity (2) extrapolation to in vivo blood concentration, and (3) reverse modeling to obtain the lowest oral hepatotoxic dose (**Figure 2**) [79].

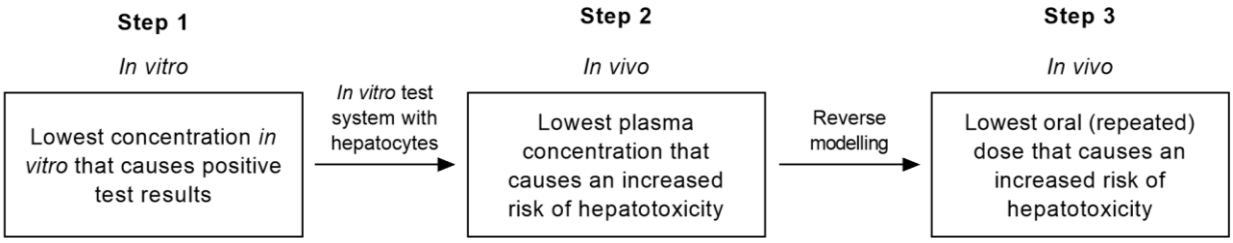

Figure 2: Concept of in vitro to in vivo extrapolation (Taken from [79]).

The basic idea behind this test system is the assumption that there is a specific relationship between hepatotoxic relevant concentrations of a test compound in vitro and the concentration in vivo, which indicates an increased risk of hepatotoxicity.

To investigate this, cytotoxicity of 28 compounds with known hepatotoxicity status for a specific dose was determined in primary human hepatocytes. Next, a blood concentration of the specific dose was determined using pharmacokinetic modeling. Subsequently, both concentrations were correlated by plotting the in vivo concentrations on the y-axis and the in vitro concentrations on the x-axis of a 2D coordinate system. The plot showed a clear separation between hepatotoxic and non-hepatotoxic compounds. Furthermore, cytotoxicity of hepatotoxic compounds was determined at in vivo relevant concentrations (**Figure 4**). This underlines that there is a specific relationship between hepatotoxic relevant in vitro and in vivo concentrations.

The separation of hepatotoxic and non-hepatotoxic compounds is of particular interest. After plotting the data pairs into the 2D coordinate system, the points can be separated utilizing a support vector machine. The support vector machine separates the non-hepatotoxic and hepatotoxic compound with a function which is a straight line in the simplest case. This allows not only the binary classification into ‘non-hepatotoxic’ and ‘hepatotoxic’ of the existing test systems (1.3) but rather the determination of the risk for hepatotoxicity. A dot on this line indicates that for the corresponding in vivo concentration there is a 50% chance of an increased risk for liver toxicity. By shifting this function parallel downright, a 10%, 1%, or arbitrary risk chance can be determined. Which risk threshold is most appropriate or acceptable needs to be addressed in further studies.

To evaluate the performance of an in vitro test method, two new metrics—the toxicity separation index (TSI) and toxicity estimation index (TEI)—were introduced, where TSI considers the separation of hepatotoxic from non-hepatotoxic compounds, and TEI estimates how well hepatotoxic blood concentrations in vivo can be estimated for hepatotoxic compounds [79].

The two metrics can not only be used to test whether a readout improves the test system, but also which test parameter is most appropriate. For example, it can be tested whether the traditionally used EC_{50} for cytotoxicity leads to better separation and estimation than values of earlier (EC_{10}) or later (EC_{80}) cytotoxicity. Similarly, it can be evaluated whether, for example, the modeled in vivo blood, plasma, or total (blood + plasma) concentration leads to a better prediction.

Exemplary data graphs of fictional data pairs describe the two indices with hepatotoxic (red) and non-hepatotoxic (green) compounds (**Figure 3**). The maximum value of both indices is 1. Thus, a TSI of 1 represents a perfect separation of hepatotoxic and non-hepatotoxic compounds and a TEI of 1 expresses that the in vivo concentration for an increased risk of liver injury is appropriately reflected by the in vitro concentration (concentration in vitro ≤ concentration in vivo for hepatotoxic compounds).

A good separation of the hypothetic compounds is illustrated by the dots and indicated by a TSI of 0.962 (**Figure 3**A/B). The good estimation is reflected by the value 0.958, which means that the in vitro values of the hepatotoxic compounds are close to the in vivo concentration, which leads to an increased risk of hepatotoxicity (**Figure 3**A/C).

In the case of poor separation, non-hepatotoxic and hepatotoxic compounds are close together, as reflected by a low TSI of 0.538 (**Figure 3**C/D). If the estimation is poor, the hepatotoxic compounds move away from the iso-line, on which in vivo and in vitro concentrations are equal, and the TEI decreases (**Figure 3**B/D). Since separation is more important for the prediction than the estimation, a high TSI is preferred to a high TEI.

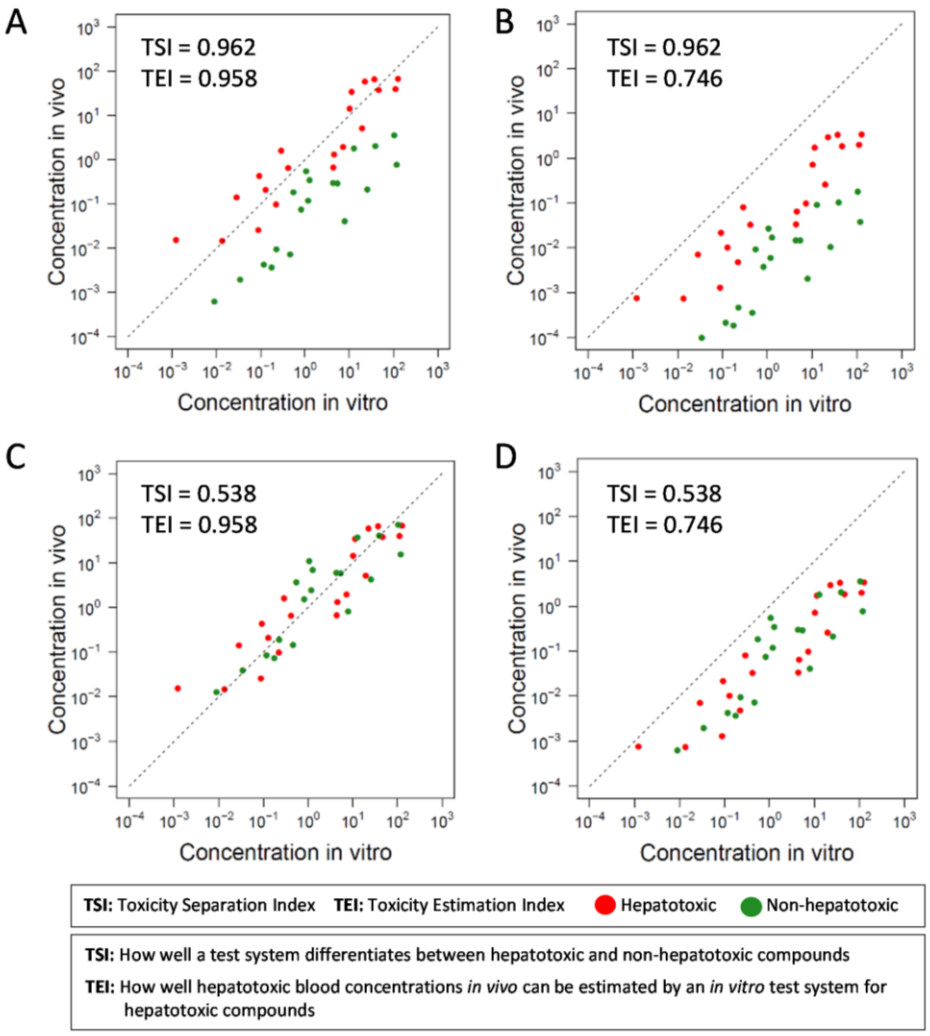

Figure 3: Concept of the toxicity separation (TSI) and toxicity estimation (TEI) indices. Fictional data pairs show exemplary constellations for different metrics values. Green dots represent non-hepatotoxic compounds and red hepatotoxic ones. Dashed diagonal line: iso-line (identical concentrations in vivo and in vitro). **(A)** Scenario with good separation and good estimation. **(B)** Scenario with good separation and worse estimation. **(C)** Scenario with worse separation and good estimation. **(D)** Scenario with worse separation and worse estimation (Taken from *[79]*).

The starting point of the doctoral thesis was the test system based on cytotoxicity in primary hepatocytes after 48 hours of exposure yielding a nearly optimal TSI of 0.996 and a TEI of 0.844 (**Figure 4**)[79]. The C_{max} (total blood 95% percentile) as in vivo parameter and the EC_{10} median as in vitro parameter resulted in the highest possible separation, which is why they were used in the further experimental approaches of this thesis.

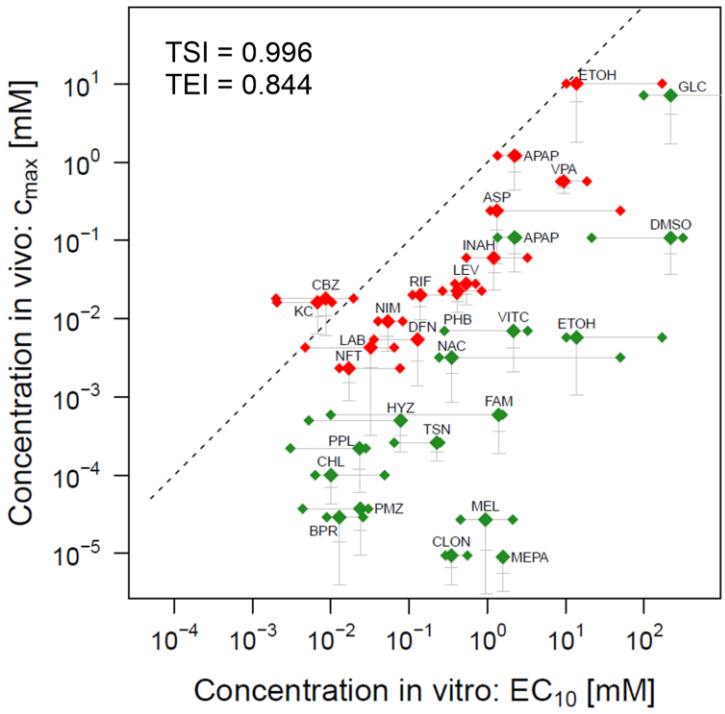

Figure 4: Test system based on 48 hours cytotoxicity test in primary human hepatocytes. Extrapolation plot of the EC_{10} median. EC_{10} values for each donor are given by a diamond, and the three diamonds corresponding to one test compound are connected by a line. The vertical lines crossing each median EC_{10} value illustrate the ranges between 5th and 95th percentiles of C_{max} (total maximal blood concentrations). The 95th percentile coincides with the median diamond, the horizontal dashes below are median values and 5th percentiles. Dashed diagonal line: iso-line (identical concentrations in vivo and in vitro). Green dots represent non-hepatotoxic compounds and red dots represent hepatotoxic compounds (Taken from [79]).

1.5 Aim of this work

The aim of this work was to improve the before introduced test system for the prediction of drug-induced liver injury in relation to blood concentrations and oral doses. It should be investigated whether the addition of functional readouts to the in vitro test battery provides an improvement compared to cytotoxicity measurement in primary human hepatocytes alone. For this purpose, in vitro approaches representing specific mechanisms involved in DILI were developed and evaluated for their performance in comparison and combination with the cytotoxicity test.

In the first approach, it is investigated whether an adaptation of the in vitro culturing situation of primary human hepatocytes to the in vivo situation improves the test system. For this purpose, the influence of bile acids in the culture medium on the cytotoxicity of test compounds is examined. Of special interest are compounds that inhibit bile acid transporters and thus lead to an accumulation of toxic bile acids.

Next, another approach is presented to detect compounds that inhibit bile acid transport. For this purpose, 5-Chloromethylfluorescein diacetate (CMFDA), a non-fluorescent molecule is used, which becomes fluorescent after uptake in the cell and is a substrate for bile acid transporters. By incubating primary human hepatocytes with a test compound and CMFDA and subsequent fluorescence measurement, it will be investigated whether inhibition of bile acid transport can be specifically detected and whether this assay is a suitable addition to the cytotoxicity test.

In the last approach, it is investigated whether the detection of drug-induced lipid accumulation improves our test system. For this purpose, HepG2 cells are incubated with free fatty acids together with a test compound, followed by staining and measuring of intracellular lipid droplets.

In conclusion, three in vitro approaches are presented and their performance is determined using the TSI and TEI. This is followed by a recommendation for or against implementation in the in vitro test battery to improve the test system and thus the prediction of DILI.

1.6 Contribution statement

Excerpts of this thesis have been published as Brecklinghaus et al., 2021 “The hepatocyte export carrier inhibition assay improves the separation of hepatotoxic from non-hepatotoxic compounds” in *Chemico-Biological Interactions* [80]. This concerns paragraph 2.2; 3.2; 4.2.

I would like to thank all the co-authors for their input and contributions. Especially I would like to thank Ahmed Ghallab for the intravital imaging (**Figure 13**) and Georgia Günther for the primary mouse hepatocyte experiments (**Figure 14**). Furthermore, I would like to thank the IfADo core facility Analytische Chemie for the glutathione measurements (**Figure 19**). Pharmacokinetic modeling by Dr. Mian Zhang, Dr. Iain Gardner, and Dr. Wiebke Albrecht was essential for this publication as well as the whole project. Dr. Wiebke Albrecht also contributed to the collection of the cytotoxicity data in PHH and HepG2 cells. Special thanks go to the statisticians Dr. Franziska Kappenberg and Julia Duda, who performed most of the statistical analyses.

Excerpts of this thesis were submitted (27.10.2021) to *Toxicology in Vitro* as Brecklinghaus et al., “Influence of bile acids on the cytotoxicity of chemicals in cultivated human hepatocytes”. I would like to thank the already before mentioned co-authors for their contributions and support especially in the PBPK modeling and statistical analysis. This concerns paragraph 2.2; 3.1; 4.1.

2 Material and Methods

2.1 Material

2.1.1 Technical equipment

Table 1: Technical equipment in the laboratory.

Equipment, Specification	Company
2-photon microscope, LSM MP7	Zeiss
Autoclave, 5075 ELV	Tuttenauer
Autoclave, Systec VX-150	Systec
Balance, EW	Kern
Bright field microscope, Primovert	Zeiss
Bunsen burner, IBS Fireboy	Integra Bioscences
Cell counter, Casy®	Innovatis
Centrifuge with cooling function, 5424R	Eppendorf
Centrifuge with cooling function, Biofuge Fresco	Heraeus
Centrifuge, Centrifuge 5415R	Eppendorf
Centrifuge, Megafuge 1.0R	Thermo Scientific
Confocal microscope, LSM880	Zeiss
Freezing container, Mr. Frosty	Thermo Fisher Scientific
Fume hood	Köttermann
Fume hood, Electronics FAZ 2	Waldner
Hemocytometer cover glasses	Marienfeld Superior
Hemocytometer Neubauer improved	Marienfeld Superior
HPLC column, Nucleodur PolarTec	Macherey-Nagel
Incubation chamber	Solent Scientific Ltd
Incubator, C150 R Hinge 230	Binder
Laminar flow hood	CLEAN AIR SYSTEMS
Laminar flow hood, HERASAFE	Heraeus
Laminar flow hood, LaminAir HBB 2472	Heraeus
Magnetic stirrer, IKAMAG RCT	IKA
Mass spectrometer, QExactive	Thermo Scientific
Microcentrifuge, Mini Spin Plus	Eppendorf
Multichannel pipette, Discovery	Abimed
Multichannel pipette, Research	Eppendorf
Multichannel pipette, Research Plus	Eppendorf
Multichannel pipette, Research Pro	Eppendorf

Equipment, Specification	Company
Multichannel pipette, Xplorer	Eppendorf
pH Meter, CG 842	Schott
Pipeteboy	Integra
Pipettes, ErgoOne	Starlab
Pipettes, Pipetman	Gibson
Pipettes, Reference	Eppendorf
Pipettes, Research	Eppendorf
Pipettes, Research Plus	Eppendorf
Plate reader, Infinite M200 Pro	Tecan
Precision balance, AE 240	Mettler
Precision balance, ALJ 200-5DA, EW150-3M	Kern & Sohn
Precision balance, ME235P	Sartorius
Reagent reservoir, Dual solution	Heathrow Scientific
Reagent reservoir, StarTub PP	Starlab
Real time PCR system, 7500 Real-Time PCR System	Applied Biosystems
Sonicator, Bandelin	SONOPLUS
Sonification bath, Labson 200	Bender& Hobein
Spectrometer, NanoDrop 2000	Thermo Scientific
Thermocycler, T-Gradient	Biometra
UHPLC system, Vanquish Horizon	Thermo Scientific
Vacuum pump, Diaphragm Vacuum Pump	Vacuumbrand
Vortex, Vortex-genie 2	Bender&Hobein
Water bath, GFL 1083	Gesellschaft für Labortechnik
Water bath, Precision GP28	Thermo Scientific
Water purification system, Maxima Ultra-Pure Water	ELGA
Water purification system, Milli-Q® Integral 15 System	Merck

Table 2: Commercial chemicals and kits.

Compound	Company	Catalog number
5-Chloromethylfluorescein diacetate	Cayman Chemicals, Ann Arbor, MI, USA	19583
Acetaminophen	Sigma-Aldrich Corp, St. Louis, MO, USA	A7085
Acetic acid	Carl-Roth, Karlsruhe, Germany	3738.5
AdipoRed™ Assay Reagent	Lonza, Basel, Switzerland	PT-7009
Amiodarone hydrochloride	Sigma-Aldrich Corp, St. Louis, MO, USA	A8423
Aspirin	Sigma-Aldrich Corp, St. Louis, MO, USA	A5376
Atorvastatin calcium salt	Cayman Chemicals, Ann Arbor, MI, USA	10493

Compound	Company	Catalog number
Atropine sulfate monohydrate	Santa Cruz, Dallas, TX, USA	sc-203322
Benztropine mesylate	Cayman Chemicals, Ann Arbor, MI, USA	16214
Bosentan hydrate	Sigma-Aldrich Corp, St. Louis, MO, USA	SML 1265
Buspirone hydrochloride	Sigma-Aldrich Corp, St. Louis, MO, USA	B7148
Carbamazepine	Sigma-Aldrich Corp, St. Louis, MO, USA	C4024
CellTiter-Blue® Cell Viability Assay	Promega, Madison, WI, USA	G8081
CellTracker™ Green CMFDA Dye	Thermo Fisher Scientific, Waltham, MA, USA	C7025
Chenodeoxycholic acid	Sigma-Aldrich Corp, St. Louis, MO, USA	C8261
Chlorpheniramine maleate	Sigma-Aldrich Corp, St. Louis, MO, USA	C3025
Clofibrate	Sigma-Aldrich Corp, St. Louis, MO, USA	C6643
Clonidine hydrochloride	Sigma-Aldrich Corp, St. Louis, MO, USA	C7897
Deoxycholic acid	Sigma-Aldrich Corp, St. Louis, MO, USA	D6750
DEPC sterile water	Thermo Fisher Scientific, Waltham, MA, USA	AM9906
Diclofenac sodium	Sigma-Aldrich Corp, St. Louis, MO, USA	D6899
Digoxin	Cayman Chemicals, Ann Arbor, MI, USA	22266
Dimethyl sulfoxide	Sigma-Aldrich Corp, St. Louis, MO, USA	34869-M
Dimethyl sulfoxide	PanReac Applichem, Darmstadt, Germany	A36720050
Diphenhydramine hydrochloride	Santa Cruz, Dallas, TX, USA	sc-204729
Disodium hydrogen phosphate	Carl-Roth, Karlsruhe, Germany	T876.2
DL-buthionine-sulfoximine	Sigma-Aldrich Corp, St. Louis, MO, USA	19176
Entacapone	BIOZOL, Eching, Germany	TGM-T2216
Ethanol	VWR Chemicals, Germany	20821.2
Glucose monohydrate	Sigma-Aldrich Corp, St. Louis, MO, USA	49159
Glycochenodeoxycholic acid	Sigma-Aldrich Corp, St. Louis, MO, USA	G0759
Glycocholic acid	Sigma-Aldrich Corp, St. Louis, MO, USA	G7132
Glycodeoxycholic acid	Sigma-Aldrich Corp, St. Louis, MO, USA	G9910
High Capacity cDNA Reverse Transcription Kit	Applied Biosystems, Waltham, MA, USA	4368813
Hoechst 33342 solution	Thermo Fisher Scientific, Waltham, MA, USA	H3570
Hydroxyzine hydrochloride	Sigma-Aldrich Corp, St. Louis, MO, USA	H8885
Ibuprofen	Sigma-Aldrich Corp, St. Louis, MO, USA	I7905
Indomethacin	Santa Cruz, Dallas TX, USA	Sc200503
Isoniazid	Sigma-Aldrich Corp, St. Louis, MO, USA	I3377
Isosorbide dinitrate	Cayman Chemicals, Ann Arbor, MI, USA	23990
Ketoconazole	Sigma-Aldrich Corp, St. Louis, MO, USA	K1003
Lovastatin	Sigma-Aldrich Corp, St. Louis, MO, USA	M2147
Melatonin	Sigma-Aldrich Corp, St. Louis, MO, USA	M5250

Compound	Company	Catalog number
Methanol	Sigma-Aldrich Corp, St. Louis, MO, USA	322415
Methotrexate	Sigma-Aldrich Corp, St. Louis, MO, USA	PHR1396
N-acetylcysteine	Sigma-Aldrich Corp, St. Louis, MO, USA	A9165
N-ethylmaleimide	Thermo Fisher Scientific, Waltham, MA, USA	23030
Nevirapine	Cayman Chemicals, Ann Arbor, MI, USA	15117
Nifedipine	Cayman Chemicals, Ann Arbor, MI, USA	11106
Nimesulide	Sigma-Aldrich Corp, St. Louis, MO, USA	N1016
Nitrofurantoin	Sigma-Aldrich Corp, St. Louis, MO, USA	N7878
Oxycodone hydrochloride	Sigma-Aldrich Corp, St. Louis, MO, USA	1378
Oxymorphone hydrochloride monohydrate	LGC Standards, Teddington, United Kingdom	MM0673.00
Pazopanib	Cayman Chemicals, Ann Arbor, MI, USA	12097
Pindolol	Sigma-Aldrich Corp, St. Louis, MO, USA	P0778
Pioglitazone hydrochloride	Sigma-Aldrich Corp, St. Louis, MO, USA	PHR1632
Potassium chloride	Fluka Chemie AG, Switzerland	60129
Potassium dihydrogen phosphate	Merck, Darmstadt, Germany	1.04873.1000
Primaquine phosphate	Santa Cruz, Dallas TX, USA	sc-205817
Primidone	Santa Cruz, Dallas TX, USA	sc-204861
Promethazine hydrochloride	Sigma-Aldrich Corp, St. Louis, MO, USA	P4651
Propranolol hydrochloride	Sigma-Aldrich Corp, St. Louis, MO, USA	P08884
Pyridoxine hydrochloride	Sigma-Aldrich Corp, St. Louis, MO, USA	P9755
Qiazol®Lysis Reagent	Qiagen Sciences, Maryland, USA	79306
Rifampicin	Sigma-Aldrich Corp, St. Louis, MO, USA	R3501
Rosiglitazone maleate	TRC, North York, ON, Canada	R693500
Rosuvastatin calcium salt	Cayman Chemicals, Ann Arbor, MI, USA	18813
ROTI®Histofix 4%	Carl-Roth, Karlsruhe, Germany	P087.X
Simvastatin	Sigma-Aldrich Corp, St. Louis, MO, USA	S6196
Sitaxentan sodium	BIOZOL, Eching, Germany	T6672
Sodium chloride	Carl-Roth, Karlsruhe, Germany	3957.2
Sodium hydroxzide	Merck, Darmstadt, Germany	1.06482
Sodium oleate	Sigma-Aldrich Corp, St. Louis, MO, USA	07501
Sodium palmitate	Sigma-Aldrich Corp, St. Louis, MO, USA	P9767
Sodium phenylbutyrate	Cayman Chemicals, Ann Arbor, MI, USA	11323
Stavudine	Cayman Chemicals, Ann Arbor, MI, USA	14975
TaqMan™ Universal PCR Master Mix	Applied Biosystems, Waltham, MA, USA	4305719
tert-Butylhydroquinone	Sigma-Aldrich Corp, St. Louis, MO, USA	112941
Tetracycline hydrochloride	Sigma-Aldrich Corp, St. Louis, MO, USA	T7660

Compound	Company	Catalog number
Tetramethylrhodamine ethyl ester perchlorate	Thermo Fisher Scientific, Waltham, MA, USA	T669
Theophylline	Cayman Chemicals, Ann Arbor, MI, USA	23760
Tolcapone	Sigma-Aldrich Corp, St. Louis, MO, USA	1670207
Tolterodine tartrate	TargetMol, Boston, MA, USA	TGM-T0099
Triclosan	Sigma-Aldrich Corp, St. Louis, MO, USA	PHR1338
Triprolidine hydrochloride	Sigma-Aldrich Corp, St. Louis, MO, USA	T6764
Triton™ X-100	Fluka Chemie AG, Switzerland	93418
Troglitazone	Cayman Chemicals, Ann Arbor, MI, USA	71750
Valproic acid	Sigma-Aldrich Corp, St. Louis, MO, USA	PHR1061
Vitamin C	Sigma-Aldrich Corp, St. Louis, MO, USA	A0278
Zaleplon	Mikromol Luckenwalde, Germany	MM1322.00

Table 3: Chemicals provided by industrial cooperation partners.

Compound	Company
Benzbromarone	Astra Zeneca
Perhexiline maleate	Astra Zeneca

2.1.2 Consumables

Table 4: Consumables.

Consumable	Company	Catalog number
CASY cups	OMNI Life Science, Bremen, Germany	OLS5651794
Cell culture microtiter plate black, 96 well	Greiner Bio-One, Kremsmünster, Austria	655986
Centrifugation tube, 15 mL	Sarstedt, Numbrecht, Germany	62.554.512
Centrifugation tube, 50 mL	Sarstedt, Numbrecht, Germany	62.547.254
CryoPure cryovials, 1 mL	Sarstedt, Numbrecht, Germany	72377992
Filtropur S 0.2 syringe filter	Sarstedt, Numbrecht, Germany	83.1826.001
Glass bottom culture dish	MatTek Corporation, Ashland, MA, USA	P35G
GravityPLUS™ hanging drop system	InSphero AG, Schlieren, Switzerland	ISP-06-001/010
IBIDI µ-Slide 4 Well	Ibidi, Gräfelfing, Germany	80426
Omnifix syringe, 10 mL	B. Braun, Melsungen, Germany	1616103V
Parafilm wrap	Cole-Parmer, Kehl/Rhein, Germany	PM-992
Pasteur pipette, glass, 150 mm	Carl Roth, Karlsruhe, Germany	4518.1
Pipette tips, 1250 µl, long	Sarstedt, Numbrecht, Germany	70.1186
Pipette tips, 1000 µl	Sarstedt, Numbrecht, Germany	70.762

Consumable	Company	Catalog number
Pipette tips, 20 µl	Sarstedt, Numbrecht, Germany	70.1116
Pipette tips, 200 µl	Sarstedt, Numbrecht, Germany	70.760.002
Pipette tips, 5000 µl	Eppendorf, Hamburg, Germany	22492080
RNaseZap® RNase decontamination solution	Ambion, Thermo Fischer Scientific, USA	AM9780/AM9782
SafeSeal, 0.5 microtube	Sarstedt, Numbrecht, Germany	72.699
SafeSeal, 1.5 mL microtube	Sarstedt, Numbrecht, Germany	72.706
SafeSeal, 2 mL microtube	Sarstedt, Numbrecht, Germany	72.695.500
SafeSeal, 5 mL microtube	Sarstedt, Numbrecht, Germany	72.701
Serological pipette, 10 mL	Sarstedt, Numbrecht, Germany	86.1254.001
Serological pipette, 25 mL	Sarstedt, Numbrecht, Germany	86.1685.001
Serological pipette, 5 mL	Sarstedt, Numbrecht, Germany	86.1253.001
Serological pipette, 50 mL	Sarstedt, Numbrecht, Germany	86.1256.001
Tail vein catheter	SAI-infusion, Lake Villa, IL, USA	MTV-01
Tissue culture flask, T175	Sarstedt, Numbrecht, Germany	83.3912.002
Tissue culture flask, T25	Sarstedt, Numbrecht, Germany	83.3910.002
Tissue culture flask, T75	Sarstedt, Numbrecht, Germany	83.3911.002
Tissue culture plate, Flat-Bottom 24 Well plate	Sarstedt, Numbrecht, Germany	83.1836
Tissue culture plate, Flat-Bottom 96 Well plate	Sarstedt, Numbrecht, Germany	83.3924
Vacuum filtration unit, 0.22 µm, 250 mL	Sarstedt, Numbrecht, Germany	83.1822.001
Weighing tray	Sarstedt, Numbrecht, Germany	719923211
Weighing tray	Sarstedt, Numbrecht, Germany	719923212

2.1.3 Cell culture supplies

Table 5: Cell culture supplies.

Supply	Company	Catalog number
CASYton solution	Roche Diagnostics GmbH, Mannheim, Germany	5651808001
Collagen lyophilized (rat tail), 10 mg	Roche Diagnostics GmbH, Mannheim, Germany	11171179001
Dexamethasone	Sigma-Aldrich Corp, St. Louis, MO, USA	D4902
Dulbecco's modified eagles medium (DMEM), high glucose (4.5 g/l), 1x concentrated	PAN Biotech GmbH, Aidenbach, Germany	P04-04500

Supply	Company	Catalog number
Dulbecco's modified eagles medium (DMEM), low glucose (1.0 g/l), 10x concentrated	BioConcept, Allschwil, Switzerland	1-25K03-I
Gentamicin sulfate, 10 mg/mL	PAN Biotech GmbH, Aidenbach, Germany	P06-03021
Hepatocyte growth factor	R&D Systems, Minneapolis, MN, USA	2207-HG-025
Insulin transferrin selenite supplement (ITS)	Sigma-Aldrich Corp, St. Louis, MO, USA	13146
Penicillin/Streptomycin, 10,000 U/mL Penicillin, 10 mg/mL Streptomycin	PAN Biotech GmbH, Aidenbach, Germany	P06-07100
Sera Plus (Special Processed FBS)	PAN Biotech GmbH, Aidenbach, Germany	3702-P103009
Stable Glutamine, 200 mM	PAN Biotech GmbH, Aidenbach, Germany	P04-82100
Trypan blue solution 0.4%	Sigma-Aldrich Corp, St. Louis, MO, USA	T8154
Trypsin 0.05 %/EDTA 0.02 % in PBS, w/o: Ca and Mg	Sigma-Aldrich Corp, St. Louis, MO, USA	P10-023100
William's E medium, w/o: L-Glutamine, w/o: Phenol red, w: 2.24 g/L NaHCO3	PAN Biotech GmbH, Aidenbach, Germany	P04-29510

2.1.4 Antibodies

Table 6: Antibodies for immunostaining.

Antibody	Company	Order number
Anti-BSEP, Polyclonal Antibody	Thermo Fisher Scientific, Waltham, MA, USA	PA5-78690
Secondary Antibody, Alexa Fluor Plus 488	Thermo Fisher Scientific, Waltham, MA, USA	A32790

2.1.5 Cell culture media and buffers

Table 7: Recipe for 5 l 10×PBS for cell culture.

Compound	Amount [g]
KCl	10
KH_2PO_4	10
Na_2HPO_4	46
NaCl	400

The reagents in **Table 7** were dissolved in double distilled water, the pH was adjusted to 7.4 and autoclaved. Unless otherwise stated, 1×PBS was used for the experiments, therefore the 10×PBS was diluted 1:10 in double-distilled water and autoclaved.

2.1.6 Primers

Table 8: TaqMan probes from Applied Biosystems for gene expression quantification.

Gene	Company	Assay ID
BSEP	Thermo Fisher Scientific, Waltham, MA, USA	Hs00994811_m1
GAPDH	Thermo Fisher Scientific, Waltham, MA, USA	Hs99999905_m1
MRP2	Thermo Fisher Scientific, Waltham, MA, USA	Hs00960488_m1

Table 9: PHH plating medium.

Component	Volume [mL]
William's E medium, w/o: L-Glutamine, w/o: Phenol red, w: 2.24 g/L $NaHCO_3$	500
Sera Plus, EU approved regions, special processed FBS, 0.2 µm sterile filtered	50
Penicillin-Streptomycin, 10,000 U/mL Penicillin, 10 mg/mL Streptomycin	5
Stable Glutamine, 200 mM	5
Gentamicin sulfate, 10 mg/mL	0.5
Dexamethasone, 2.5 mM in EtOH	0.02
ITS supplement, 1.0 mg/mL recombinant human insulin, 0.55 mg/mL human transferrin, 0.5 µg/mL sodium selenite	0.005

Table 10: PHH culture medium.

Component	Volume [mL]
William's E medium, w/o: L-Glutamine, w/o: Phenol red, w: 2.24 g/L $NaHCO_3$	500
Penicillin-Streptomycin, 10,000 U/mL Penicillin, 10 mg/mL Streptomycin	5
Stable Glutamine, 200 mM	5
Gentamicin sulfate, 10 mg/mL	0.5
Dexamethasone, 2.5 mM in EtOH	0.02
ITS supplement, 1.0 mg/mL recombinant human insulin, 0.55 mg/mL human transferrin, 0.5 µg/mL sodium selenite	0.005

Table 11: HepG2 culture medium.

Component	Volume [mL]
DMEM, w: 4.5 g/L Glucose, w: stable Glutamine, w/o: Sodium pyruvate, w: 3.7 g/L NaHCO3	500
Heat inactivated Sera Plus, EU approved regions, special processed FBS, 0.2 µm sterile filtered	50
Penicillin-Streptomycin, 10,000 U/mL Penicillin, 10 mg/mL Streptomycin	5

For heat inactivation FBS was placed in a water bath at 56 °C for 30 minutes and rotated every 10 minutes.

Table 12: PMH Aggregation medium.

Component	Volume [mL]
William's E medium, w/o: L-Glutamine, w/o: Phenol red, w: 2.24 g/L NaHCO3	8
Sera Plus, EU approved regions, special processed FBS, 0.2 µm sterile filtered	2
Penicillin-Streptomycin, 10,000 U/mL Penicillin, 10 mg/mL Streptomycin	0.1
Stable Glutamine, 200 mM	0.1
Hepatocyte growth factor (20 µg/mL)	0.01

2.1.7 Cell line and cryopreserved human hepatocytes

2.1.7.1 Primary cells

Cryopreserved human hepatocytes were purchased from BioIVT (product numbers M00995-P, F00995-T-CERT, and F00995-P) and Lonza (catalog number HUCPI) and stored in the vapor phase of liquid nitrogen. Detailed information about the donors is given in the Electronic supplement.

2.1.7.2 Secondary cell line

The HepG2 cell line is an adherent human hepatocellular carcinoma cell line derived from cells of a 15-year-old male Caucasian donor. Frozen HepG2 cells were purchased from ATCC LGC Standards (product number HB-8065) and stored in the vapor phase of liquid nitrogen.

2.2 Methods

2.2.1 Collagen coating of cell culture plates

To achieve cell adhesion of primary human hepatocytes, cell culture plates were coated with collagen before plating. Similarly, this was done for HepG2 cells to have a more uniform cell layer, no clump formation, and to allow greater comparability between HepG2 and PHH cultures.

Monolayer (ML): For collagen coating of cell culture plates, 0.25 mg/mL collagen solution was prepared by dissolving 10 mg lyophilized rat tail collagen I for at least 4 hours at 4 °C in 40 mL 0.2% sterile acetic

acid. Next, 100 µL of the collagen solution was transferred into each well of a 96-well plate and removed after 1-2 minutes incubation time. The plates were left to dry for at least 2 hours (ideally overnight) and were washed 3 times with PBS before usage. 4-well IBIDI chambers were coated with 350 µL per well using the same procedure.

Sandwich (SC): 1.1 mg/mL collagen solution was prepared by dissolving 10 mg lyophilized rat tail collagen I for at least 12 hours at 4 °C in 9 mL 0.2% sterile acetic acid. Before coating, 1 mL of 10×DMEM was added followed by NaOH titration till a pink color change occurred, resulting in a final concentration of 1 mg/mL. For a 4-well IBIDI chamber, 200 µL collagen solution was transferred into each well and polymerized at 37 °C in the incubator for 45 minutes. After plating, attachment, and washing of the cells the second layer, 200 µL of 1 mg/mL collagen solution, was added and polymerized for 30 minutes at 37 °C in the incubator.

2.2.2 Cell culture of primary human hepatocytes

Cryopreserved human hepatocytes were thawed for 2 minutes in a 37 °C water bath and one vial (≥ 5 × 10^6 cells) was transferred into 5 mL pre-warmed plating medium (**Table 9**) .Cell number and vitality were determined via the trypan blue exclusion method using a hemocytometer. Therefore 50 µL cell suspension was added to 350 µL plating medium and 100 µL trypan blue solution. The mixture was filled into the hemocytometer and vital, unstained cells as well as dead, blue-colored cells were counted and the cell yield, as well as the cell viability, was calculated.

Cell yield [cells/mL] = (total number of cells / number of counted square grids) × 10^4 × 10 (dilution factor)

Cell viability [%] = (number of vital cells / total number of cells) × 100

For 96-well plates, the cell suspension was diluted with plating medium to a final concentration of 0.5 × 10^6 cells/mL and subsequently 100 µL were transferred into each well. To avoid edge effects, the outer wells were filled with PBS only. After 3 – 4 hours of attachment, the cells were washed gently three times with PBS to get rid of cell debris, dead cells, and serum. Finally, cultivation medium was added (**Table 10**) and the cells were maintained under standard cell culture conditions (37 °C in a humidified atmosphere with 5% CO_2).

2.2.3 Cell culture of primary mouse hepatocytes

The performed experiments were approved by the animal welfare authority. Mice were handled according to the Principles of Laboratory Care and recommendations of the Society of Laboratory Animal Science (Gesellschaft für Versuchstierkunde, GV-SOLAS, Germany).

Mouse hepatocytes were isolated using a published standard operating procedure [81]. Hepatocytes from tdTomato mice (Gt(ROSA)26Sortm14(CAG-tdTomato)Hze, Jackson lab, male, 8 – 12 weeks old) were used to establish spheroid and sandwich cultures.

Spheroid cultures were established using the GravityPLUS™ Hanging Drop System (InSphero AG). First, 5 mL of 0.5×PBS with 0.1% Triton X-100 was added to the bottom of the 96-well reservoir plate. Next, 40 µL of aggregation medium (**Table 12**) was pipetted with a multichannel pipette at 1000 cells per well. The cell suspension was gently agitated before each pipetting. Afterward, the plate was incubated for 5 days at 37 °C and 5% CO_2. Spheroids were rinsed into the petri dish placed below by adding 100 µL of aggregation medium without FCS. Finally, the spheroids were collected individually and fixed in a collagen-coated 35 mm, 1.5 coverslip and 14 mm glass diameter culture dish.

For sandwich cultures, primary mouse hepatocytes were cultivated in the same medium as primary human hepatocytes (**Table 9**, **Table 10**). Hepatocytes were isolated from the same mouse strain (tdTomato) and 2 mL plating medium with 1×10^6 cells of primary mouse hepatocytes (tdTomato) were seeded on a glass-bottom culture dish pre-coated with a first layer of 200 µL collagen (0.25 mg/mL rat tail collagen I solution). Three hours after attachment, the cells were washed with culture medium and 250 µL of the second layer (1 mg/mL collagen solution) was added and incubated for 30 minutes at 37 °C and 5% CO_2. Finally, the cells were covered with 2 mL culture medium and maintained in the incubator. The medium was changed every second day during cultivation.

Mouse perfusion and cultivation of hepatocytes were carried out at the IfADo by Georgia Günther.

2.2.4 Cell culture of the HepG2 cell line

2.2.4.1 Cultivation and seeding of HepG2 cells

HepG2 cells were cultivated in Dulbecco's modified eagle's medium (DMEM) containing 4.5% glucose, 1% penicillin/streptomycin mixture, and 10% heat-inactivated FBS (**Table 11**). The cells were maintained in conventional T75 cell culture flasks and kept at 37 °C with constant humidity and 5% CO_2 content. The medium was changed every 2 – 3 days.

When reaching 80 – 90% confluency, the cells were sub-cultured or plated for experiments. First, the cells were washed with PBS and then dissolved with 1 mL trypsin for 5 minutes at 37 °C. The enzymatic reaction was stopped by adding 9 mL medium and after transfer to a 50 mL centrifugation tube, the cell suspension was pelleted for 5 minutes at 600 rpm. After discarding the supernatant, the pellet was carefully dissolved in 1 mL of medium and then diluted with another 9 mL. For sub-culturing, 1:3 or 1:10 dilutions of cell suspension:medium were made and transferred into a new T75 cell culture flasks. For seeding, cell yield and viability were determined with a hemocytometer (2.2.3) or a CASY cell

counter. For the CASY cell counter, 100 µL of cell suspension was transferred to 10 mL of CASYton and then measured. Finally, the cell suspension was diluted to the desired concentration and the cells were plated in the respective plate format for the corresponding assays. Cell number and plate format are specified in the respective chapters.

2.2.4.2 Storage of HepG2 cells

For storage, HepG2 cells cultured in T75 cell culture flasks were first washed with PBS and then detached with 1 mL trypsin at 37 °C for approximately 5 minutes. The reaction was stopped by adding 9 mL culture medium and the cell suspension was centrifuged at 600 rpm for 5 minutes. After aspiration of the supernatant, the pellet was resuspended with 3 mL of freezing solution (90% FBS + 10% DMSO) and transferred into a cryovial (1 mL per vial). The vials were stored for at least one day at -80 °C in a freezing container filled with isopropanol e.g. Mr.Frosty and transferred to the vapor phase of a nitrogen tank for long-term storage after a mycoplasma test was performed.

2.2.4.3 Thawing of HepG2 cells

For thawing, cryopreserved HepG2 cells were defrosted at 37 °C in a water bath and subsequently diluted with 10 mL culture medium in a 50 mL centrifugation tube. The cell solution was then centrifuged for 5 minutes at 600 rpm and the supernatant was aspirated. Subsequently, the pellet was resuspended with 1 mL of culture medium and transferred to a T75 cell culture flask with additional 9 mL of culture medium. Before being used for experiments, each passage was sub-cultured at least 2 times after thawing.

2.2.5 Compound treatment

Depending on the solubility, test compounds were either dissolved directly in medium or a solvent stock with DMSO or EtOH was prepared, which was then added to the medium. The maximum solvent concentration was limited to 0.5% and appropriate solvent controls were included. Otherwise, medium was used as a control. Usually, 5 concentrations with a dilution factor of $\sqrt{10}$ were applied. Exceptions and a detailed list of all concentrations used are provided in the Electronic supplement.

To remove the culture medium for the treatment, 96-well plates were tapped on paper towels one day after the cells were plated. This procedure is faster than the aspiration of single wells, which prevents the cells from drying out and also avoids the risk of damaging or aspirating cell lawns. Afterward, the cells were exposed with the test compounds and the appropriate controls using a multichannel pipette. For larger culture plate formats, the medium was aspirated with a vacuum pump.

2.2.6 CellTiter-Blue assay (CTB assay)

The CellTiter-Blue (CTB) assay is a commercially available fluorescent method to monitor cell viability [82]. The assay is based on the metabolic capacity of living cells to convert a slightly fluorescent redox dye (resazurin) into a highly fluorescent end product (resorufin). Living cells have a high metabolic capacity, which leads to an increase in fluorescence in the cell culture supernatant after the addition of CTB. In dead or non-viable cells, the reduction reaction does not take place or only to a limited extent, resulting in no or only a weak fluorescent signal. In this work, the CTB assay was used to determine the viability of primary human hepatocytes and HepG2 cells. Due to the light sensitivity, work was carried out in the dark and the CTB reagent was covered with aluminum foil. Since the protocol was adapted in the course of the thesis, there are different procedures, which have the following steps in common: After reaching the intended exposure time, the cell culture plates were washed 3 times with PBS to exclude possible interference with the test compound. A 20% CTB mixture consisting of one part CTB reagent and four parts culture medium was then applied to each well. Wells without cells but with CTB mixture were used as background control. After a color change was visible to the bare eye, the fluorescent signal was measured in a black 96-well plate using the Tecan Infinite M200 Pro plate reader (i-control software version 1.7.1.12) at 540 nm excitation and 594 nm emission.

PHH (old): In the old protocol, 0.5×10^5 living cells were seeded on collagen-coated clear 96-well plates in 200 µL plating medium (2.2.1; 2.2.2). After compound exposure and washing of the cells, 100 µL CTB mixture was added. Following color change after 3 – 4 hours, 100 µL of each well was transferred to a black 96-well plate and finally fluorescence was measured.

PHH (new): To save time and reduce the risk of errors, the cells were directly plated on a collagen-coated black 96-well plate, incubated with the test compound, and subsequently the CTB fluorescence was measured. Before changing the protocol, the reproducibility of both methods was confirmed in detail with and without test compounds in several donors.

HepG2 (old): 0.625×10^5 cells in 0.5 mL were seeded on clear 24-well plates without collagen coating (2.2.4.1). After compound incubation and washing, 0.5 mL CTB mixture was transferred into each well. Following color change (approximately 1 hour), 100 µL of one well was transferred each into 3 wells of a black 96-well plate, resulting in 3 technical replicates. Subsequently, fluorescence was determined with the plate reader.

HepG2 (new): To simplify the work and harmonize the cytotoxicity determination between the two cell culture systems, 0.15×10^5 HepG2 cells were plated on collagen-coated black 96-well plates (2.2.1; 2.2.4.1). Following compound exposure and washing of the cells, 100 µL CTB mixture was added and the fluorescence was determined after a visible color change (approximately 1 hour).

All cytotoxicity experiments were performed in at least three biological replicates with at least 3 technical replicates each. For primary hepatocytes, cells from different donors were counted as biological replicates and 3 simultaneously incubated wells from one donor were used as technical replicates. For HepG2 cells, different passages were used as biological replicates and 3 identically exposed wells of one passage (new protocol) or one well divided into three (old protocol) were considered as technical replicates. All cytotoxicity curves and the corresponding raw and processed data are in the Electronic supplement.

2.2.7 Bile acid mix assay (BAM assay)

The purpose of the bile acid mix (BAM) assay was to investigate the effect of a bile acid mix on the cytotoxicity of test compounds in primary human hepatocytes. For this, PHH were exposed to a test compound and a bile acid mix and subsequently the viability was determined using the CTB assay.

In detail, 0.5×10^5 living PHH were plated on a collagen-coated black 96-well plate (2.2.1; 2.2.2). The next day after plating, the cells were exposed to 100 µL of the test compound for 2 hours. Subsequently, 100 µL consisting of the test compound and bile acid mix was added. This did not change the concentration of the test compound but increased the final DMSO concentration by 0.1% which was taken into account in the corresponding control. The bile acid mix composition was adapted from Chatterjee and colleagues [83] and consisted of 46.5% glycochenodeoxycholic acid (GCDCA), 13.7% chenodeoxycholic acid (CDCA), 13.4% glycodeoxycholic acid (GDCA), 14.1% deoxycholic acid (DCA), and 12.3% glycocholic acid (GCA). For the treatment a total bile acid concentration of 0.5 mM was applied. Following additional 46 hour incubation time, viability was determined using the CTB assay (2.2.6). As a control for comparison, cells were incubated with the same protocol but without the bile acid mix.

All experiments were performed with at least three biological and three to four technical replicates. The raw data, processed data, and related cytotoxicity curves can be found in the Electronic supplement.

2.2.8 Chloromethylfluorescein diacetate assay (CMFDA assay)

The CMFDA assay is used to investigate the inhibition of bile salt carriers in PHH. The assay is based on 5-chloromethylfluorescein diacetate (CMFDA), which is converted intracellularly into fluorescent 5-CMF. As a substrate of important bile acid transporters, 5-CMF accumulates upon inhibition of these transporters, leading to a detectable increase in intracellular fluorescence (**Figure 12**).

In detail, 0.5×10^5 living PHH were plated on a collagen-coated black 96-well plate (2.2.1; 2.2.2). On the next day, the cells were incubated with 200 µL of the respective test compound for one hour. A

fresh CMFDA solution was prepared by mixing 1 mL of culture medium and 20 µL of CMFDA stock [1 mg/mL in DMSO]. Next, 10 µL of this solution was added to the cells. After another 20 minutes, 100 µL of the cell culture supernatant was transferred to a black 96-well plate and fluorescence was determined at 520 nm emission with 485 nm excitation. Subsequently, the cells were washed 3 times with 200 µL of culture medium, covered with 100 µL of culture medium, followed by fluorescence measurement with a plate reader at 485 nm excitation and 520 nm emission.

To control for possible quenching effects, the test compounds were incubated with 2',7'-Dichlorofluorescein in a concentration-dependent manner and subsequently the fluorescence was detected with the plate reader (Appendix Table 24).

The CMFDA assay was performed in hepatocytes of 3 different human donors each with 3 technical replicates. Raw data, processed data, and concentration-response curves of the CMFDA assay are documented in the Electronic supplement.

2.2.9 AdipoRed assay (AR assay)

The AdipoRed (AR) assay examines the effect of a test compound on lipid droplet accumulation in HepG2 cells. For this purpose, HepG2 cells are incubated with a test compound in the presence of free fatty acids (FFA). Subsequently, the lipid droplets are stained with AdipoRed, a commercially available dye that binds to intracellular lipids and Hoechst to stain the cell nuclei for normalization, intracellular fluorescence is then measured with a plate reader.

In detail, 0.15×10^5 HepG2 cells per well were seeded on collagen-coated 96-well plates (2.2.1; 2.2.4) and incubated for 24 hours. Next, the cells were exposed with the test compound and FFA for 48 hours. For this purpose, 0.413 µL Palmitate [50 mM MeOH stock] and 0.827 µL Oleate [50 mM DMEM stock] per mL culture medium were mixed and incubated at 37 °C for 30 minutes in an ultrasonic bath. Afterward, the test compound was added and the cells were exposed to 200 µL of the compound-FFA solution for 48 hours. Subsequently, the plates were washed 3 times with PBS and stained with AdipoRed and Hoechst. For this purpose, 200 µL staining solution (195 µL PBS + 5 µL AdipoRed + 0.2 µL 16.2 mM Hoechst solution) was applied to each well and stored for 10 minutes at room temperature in the dark. Finally, intracellular fluorescence was detected at 460 nm and 572 nm emission with excitation of 340 nm and 485 nm for Hoechst and AdipoRed, respectively. Empty wells without cells but staining solution were used as a background control. The AdipoRed assay was performed in 3 biological replicates with 4 technical replicates. Raw data, processed data, and concentration-response curves of the AdipoRed assay are documented in the Electronic supplement.

To study the effect of increasing fatty acids on mitochondrial membrane potential, cells were exposed to FFA as described before (2.2.9) and stained for 10 minutes with tetramethylrhodamine ethyl ester (TMRE) and Hoechst at room temperature in the dark. Therefore, 200 µl staining solution (200 µl PBS + 0.2 µl 16.2 mM Hoechst solution + 0.1 µl 2 mM TMRE stock) was transferred to each well and subsequently fluorescence was measured with a plate reader at 584 nm and 460 nm emission with excitation of 545 nm and 340 nm for TMRE and Hoechst, respectively. Wells with staining solution but without cells served as background control.

2.2.10 Measurement of GSH in primary human hepatocytes

To obtain further insight into the mechanism and to clarify if the thiol concentration influences the CMFDA assay, primary human hepatocytes of three different donors were incubated for 48 hours with DL-buthionine-sulfoximine (BSO), a selective inhibitor of glutathione synthesis, and the antioxidant tert-butylhydroquinone (tBHQ). Afterward, the CTB and CMFDA assays were performed and total reduced glutathione (GSH) and oxidized glutathione (GSSG) were analyzed by mass spectrometry. Here, samples were derivatized using N-ethylmaleimide as described by New and Chan [84], followed by separation on a 3 × 150 mm Nucleodur PolarTec (3 µm) reversed phase column using a Vanquish Horizon UHPLC coupled online to a QExactive mass spectrometer (both ThermoFisher, Germany) operating in PRM-mode. Generated data were quantified using Skyline [85].

GSH and GSSG quantification was carried out by the IfADo core unit of Analytical Chemistry (Dr. Jörg Reinders).

2.2.11 Gene expression analysis in primary human hepatocytes

2.2.11.1 RNA isolation

Gene expression experiments were performed for three different human donors by culturing 1.5×10^6 cells for 24 hours on collagen-coated 6-well plates (2.2.1; 2.2.2). Afterward, the plates were transferred on ice and the medium was aspirated immediately. Cells were lysed with 1 mL QIAzol lysis reagent and mechanical scraping, followed by transfer of the solution into a sterile 2 mL Eppendorf tube. As a control, 1.5×10^6 freshly thawed cells were transferred into a 2 mL Eppendorf tube and centrifuged for 5 minutes at 500 rpm and 4 °C. The supernatant was discarded and the pellet dissolved in 1 mL QIAzol lysis reagent. Subsequently, the samples were sonicated on ice for 30 seconds (5 second pulse, 2 second pause). For phase separation, the samples were mixed with 200 µL chloroform, shaken vigorously for 15 seconds, and then incubated for 2 – 3 minutes at room temperature followed by centrifugation at 12000 rpm and 4 °C for 15 minutes. The colorless upper aqueous phase was mixed with 500 µL isopropanol in a new 1.5 mL RNase-free Eppendorf tube and incubated for 10 minutes at

room temperature. Next, the sample was centrifuged at 12000 rpm for 20 minutes at 4 °C, the supernatant was discarded, and the pellet was washed with 800 µL of 100% ethanol. After vortexing for 20 seconds and centrifugation for 5 minutes at 10000 rpm at 4 °C, the supernatant was discarded and 800 µL of 75% ice-cold ethanol was added to the pellet. Following 20 seconds of vortexing, the pellet was centrifuged again at 10000 rpm for 5 minutes at 4 °C, the supernatant was discarded, and the pellet was dried for 5 minutes. Finally, the pellet was dissolved with 15 µL DEPC water and the RNA concentration was determined photometrically with the NanoDrop 2000.

2.2.11.2 cDNA synthesis

For quantification of gene expression, the isolated RNA had to be reversely transcribed into cDNA. The cDNA synthesis was performed using the High Capacity cDNA Reverse Transcription Kit from Applied Biosystems according to the manufacturer's protocol. For this purpose, the reagents in **Table 13** were mixed on ice and then processed in a thermo cycler according to the protocol in **Table 14.**

Table 13: Reaction mix for cDNA synthesis.

Compound	Volume per reaction
Mixture 1	10 µL
RNA	500 ng – 2 µg
DEPC H_2O	up to 10 µL
Mixture 2	10 µL
10x RT buffer	2 µL
Random primers	2 µL
dNTPs	0.8 µL
Reverse transcriptase	1 µL
DEPC H_2O	4.2 µL
Final volume	20 µL

Table 14: Thermal conditions for cDNA synthesis.

Step	Temperature	Time
Incubation	25 °C	10 min
Reverse transcription	37 °C	120 min
Inactivation	85 °C	5 sec
	4 °C	hold

2.2.11.3 Quantitative real-time PCR (RT-qPCR)

During the RT-qPCR, cDNA is amplified using DNA polymerase, non-targeted primers, and targeted primers and allows quantification by combining each amplification cycle with a fluorescent signal. Every amplification step increases the PCR product concentration and fluorescence signal resulting in

a so-called cycle threshold (Ct) which represents the number of cycles needed to reach a certain fluorescence threshold.

For quantitative real-time PCR the TaqMan™ Universal PCR Master Mix from Applied Biosciences was used. The reagents in **Table 15** were mixed and then processed according to the protocol in **Table 16** using a 7500 Real-Time PCR System.

Table 15: Reaction mix for qPCR.

Component	Volume
Universal PCR Master Mix	10 µL
DEPC H_2O	6.5 µL
Taqman probe	1 µL
10 ng/µl cDNA	2.5 µL
Final volume	20 µL

Table 16: Thermal conditions for qPCR.

Stage	Temperature	Time	Repetitions
1	50 °C	2 min	1
2	95 °C	10 min	1
3	94 °C	15 sec	40 – 45
	60 °C	30 sec	
	72 °C	35 sec	
4	95 °C	15 sec	1
	60 °C	20 sec	
	95 °C	15 sec	
	60 °C	15 sec	

Analysis was performed using the commonly known $2^{-\Delta\Delta CT}$ method [86]:

Equation 1: D & C correspond to the target gene (in this thesis BSEP) and B & A to a reference gene (in this study GAPDH).

$$\Delta\Delta CT = \Delta CT(target\ sample) - \Delta CT(reference\ sample) = (CT_D - CT_B) - (CT_C - CT_A)$$

2.2.12 Intravital imaging in mice

The performed experiments were approved by the animal welfare authority. Mice were handled according to the Principles of Laboratory Care and recommendations of the Society of Laboratory Animal Science (Gesellschaft für Versuchstierkunde, GV-SOLAS, Germany).

Functional intravital imaging of CMFDA clearance in the livers of mT/mG mice was performed using an inverted two-photon microscope LSM MP7 with an LD C-Apochromat 40×/1.1 water immersion objective, as previously described [87], [88]. A bolus of 20 µg CMFDA was intravenously administered using a tail vein catheter. Quantification of mean fluorescence intensity of 5-CMF in the hepatic

sinusoids, hepatocytes, and bile canaliculi was done in a specified region of interest using ZEN software (Zeiss, Jena, Germany) as indicated in the corresponding figures (**Figure 13**).

Measurements and quantifications were carried out at the IfADo by Dr. Ahmed Ghallab

2.2.13 Fluorescence microscopy

2.2.13.1 CMFDA kinetics in primary mouse hepatocytes

To study the CMFDA kinetics, the spheroid (2.2.3) was exposed to 800 µL William's E medium containing a final concentration of 3.2 µM CMFDA and maintained at 37 °C and 5% CO_2 in an incubation chamber. Images were acquired using a custom-made inverted LSM 7MP with an LD C-Apochromat 40×/1.1 water immersion objective. For two-photon excitation, a Chameleon Ultra II laser (Coherent) tuned to 870 nm was used.

For sandwich culture the cells were cultivated for three days (2.2.3), next culture medium was removed and 800 µL fresh William's E medium with 0.05 mM Hoechst dye was added. CMFDA at a final concentration of 1.6 µM in the medium was repeatedly added. Images were acquired by the same microscope (LSM 7MP) as for spheroid cultures.

Cultivation, measurement, and quantification were carried out at the IfADo by Georgia Günther.

2.2.13.2 CMFDA kinetics in primary human hepatocytes

For CMFDA kinetic studies in primary human hepatocytes, 2×10^5 cells were seeded in monolayer and sandwich format in 4-well IBIDI chambers (2.2.1; 2.2.2). The day after seeding, cells were acclimatized in the climate-control chamber at 37 °C and 5% CO_2, images were taken on a Zeiss LSM880 confocal microscope with the corresponding software and an EC Plan-Neofluar 40×/1.30 Oli DIC (monolayer) and LD C-Apochromat 40×/1.1 water immersion (sandwich) objective. Image acquisition was performed with a 488 nm Argon laser and emission bands set to 503 nm and 558 nm. Pictures were taken before and after the treatment with 2 µM CMFDA.

2.2.13.3 Immunofluorescence staining of BSEP in PHH

To detect the localization of BSEP in monolayer cultured hepatocytes, 2×10^5 cells were seeded in collagen-coated 4-well IBIDI chambers (2.2.1; 2.2.2). The day after seeding, the cells were washed 2 times with PBS and fixed with 4% paraformaldehyde (ROTI®Histofix) for 20 minutes. After washing with PBS for 5 minutes, the samples were permeabilized with 0.5% Triton X-100 in PBS for 10 minutes and washed again 3 times with PBS for 5 minutes each. After blocking with 5% BSA in PBS for 90 minutes, cells were stained overnight on a shaker at 4 °C with the primary antibody PA5-78690 (1:200) in PBS + 2% BSA. The next day, after washing 3 times with PBS + 2% BSA, the cells were stained with the

corresponding secondary antibody A32790 (1:200) for 2 hours. This was followed by washing for 5 minutes with PBS and staining for 30 minutes with Hoechst 33342. After washing 3 times, the cells were covered with culture medium. Images were taken on a Zeiss LSM880 confocal microscope using an EC Plan-Neofluar 40×/1.30 Oil DIC objective and the manufacturer's provided software. Emission bands were set to 423 - 475 nm and 500 – 608 nm with excitation at 405 nm and 488 nm for Hoechst and BSEP, respectively.

2.2.13.4 Microscopic analysis of lipid accumulation in HepG2 cells

For the observation of lipid accumulation in HepG2 cells at increasing fatty acid concentrations, 0.75 × 10^5 cells were plated on collagen-coated IBIDI 4-well chambers (2.2.1; 2.2.4.1). The next day, the cells were exposed to a free fatty acid mix (1:2 palmitate:oleate) for 48 hours. Subsequently, cells were washed 3 times with PBS and stained with 700 µL culture medium + 17.5 µL AdipoRed + 0.7 µL Hoechst [16.2 mM stock]. Image acquisition was performed after 15 minutes of incubation using a LSM880 confocal microscope with a C-Apochromat 63×/1.20 water immersion objective and the appropriate software. Emission bands were set to 421 – 479 nm and 560 – 615 nm with excitation at 405 nm and 488 nm for Hoechst and AdipoRed, respectively.

2.2.14 Transporter prediction

Quantitative Structure-Activity Relationship (QSAR) describes mathematical models that explore the relationship between pharmacological, chemical, and biological activities of a given compound and its chemical structure. The correlation is used to develop a reliable prediction model and estimate the activity of an unknown compound based on its chemical structure [89], [90].

In this thesis, a publicly available web service was used that predicts if small molecules inhibit the export carriers BSEP, MRP3, and MRP4 of hepatocytes [91]. The web service predicts a binary outcome, indicating whether the query compound is active or not. Each transporter model is based on a different classifier and the structure of the molecules is described with RDKit descriptors. A detailed description of the models is given at https://livertox.univie.ac.at [91].

2.2.15 Statistical analyses

Statistical analyses were performed in close cooperation with the statisticians Prof. Dr. Jörg Rahnenführer, Dr. Franziska Kappenberg, and M.Sc. Julia Duda from the Department of Statistics at the TU Dortmund University.

Statistical analyses were performed with the statistical programming language R-version 4.0.0 [92].

2.2.15.1 Curve fitting and calculation of EC values

Concentration-response curves were generated from the CTB data to determine effective concentration values (EC values). Effective concentrations (EC_x) are concentrations at which (100-x)% viability is reached. For example, EC_{10} is the concentration at which 90% viability is present. For the determination, three models were initially fitted to the data and the most appropriate was selected. After normalization, the EC values were finally calculated.

First, the background signal was subtracted by averaging the fluorescence of wells without cells but with CTB medium mixture and then subtracting this value from all fluorescence values. Fluorescence values of all technical replicates were assigned to the corresponding concentrations and divided by the corresponding averaged control values and multiplied by 100 to obtain percentages. The obtained data were subsequently fitted with three models utilizing the drc-package version 3.0-1 [93]; a four-parameter log-logistic model (4pLL), a Brain-Cousens model (BC) [94], and a flat profile with the following equations:

Equation 2: 4pLL function. The concentration is represented by x, b indicates the slope, c and d denote lower and upper asymptote value, respectively and e > 0 is the inflection point, where the half-maximal effect can be observed.

$$f(x, b, c, d, e) = c + \frac{d - c}{1 + exp(b(log(x) - log\ (e)))}$$

Equation 3: BC function. The parametric function of the Brain-Cousens model differs from the 4pLL-model in the addition of a fifth parameter $f > 0$, that indicates the strength of the hormesis effect. The concentration is represented by x, c and d denote lower and upper asymptote value, respectively and b and $e > 0$ do not have a direct interpretation anymore.

$$f(x, b, c, d, e, f) = c + \frac{d - c + fx}{1 + exp(b(log(x) - log\ (e)))}$$

Equation 4: Flat profile. A flat profile means that no relevant changes in cytotoxicity occurred with respect to the test compound concentrations. In this case a constant, calculated as the mean viability across all concentrations, was fitted to the cytotoxicity data. Here yi denotes the response for a concentration xi and n the number of concentrations.

$$f(x) = \frac{\sum_{i=1}^{n} y_i}{n}$$

For model selection, the Akaike Information Criterion (AIC) [95], an estimator of prediction error, was calculated for each model and the one with the lowest AIC value was selected. The data was then normalized. In the case of the 4pLL function, the data was divided by the value of d (upper asymptote) and multiplied by 100. For the BC function, the left asymptote was used instead of the upper

asymptote, and for the flat profile, the average was set to 100%. The confidence intervals of the EC values were calculated by the delta method [96].

To check how well the fitted model matches the data, a goodness of fit (GoF) was calculated. It should be mentioned that for the flat function the GoF is always = 0 and therefore only for the 4pLL and BC function reasonable GoF can be determined.

Equation 5: Godness of fit.

$$GoF = 1 - \frac{\sum(data\ points - fitted\ curve)^2}{\sum(data\ points - mean\ response)^2}$$

A GoF of 1 indicates a perfect fit. A GoF close to 0 indicates a poor fit. For the EC value determination, only curves with a GoF > 0.55 and a response at the highest tested concentration < 90% were used. If one or both of these criteria were not fulfilled, the EC value was set to > highest concentration tested. Similarly, only EC values that were within the range 0.2 × lowest concentration tested to 5 × highest concentration tested were accepted. Those below or above this range were marked as < lowest concentration tested and > highest concentration tested. A penalty factor of 5 was applied to calculate minimum, median, and maximum. EC values < lowest concentration tested were divided by 5 (0.2 × lowest concentration tested) and > highest concentration tested multiplied by 5 (5 × highest concentration tested). If a donor of cryopreserved human hepatocytes was used twice, both resulting EC values with a weight of 0.5 were used to calculate the minimum, median, and maximum over all donors.

For the CMFDA assay, concentration-response curves were also generated to derive an effective concentration. Since the curve shape was uncertain in comparison to the cytotoxicity, the MCP-Mod (Multiple Comparison Procedure and Modeling), a two-step modeling approach that considers model uncertainty [97], was applied by fitting several candidate models to the data and then determining the most appropriate one. The package DoseFinding version 0.9-17 [98] was used for this purpose.

For this purpose, the averaged background fluorescence for the cell- (well with cells without CMFDA) and the supernatant data (well without cells with CMFDA) was determined and subtracted from the respective fluorescence values. After assigning the corresponding concentrations, the values were divided by the corresponding averaged control values and multiplied by 100 to obtain percentages. Based on MCP, each concentration-response model was evaluated with respect to the compound effect, considering candidate models as illustrated in **Figure 5**. For the set of candidate models, a multivariate two-sided contrast t-test tailored to the shapes of the candidate models was calculated for each concentration-response data set at a family-wise error rate of α = 0.05 to adjust for multiple

testing. Either the test selected one model according to the AIC (in case at least one p-value < 0.05) or, if no model was selected (in case all p-value ≥ 0.05), a flat concentration-response profile was assumed indicated by a horizontal red line as the concentration-response curves. In the Mod-step, the chosen model was fitted to the data.

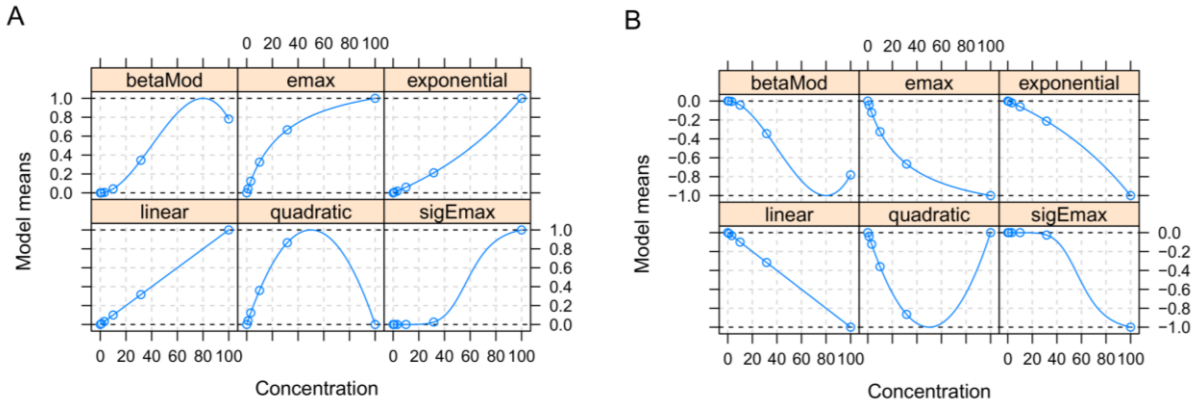

Figure 5: MCP-Mod candidate models. (A) Increasing candidate models and **(B)** decreasing candidate models. The associated functions are given in the Appendix Table 25 (Taken and adapted from [80]).

To compensate for uncertainties and increase sensitivity, the difference between the cell and supernatant data was also calculated. For this purpose two methods were used, in the first one the obtained concentration-response curves of the cell and supernatant data of a compound were subtracted from each other and in the second one the corresponding supernatant raw data were subtracted from the cell raw data and the MCP-Mod procedure was applied again. Consequently, three 'measurements' were generated; (1) cells, (2) supernatant, and (3) difference divided into (3.1) model-difference and (3.2) data-difference (**Figure 6**). The curves were shifted so that at control (concentration 0) they were 100% for (1) and (2) and 0% for (3). EC_x values were calculated as the lowest concentration where the curve attains the response of (100+x)% for (1), (100-x)% for (2), x% for (3). Subsequently, the minimum, median, and maximum for the three donors were determined across all EC_x values. For the cases where no EC_x value could be calculated, the previously mentioned penalty factor was used. In this case, the EC value was set to 5 × highest tested concentration for the calculation. This was used for the analyses where the CMFDA assay was considered alone. When analyzing the combination of CMFDA assay-based EC_x values and CTB assay-based EC_x values, the compound-wise minimum was used and only the CTB assay-based values were replaced by 5 x highest tested concentration in the case of missing values.

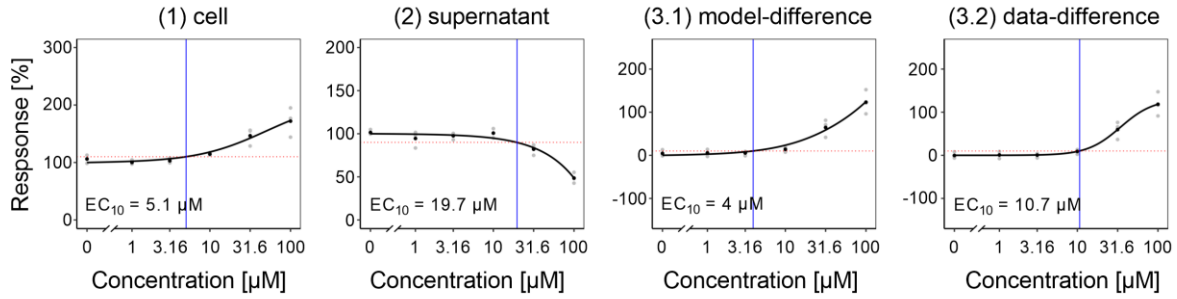

Figure 6: Exemplary curves of the CMFDA assay. Fitted concentration-response curves of the CMFDA assay after 1 hour rifampicin exposure as an example for the different measurements. Black dots represent the mean value of three technical replicates (gray). The intersection of the red and blue lines marks the EC_{10} (Taken from [80]).

Concentration-response curves for the AdipoRed assay were generated using the same principle as for the CMFDA cell data. First, the background fluorescence (well with dye, without cell) was subtracted from the fluorescence values obtained. Then, the AdipoRed signal was divided by the Hoechst signal for normalization. The MCP-Mod procedure was applied to the normalized data. Briefly, several candidate models (**Figure 5**) were fitted to the normalized data and the most appropriate model was selected using the AIC. If no model fitted (in case all p-value ≥ 0.05), a flat concentration-response profile was assumed and plotted as a red line. EC_x values were calculated as the lowest concentration where the curve attains the response of (100+x)%. For the cases where no EC_x value could be calculated, the previously mentioned penalty factor was used. In this case, the EC value was set to 5 × highest tested concentration for the calculation. This was used for the analyses where the AdipoRed assay was considered alone. When analyzing the combination of AdipoRed assay-based EC_x values and CTB assay-based EC_x values, the compound-wise minimum was used and only the CTB assay-based values were replaced by 5 x highest tested concentration in the case of missing values.

2.2.15.2 Calculation of toxicity separation and toxicity estimation index

For quantitative evaluation of the test system, two recently introduced indices were used [79]. The toxicity separation index (TSI) quantifies how well a test method or chosen test parameter differentiates between hepatotoxic and non-hepatotoxic compounds, and the toxicity estimation index (TEI) measures how well hepatotoxic blood concentrations in vivo can be estimated by an in vitro test system [79].

Input data for TSI calculation are the effective concentrations derived by the different in vitro assays (e.g. EC_{10}) and the in vivo modeled blood concentrations (C_{max}) derived from specific human doses. Furthermore, the toxicity status for the specific human dose is needed.

First, the difference is calculated as the ratio between the in vitro concentrations for a given scenario and the in vivo concentrations for each compound on a $\log_{10}$ scale.

Equation 6: Calculation of in vivo in vitro difference. C represents the concentration.

$$\Delta = \log_{10} \frac{C(in\ vivo)}{C(in\ vitro)}$$

Next, the differences (Equation 6) are sorted in ascending order and for each interval between two consecutive differences, a cutoff value (CV) is selected. Furthermore, one cutoff value below the minimal difference and one cutoff value above the maximal difference are chosen. Thus, all possible cutoff values are present in the range of the calculated differences, since all cutoff values in the same interval have the same sensitivity and specificity.

Sensitivity and specificity can then be calculated for each cutoff value by classifying a compound 'toxic' if the difference is greater than the cut of value ($\Delta > CV$) or 'non-toxic' if the difference is equal to or smaller than the cutoff value ($\Delta \leq CV$) and subsequently comparing this classification to the true toxicity status (Equation 7).

Equation 7: Equations to calculate sensitivity and specificity.

$$Sensitivity = \frac{TP}{TP + FN} = \frac{True\ positive}{True\ positive + false\ negative}$$

$$Specificity = \frac{TN}{TN + FP} = \frac{True\ negative}{True\ negative + false\ positive}$$

Finally, the TSI is calculated by plotting 1-specificity against the sensitivity for each cutoff and calculating the area under the ROC curve. For calculations, the R package pROC version 1.13 was used [99]. The TSI ranges from 0.5 to 1, where 1 stands for perfect separation and 0.5 for random distribution of the compounds.

Since the TEI measures how well hepatotoxic blood concentrations in vivo can be estimated only toxic compounds are considered for calculation. Input parameters are the effective concentrations derived by the different in vitro assays (e.g. EC_{10}) and the in vivo modeled blood concentrations (C_{max}) derived from specific human doses.

Equation 8: TEI equation where i=1,…,n represent the compounds in question, x(i) and y(i) the in vitro value and the in vivo value of compound i, respectively, and 1_((condition))(i) the indicator function which takes the value 1 if the condition is fulfilled by the compound i, otherwise 0.

$$TEI = 1 - \frac{1}{5} \frac{\sum_{i=1}^{n} \mathbb{1}_{toxic}(i) \mathbb{1}_{x(i)>y(i)} \left| log_{10} \left(\frac{y(i)}{x(i)} \right) \right|}{\sum_{i=1}^{n} \mathbb{1}_{toxic}(i)}$$

Among the test compounds (i), only those that fulfill the conditions ($\mathbb{1}_{toxic}$) and ($\mathbb{1}_{x(i)>y(i)}$) are included in the calculation; in detail, only hepatotoxic compounds where the in vitro concentration

$(x(i))$ is greater than the in vivo concentration $(y(i))$. For these compounds, the absolute difference of the in vivo and in vitro concentration is calculated ($|\log_{10}(\frac{y(i)}{x(i)})|$). Subsequently, the sum of the differences is calculated and divided by the total number of hepatotoxic compounds. Finally, it is multiplied by a factor of 0.2 and subtracted from 1. As a result, a perfect estimation yields a TEI of 1 and a reduction of the TEI by 0.2 corresponds to an average distance of the compounds from the iso-line by a factor of 10.

2.2.15.3 Calculation of significance

Statistical analyses were performed using GaphPad Prism Version 9 (Graphpad Software, Inc.). Statistical significance was calculated using a one-way ANOVA with post-hoc Dunnett's test for multiple comparison. The number of replicates used is indicates in the figure description.

2.2.16 Physiologically based pharmacokinetic modeling (PBPK)

In order to compare the concentrations generated in vitro with the situation in vivo, blood concentrations were obtained for specific human doses using physiologically based pharmacokinetic (PBPK) modeling.

PBPK modeling involves the generation of compound-specific models that can be used to determine blood concentrations for a given dose. This requires data on both the compound and the organism [100]. The organism's information includes the anatomy and physiology such as the organ volumes, the blood flow rate, and the expression of certain enzymes. For the compound, information about the absorption, distribution, metabolism, and elimination (ADME), as well as its physicochemical properties are required. The ADME data can be determined either by in vitro or in vivo experiments or predicted by a program based on the compound's physicochemical properties.

For each test compound, a PBPK model was constructed as described in Albrecht et al., 2019 [79] using the Simcyp Simulator (commercial software, Version 15, 18, 19; SimCyp, Sheffield, UK). The simulations were done with a virtual population of 100 healthy North European Caucasian subjects, half female, half male, aged 20 – 50. Compound information was taken from the literature or predicted. All treatment regimens of the analyzed compounds and input parameters of the pharmacokinetic simulations are given in the Electronic supplement. Certera UK (Simcyp Division) granted free access to the Simcyp Simulators through an academic license (subject to conditions).

The simulations were performed by Dr. Iain Gardner and Dr. Mian Zhang from Certara UK (Simcyp Division) and Dr. Wiebke Albrecht from the IfADo.

3 Results

3.1 Bile acid mix assay

Inhibition of export carriers in hepatocytes is one mechanism by which drugs can damage the liver. In addition, higher intracellular bile acid concentrations are observed in vivo compared to in vitro, which may have an impact on cytotoxicity. As an addition to the in vitro test battery of the presented test system (1.4), a concept was elaborated to detect this mechanism in vitro and thus drugs that inhibit bile acid export carriers or the bile acid transport. This concept resulted in the bile acid mix assay.

3.1.1 Concept of the bile acid mix assay

In vivo (**Figure 7**, *top row*), bile acids are absorbed from the intestine and transported to the liver via the portal vein. Here they are taken up into the cell via the carriers NTCP and OATP. In addition, bile acids are also synthesized intracellularly via cholesterol, but this contributes only a smaller amount of bile acids per time unit. After uptake into hepatocytes, bile acids are secreted into the bile canaliculi primarily by the bile acid carriers BSEP and MRP2. When the export of these carriers is inhibited, intracellular bile acid concentrations increase and may exceed cytotoxic thresholds. Under standard in vitro conditions (**Figure 7**, *middle row*), intracellular bile acid concentrations usually do not reach cytotoxic levels because the culture medium does not contain bile acids and the rate of synthesis in hepatocytes is low. To simulate the in vivo situation and to investigate the cytotoxicity of compounds that inhibit bile acid transport or the corresponding export carriers, bile acids were added to the culture medium in vitro (**Figure 7**, *bottom row*).

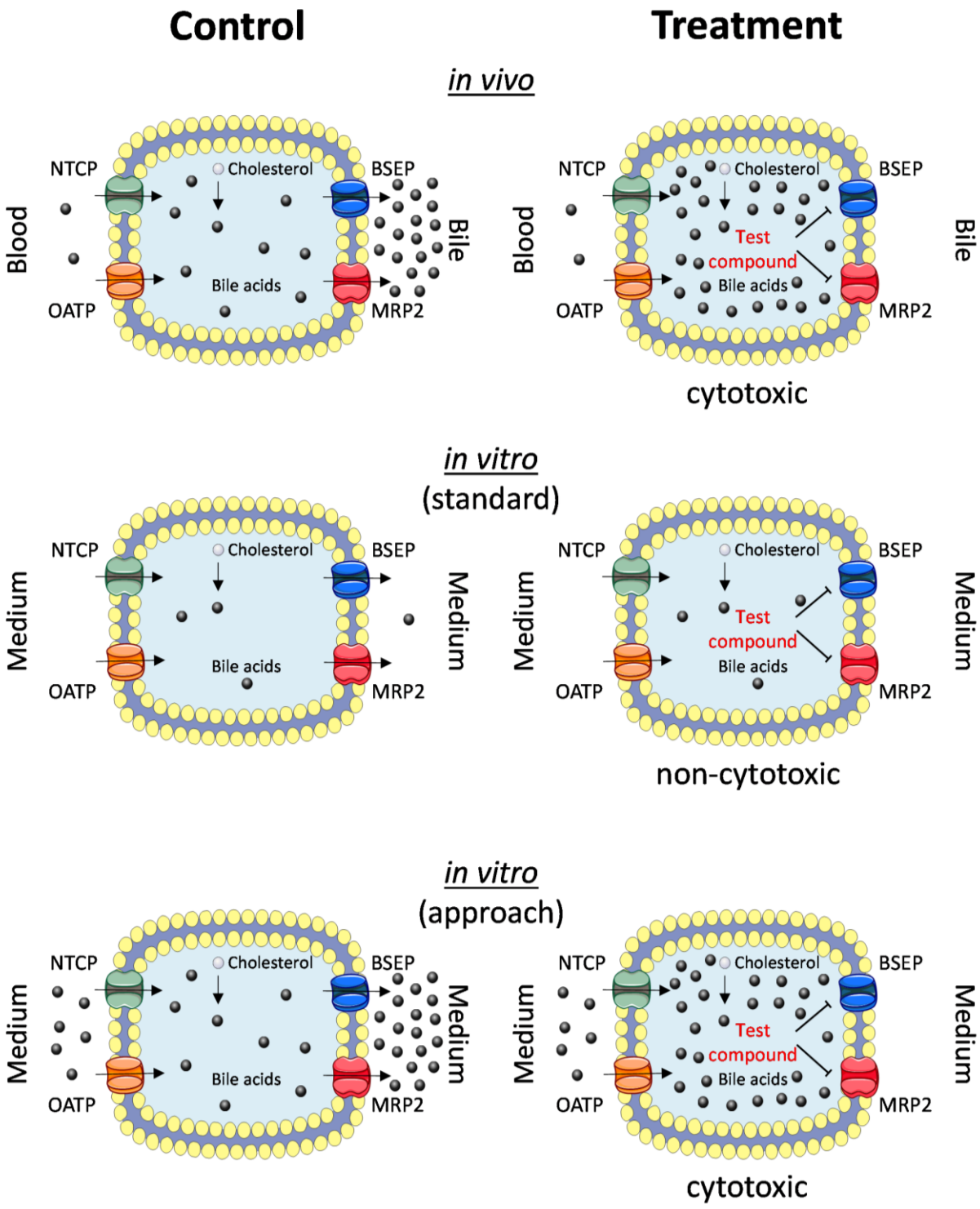

Figure 7: Concept of bile acid induced cytotoxicity in vivo and in vitro due to the inhibition of bile acid export inhibitors. NTCP = Na+-taurocholate cotransporting polypeptide, OATP = Organic anion transporting polypeptide, BSEP = Bile salt export pump, MRP2 = Multidrug resistance-associated protein 2. Graphical elements were taken from Servier Medical Art by Servier.

3.1.2 Cytotoxicity of bile acids in primary human hepatocytes

Cytotoxic bile acid concentrations were first determined in cultured PHH to identify concentrations where cytotoxicity was not yet evident, for example slightly below or at the onset of cytotoxicity, e.g. 50% of the EC_{10}. This was necessary since a relatively small increase in intracellular bile acid concentration due to the inhibition of bile acid carriers by a test compound may then exceed cytotoxic thresholds leading to cell death.

For this purpose, PHH were incubated with a physiologically relevant bile acid mix (BAM) consisting of the five most common bile acids in a ratio that is present in human bile. The bile acid mix consisted of 46.5% glycochenodeoxycholic acid (GCDCA), 14.1% deoxycholic acid (DCA), 13.7% chenodeoxycholic acid (CDCA), 13.4% glycodeoxycholic acid (GDCA), and 12.3% glycocholic acid (GCA). Primary human hepatocytes were exposed to the mix for 48 hours and viability was determined using a CellTiter-Blue assay.

The cytotoxicity test in primary human hepatocytes from four different donors revealed beginning cytotoxicity (EC_{10}) of the bile acid mix at 0.91 – 1.08 mM and almost complete cell death (EC_{90}) at 1.20 – 1.61 mM (**Figure 8**). Based on this observation 0.5 mM was determined as the appropriate bile acid concentration in the culture medium during exposure to the test compound since cytotoxicity was not yet evident, but a relatively small increase in bile acids due to inhibition of bile acid carriers would induce cell death.

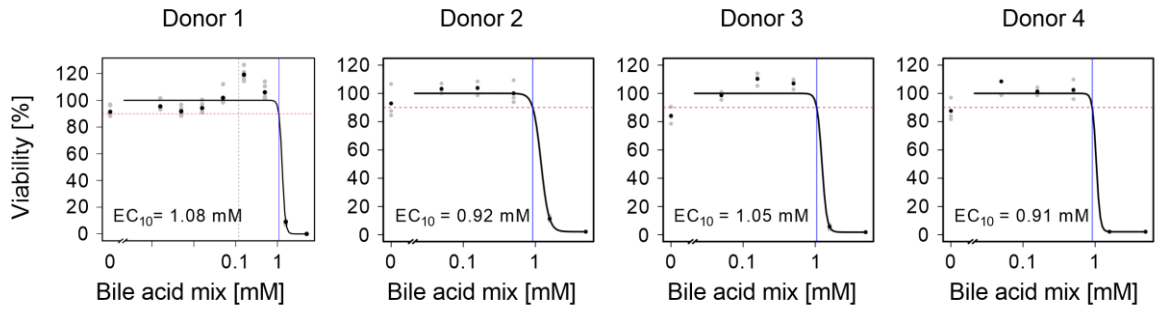

Figure 8: Cytotoxicity test with cultivated human hepatocytes with the addition of a bile acid mix. Primary human hepatocytes were cultured on collagen and exposed for 48 hours to increasing concentrations of the bile acid mix. Grey dots represent technical replicates and black dots the mean. The red and blue lines indicate the EC_{10} and the dotted grey line the confidence interval of the EC_{10}.

3.1.3 Influence of bile acids on the cytotoxicity of test compounds

After the determination of an appropriate bile acid concentration, the next step was to investigate whether the addition of 0.5 mM bile acid mix to the culture medium of PHH would increase the cytotoxicity of the test compounds. Since we have shown that 48 hours incubation time was adequate

for separation of non-hepatotoxic and hepatotoxic compounds based on cytotoxicity [79], this incubation period was also used for the bile acid mix assay. To ensure that the bile acid carriers are successfully inhibited before being exposed to the BAM, a protocol was used where bile acids were added 2 hours after the test compounds, followed by cytotoxicity measurement (**Figure 9**). As a control, cells were exposed to the test compound for 48 hours without the addition of the bile acid mix. Subsequently, the CTB assay was performed. The whole approach was applied to a set of test compounds consisting of 18 compounds with known hepatotoxicity status for specific human doses (**Table 17**). For two compounds (acetaminophen and ethanol) a hepatotoxic and a non-hepatotoxic scenario was available.

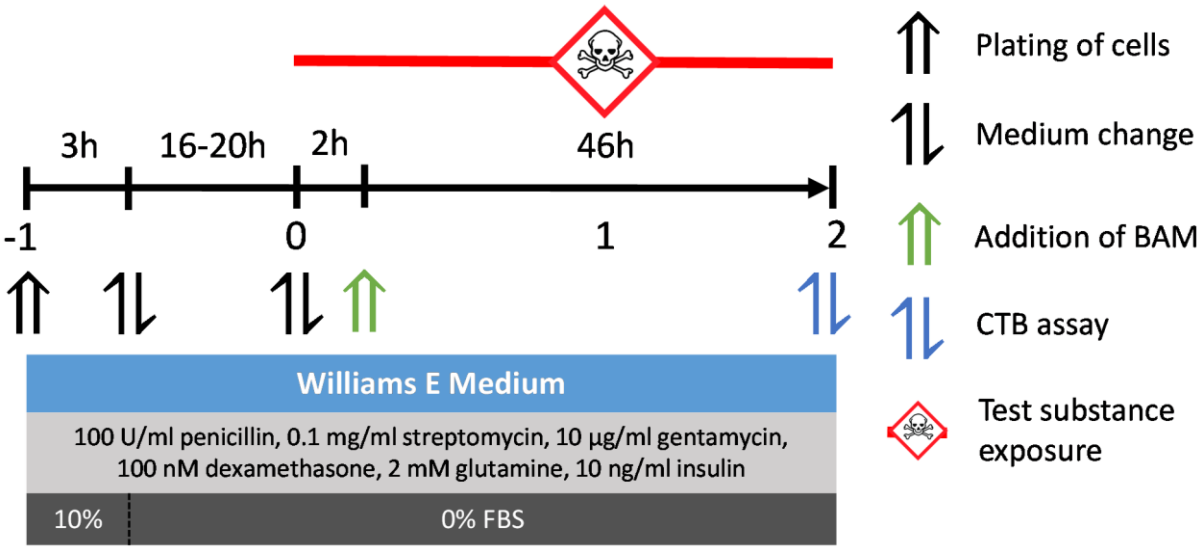

Figure 9: Experimental schedule of the cytotoxicity test with and without the addition of a bile acid mix. BAM = Bile acid mix; CTB = CellTiter-Blue; FBS = Fetal bovine serum.

The cytotoxicity data shows different effects of the bile acid mix on the cytotoxicity of the test compounds. Both, increased and decreased cytotoxicity were observed, which is illustrated by the example of two test compounds (**Figure 10**). For promethazine there was no bile acid induced cytotoxicity observed with EC_{10} values of 0.014; 0.027 and 0.005 mM for three donors without bile acid mix and 0.023; 0.027 and 0.002 mM with additional bile acid exposure, respectively. For cyclosporin A increased cytotoxicity was observed for all three donors, whereby EC_{10} values decreased from 0.013; 0.016 and 0.019 mM to 0.003; 0.008 and 0.007 mM with BAM exposure, respectively (**Figure 10**). In summary, a protocol was established that allows the analysis, if addition of a bile acid mix to the cell culture medium enhances the cytotoxicity of individual test compounds.

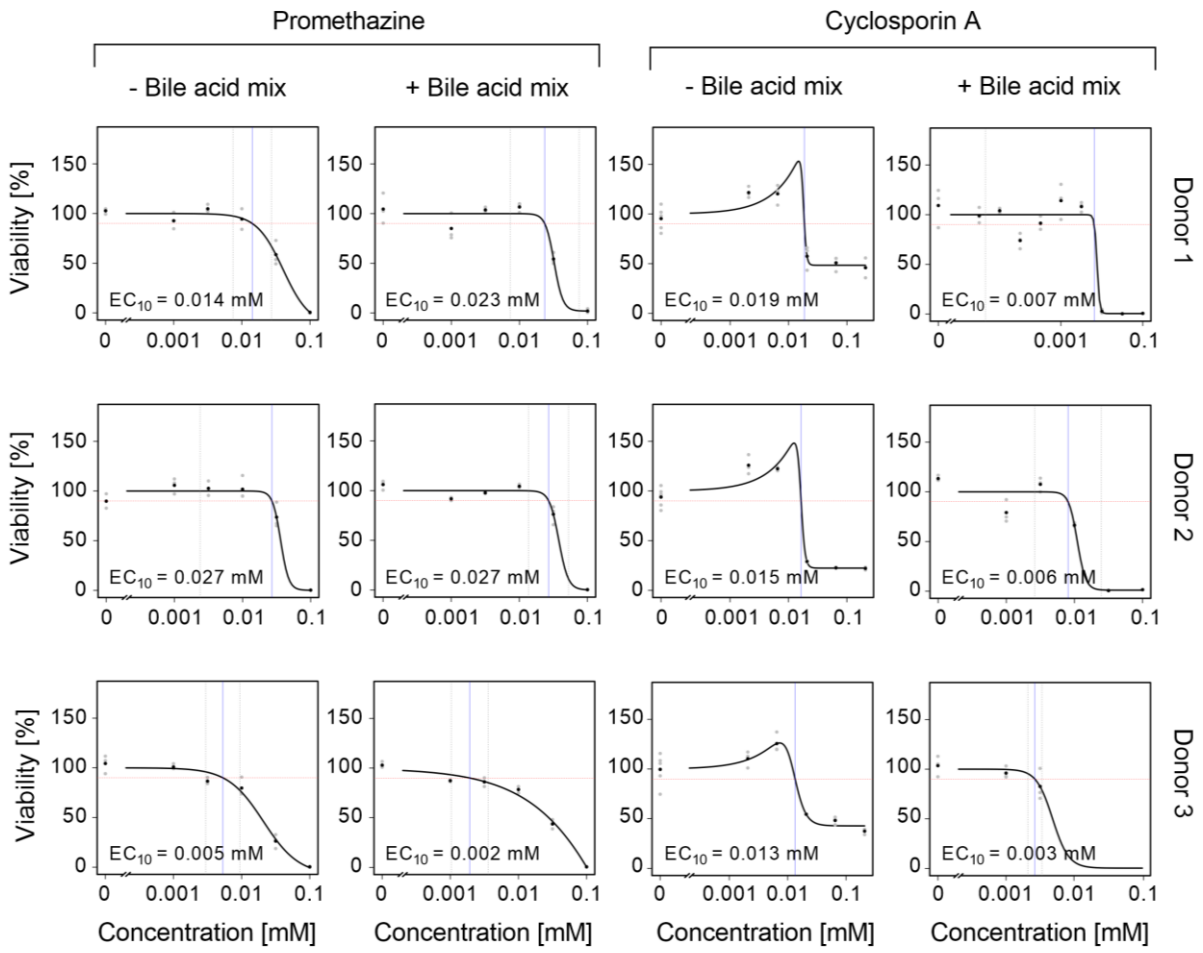

Figure 10: Exemplary curves of the cytotoxicity test with and without the addition of a bile acid mix. Examples of concentration-response curves obtained from primary human hepatocytes incubated with promethazine and cyclosporine A without and with addition of the bile acid mix. Grey dots represent technical replicates and black dots the mean. The red and blue lines indicate the EC_{10} and the grey lines the confidence interval of the EC_{10}.

Table 17: Summary of the results of the cytotoxicity test with and without bile acid mix and pharmacokinetic modeling of the test compounds. Minimum, median, and maximum values were calculated from experiments with hepatocytes from at least three different human donors. All generated data including the raw data can be found in the Electronic supplement. Inhibition of hepatocellular carriers was indicated as "yes" if documented in at least one previous study together with an IC_{50}-value. "#" indicates that contradicting information has been reported, "N/A" indicates that no information could be identified. The in vivo concentration is the 95% percentile of the peak total systemic blood concentration modeled for a specific dose.

Compound	Abbre-viation	Hepato-toxicity reported	In vivo C_{max} whole blood 95% total [mM]	In vitro cyto-toxicity -BAM EC_{10} [mM] median [min/max]	In vitro cyto-toxicity +BAM EC_{10} [mM] median [min/max]	Inhibition of hepato-cellular export [BSEP/MRP2]	
Acetaminophen	APAP	no/ yes	1.09×10^{-1} $1.21\times10^{+0}$	1.403 [0.500/2.833]	2.398 [0.826/3.596]	no	no
Aspirin	ASP	yes	2.4×10^{-1}	2.004 [0.335/4.179]	2.122 [0.843/3.209]	no	no
Atorvastatin	AVS	yes	1.5×10^{-5}	0.138 [0.064/0.208]	0.076 [0.068/0.148]	yes	yes

Compound	Abbre-viation	Hepato-toxicity reported	In vivo C_{max} whole blood 95% total [mM]	In vitro cyto-toxicity -BAM EC_{10} [mM] median [min/max]	In vitro cyto-toxicity +BAM EC_{10} [mM] median [min/max]	Inhibition of hepato-cellular export [BSEP/MRP2]	
Chlorpheniramine	CHL	no	6.49×10^{-5}	0.044 [0.014/0.155]	0.024 [0.024/>0.316]	no	no
Clonidine	CLON	no	9.4×10^{-6}	0.317 [0.0.057/ 0.555]	0.082 [0.066/ 0.911]	no	N/A
Cyclosporin A	CSA	yes	7.34×10^{-3}	0.014 [0.008/0.031]	0.007 [0.003/0.008]	yes	yes
Ethanol	ETOH	no/ yes	5.76×10^{-3} $1.01\times10^{+1}$	10.218 [2.050/ 170.502]	>1000 [>1000/ >1000]	N/A	N/A
Glucose	GLC	no	$7.15\times10^{+0}$	119.713 [71.940/ >316]	63.808 [21.775/ 95.325]	N/A	N/A
Ketoconazole	KC	yes	1.62×10^{-2}	0.026 [0.008/0.100]	0.013 [0.009/0.023]	yes	no
Lovastatin	LO	yes	8.48×10^{-6}	>0.245 [0.024/ >0.245]	>0.245 [>0.245/ >0.245]	yes	yes
Melatonin	MEL	no	2.7×10^{-5}	0.687 [0.040/>5]	0.795 [0.029/1.207]	no	no
Promethazine	PMZ	no	3.72×10^{-5}	0.014 [0.004/0.032]	0.023 [0.002/0.027]	no	no
Propranolol	PPL	no	2.2×10^{-4}	0.021 [0.003/0.080]	0.025 [0.004/0.033]	no	no
Rifampicin	RIF	yes	2.01×10^{-2}	0.262 [0.121/0.424]	0.053 [0.049/0.146]	yes	yes
Triclosan	TSN	no	2.6×10^{-4}	0.136 [0.047/0.250]	0.107 [0.052/0.107]	N/A	N/A
Troglitazone	TROG	yes	2.21×10^{-3}	0.011 [0.009/0.022]	0.017 [0.010/0.020]	yes	yes#
Valproic acid	VPA	yes	5.69×10^{-1}	10.134 [8.462/22.132]	10.006 [3.202/12.068]	no	no
Vitamin C	VITC	no	6.98×10^{-3}	3.701 [0.282/>10]	3.005 [1.546/>10]	no	no

3.1.4 Evaluation of the bile acid mix assay

Finally, we studied if the addition of the bile acid mix to hepatocytes improves the separation of hepatotoxic and non-hepatotoxic compounds and the estimation of hepatotoxic blood concentrations. For this purpose, the toxicity separation index (TSI) and the toxicity estimation index (TEI) were used. These indices were calculated based on the C_{max} (whole blood concentration; total – free and protein

bound –concentration, 95% percentile) as in vivo value and the EC_{10} (median) as in vitro value (**Table 17**).

Cytotoxicity of hepatocytes without the addition of the bile acid mix led to a TSI of 0.79 and a TEI of 0.73 for the analyzed set of test compounds (**Table 18**A). The addition of the bile acid mix decreased the indices slightly to 0.77 and 0.69 for TSI and TEI, respectively. In addition to the individual analysis, a combination of both approaches was also evaluated as it might show a beneficial effect. A combination was achieved by using the lower EC_{10} median value from both approaches for each compound which resulted in a slightly increased TSI of 0.80 and TEI of 0.76. In order to visualize the results, in vitro-in vivo plots were generated using the approach with and without bile acid mix, either alone or as a combination of both (**Figure 11**A, B, C).

In previous studies, the EC_{10} (median) was used because it allowed the best separation of hepatotoxic and non-hepatotoxic compounds based on cytotoxicity. To verify whether another parameter would give better results for this study, a comprehensive TSI and TEI analysis was performed with all cut-offs (EC_{10}-EC_{90}) and measures (minimum, median, and maximum). For the cytotoxicity test without bile acid mix, the best parameter was the EC_{60} minimum with a TSI of 0.86 and TEI of 0.69 (**Table 18**B). Compared to this, the best parameter (EC_{60} maximum) for the approach with bile acid mix performed slightly worse with 0.84 and 0.63 for TSI and TEI, respectively. The highest TSI (0.86) and TEI (0.76) for the combination of both assays were reached by using the EC_{40} and EC_{30} minimum from the approach without and with bile acid mix, respectively. In conclusion, only minor differences for the separation of hepatotoxic and non-hepatotoxic compounds were obtained between the two approaches with and without the addition of a bile acid mix for cytotoxicity testing.

Table 18: Toxicity separation index (TSI) and toxicity estimation index (TEI) for the cytotoxicity assay with and without bile acid mix alone and in combination.

A TSI and TEI based on the EC_{10} values of both approaches

Approach	EC value	Classification	TSI	TEI
Without bile acid mix	EC_{10}	median	0.79	0.73
With bile acid mix	EC_{10}	median	0.77	0.69
Combination	EC_{10}	median	0.80	0.76

B TSI and TEI for all possible parameter combinations considering EC_{10}, EC_{20}, …, EC_{90} as well as median, minimum and maximum values. The parameters resulting in the highest TSI are given for both approaches alone and in combination.

Approach	EC value	Classification	TSI	TEI
Without bile acid mix	EC_{60}	minimum	0.86	0.69
With bile acid mix	EC_{60}	maximum	0.84	0.63
Combination [without/with]	[EC_{40}/EC_{30}]	minimum	0.86	0.76

Results

To obtain an overview of the influence of the bile acid mix on cytotoxicity of the test compounds, the donor-specific ratios of the EC_{10} values (median) without and with bile acids (log_2 ratios) were calculated (**Figure 11**D). Log_2 ratios higher than zero indicate that the susceptibility of the hepatocytes was increased by the addition of the bile acid mix, while values lower than zero indicate increased resistance. For ten compounds the ratio was higher than zero of which only five were hepatotoxic compounds known to inhibit canalicular export. Whereas five compounds had a calculated log_2 ratio smaller than zero. For ethanol, lovastatin, and vitamin C no ratio could be calculated as no cytotoxicity was reached up to the highest test concentration in at least two donors. In conclusion, the results demonstrate that the co-exposure of cultivated hepatocytes to test compounds and to a bile acid mix did not improve the separation of hepatotoxic and non-hepatotoxic compounds, because the susceptibility increased for both hepatotoxic as well as some non-hepatotoxic compounds. Furthermore, the influence of the bile acid mix appears to be complex, because it also decreased susceptibility to some known hepatotoxic compounds.

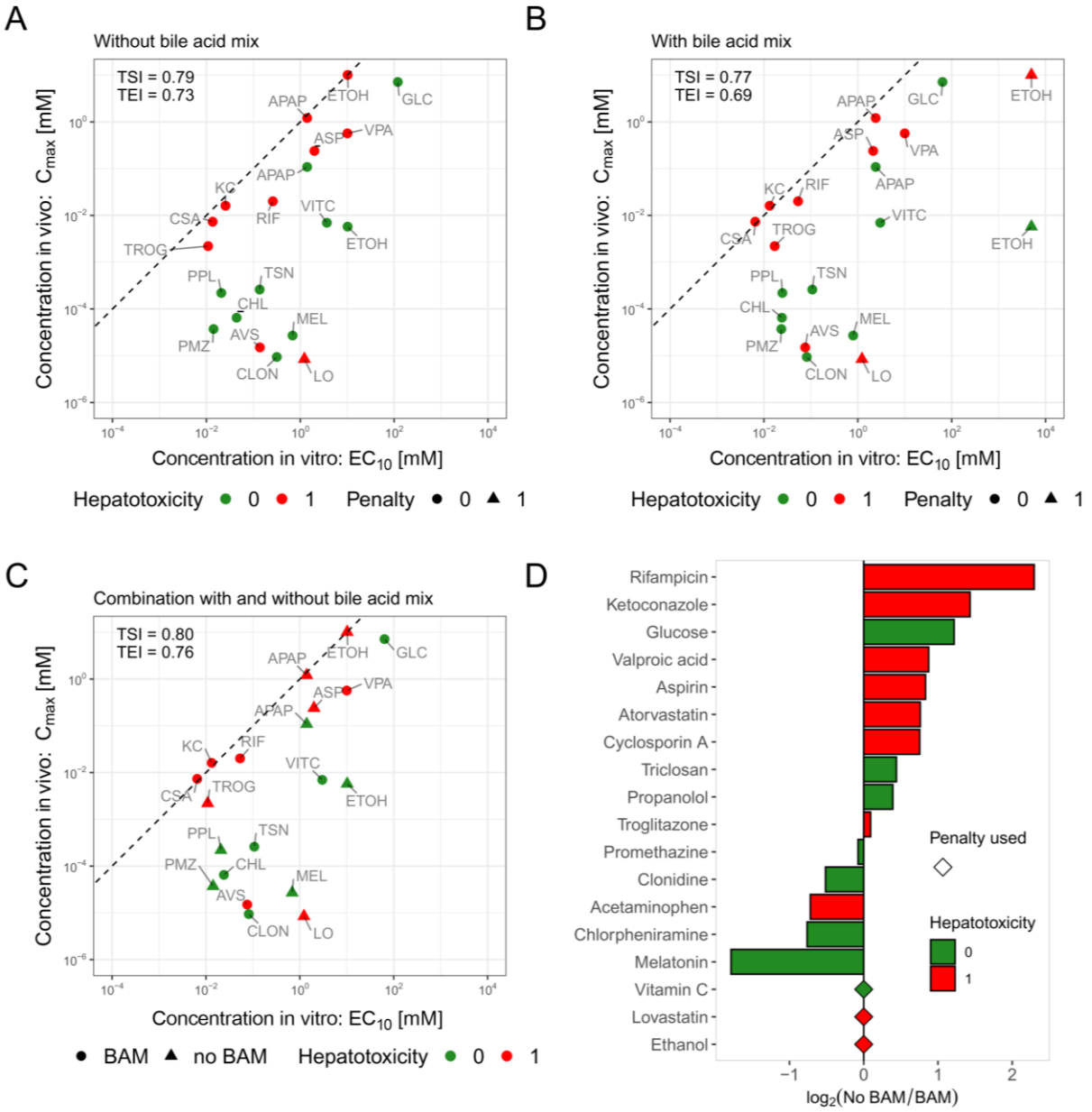

Figure 11: In vitro–in vivo plots of the BAM assay. (A) In vitro-in vivo plot of the C_{max} (whole blood, total concentration, 95% percentile) and the EC_{10} median of compound exposure without the bile acid mix. **(B)** in vitro-in vivo plot of the C_{max} (whole blood, total concentration, 95% percentile) and the EC_{10} median of compound exposure with bile acid mix. **(C)** in vitro-in vivo plot of the C_{max} and the EC_{10} median of the combination of both approaches. **(D)** Donor-specific log_2 ratio plot comparing cytotoxicity with and without bile acid mix. For the calculation, EC_{10} median values were used and a diamond indicates when this value was not reached up to the highest tested concentration in at least 2 donors of one approach.

3.2 CMFDA assay

Since the bile acid mix assay was not a suitable candidate for the in vitro battery, a new concept was developed to detect export carrier inhibiting compounds. This concept resulted in the so-called CMFDA assay.

3.2.1 Concept of the CMFDA assay

In the following, a schematic illustration of the principle of the CMFDA assay is given. In this assay, primary human hepatocytes are incubated with the membrane-permeable, non-fluorescent compound, 5-chloromethylfluorescein diacetate (CMFDA), which is catalyzed to fluorescent 5-chloromethylfluorescein (5-CMF) upon entering the cell by non-specific cytosolic esterases. Importantly, 5-CMF is unable to cross the cell membrane, but instead can be actively exported by membrane transporters, such as BSEP and MRP2, either on its own or conjugated to glutathione (GSH) [101]. Consequently, the CMFDA assay can be used to investigate export inhibition by test compounds by detecting the delayed clearance of 5-CMF-associated green fluorescence from hepatocytes, or the delayed increase in fluorescence in the culture medium.

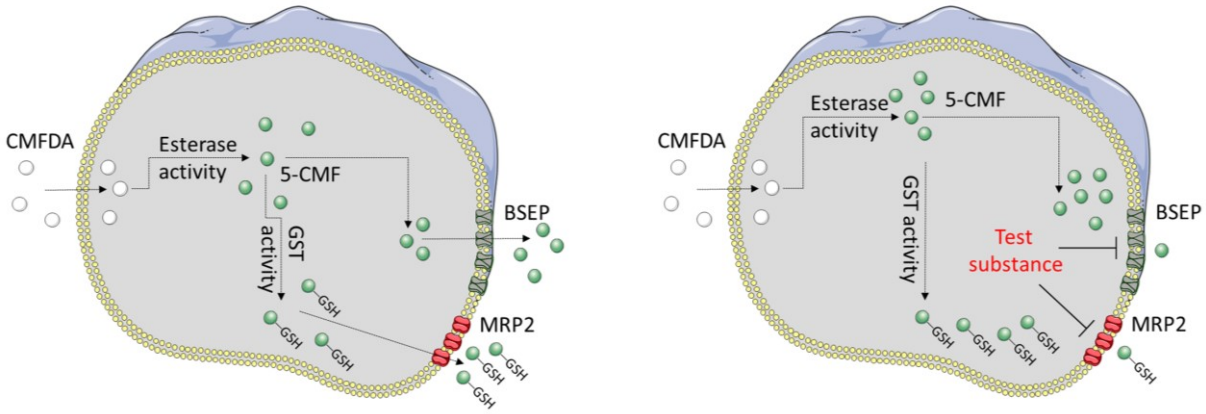

Figure 12: Principle of the CMFDA assay. 5-chloromethylfluorescein (CMFDA) freely passes through cell membranes into the cytoplasm, where it is transformed to the highly fluorescent 5-chloromethylfluorescein (5-CMF) by esterases. 5-CMF is actively exported by the bile salt export pump (BSEP) or multidrug resistance-associated protein 2 (MRP2) either as parent compound or after conjugation with glutathione (GSH). Therefore, inhibitors of BSEP or MRP2 increase intracellular fluorescence while extracellular concentrations of 5-CMF or its GSH conjugate decrease. Graphical elements were taken from Servier Medical Art by Servier. (Taken from [80]).

3.2.2 CMFDA kinetics in vivo (mouse)

First, the question arose which cultivation format is suitable to investigate 5-CMF secretion, as there are several different techniques for cultivating cells, especially primary hepatocytes, with advantages and disadvantages. Hepatocytes can be cultivated for example as three-dimensional spherical cellular aggregates, further named spheroid cultures, or as sheets of cells that can either be cultivated between two layers of collagen (sandwich culture) or on a collagen-coated dish, further referred to as monolayer. Since previous studies recommended the use of spheroids for in vitro tests due to their higher complexity and possible longer cultivation times, our first aim was to clarify if spheroid or sandwich cultures are more suited for the CMFDA assay. To investigate whether in vivo relevant

mechanisms are captured in the CMFDA assay and which culture format is most suitable for the primary human hepatocytes, we wanted to compare 5-CMF secretion in vitro to in vivo. Due to the limitations of live imaging in humans, we used intravital imaging in mice and compared the 5-CMF secretion results to the results of isolated mouse hepatocytes cultivated in spheroid and sandwich format. To analyze hepatocyte secretion of 5-CMF in vivo, we applied a previously established two-photon microscopy technique in anesthetized mice [102], [103] using the mT/mG mouse strain which has red fluorescence on all cell membranes due to a membrane-targeted tandem dimer tomato sequence [102]. After injection of CMFDA into the tail vein, 5-CMF-associated green fluorescence transiently increased in hepatocytes, followed by accumulation in bile canaliculi. Intracellular fluorescence increased rapidly during the first 10 minutes and decreased consistently thereafter. In the bile canaliculi, the maximum fluorescence was much higher, as expected, and reached its peak after about 12 minutes (**Figure 13**).

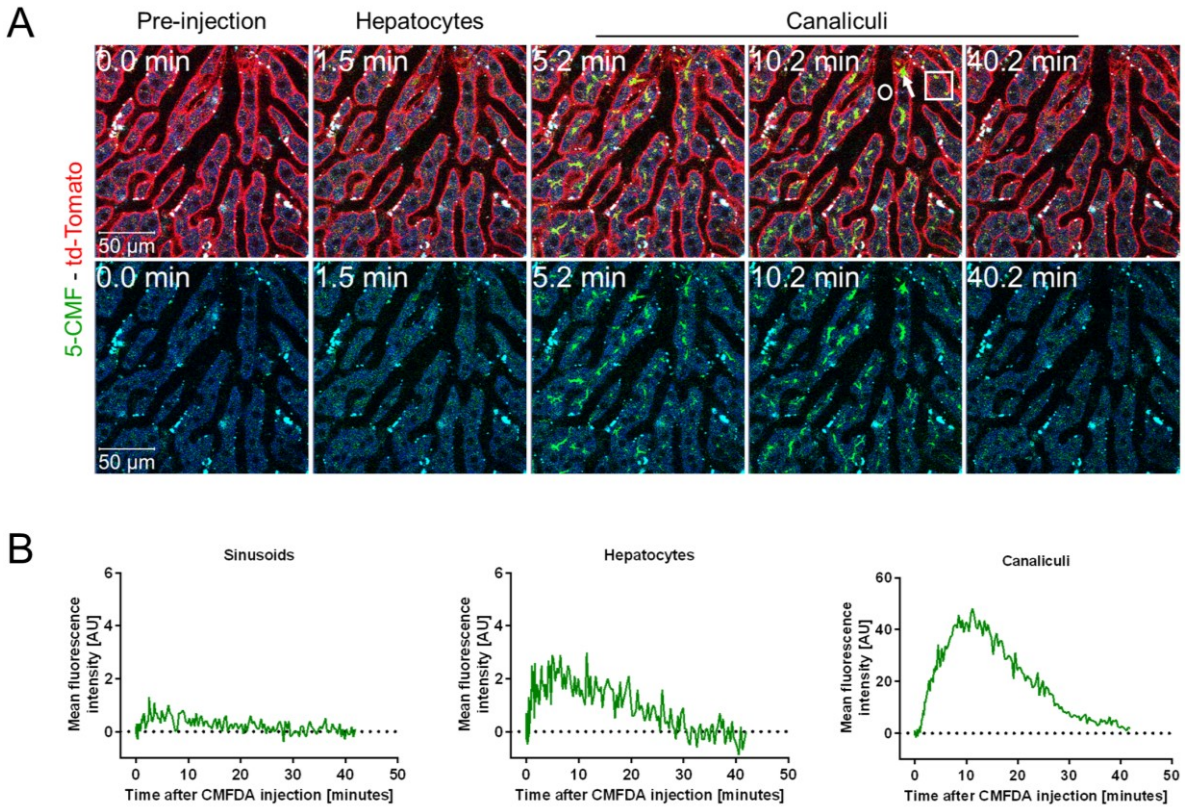

Figure 13: Intravital imaging of the mouse liver after CMFDA injection. (A) Stills of intravital two-photon imaging of 5-CMF secretion by mouse hepatocytes into bile canaliculi after tail vein injection of CMFDA. Green fluorescence occurs initially in the cytoplasm of hepatocytes and subsequently is enriched in bile canaliculi. **(B)** Quantification of 5-CMF associated fluorescence in the indicated regions of interest. Circle: sinusoid; square: hepatocyte; arrow: bile canaliculus. Time after injection of CMFDA is given in the upper left corner of the panels. Td-tomato: membrane targeted tandem dimer tomato sequence that expresses red fluorescence on the cell membrane. The upper panel shows the merged image of the td-tomato (red) and the 5-CMF (green) associated fluorescence, the lower panel only the green signal of 5-CMF. (Taken from [80]).

3.2.3 CMFDA kinetics in primary mouse hepatocytes

Next, we performed the in vitro experiments, for which we used hepatocytes from the same mT/mG mouse strain, which allowed us to directly compare the 5-CMF export to that observed in vivo.

Hepatocyte spheroids showed an increase in fluorescence (**Figure 14**A, B) followed by canalicular secretion (**Figure 14**C). However, hepatocytes at the margin of the spheroid showed a much stronger 5-CMF associated signal than cells at the center of the spheroid. Quantification of the time-fluorescence profile of 13 hepatocytes along the diameter of the spheroid demonstrated a large heterogeneity among hepatocytes (**Figure 14**B), which hampers the establishment of a quantitative assay.

In contrast, 5-CMF associated fluorescence was homogeneous among all 19 hepatocytes quantified in hepatocytes that were cultivated in a sandwich format as one cell layer between two layers of collagen (**Figure 14**D). Interestingly, adding CMFDA four times to the culture medium still led to a similar transient increase in green fluorescence in hepatocytes, supporting the suitability of this model for the export assay. In addition, excretion of 5-CMF occurred faster in the sandwich culture compared to the spheroid culture. Since homogeneity among hepatocytes is important for the establishment of automated quantification, and considering that in vivo hepatocytes are organized in sheets that rather resemble layers than spheroids along the blood sinusoids (**Figure 13**A), we conducted all further experiments using hepatocytes cultivated as sheets, i.e. as sandwich or monolayer cultures.

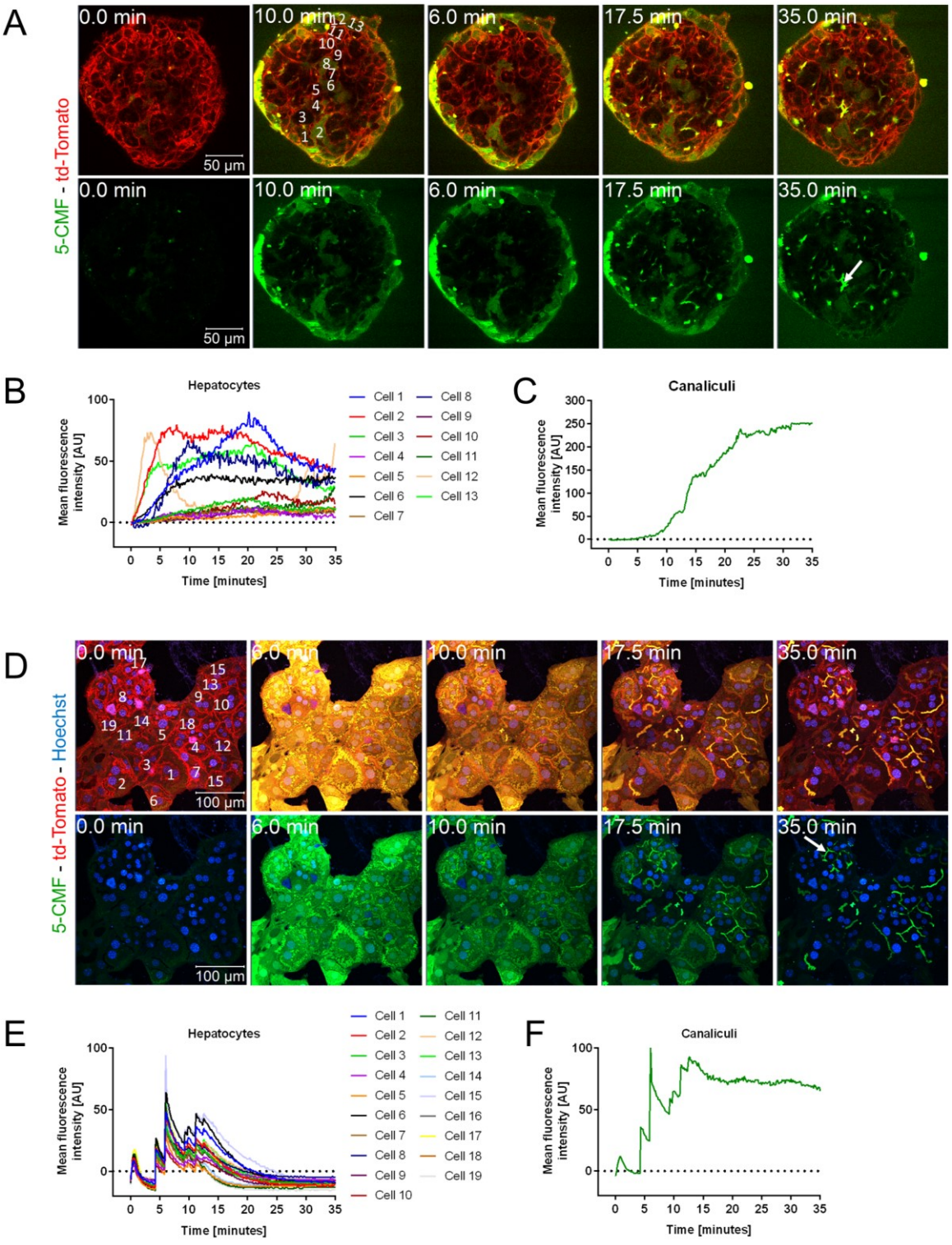

Figure 14: Export of 5-CMF from cultivated mouse hepatocytes. (A-C) Spheroid cultures. (D-F) Sandwich cultures. **(A)** Stills from an intravital video. The upper panel shows merged red and green fluorescence, the lower panel only the green signal. Time after the addition of CMFDA is given in the upper left corner. The numbers in the spheroid (top panel, 2nd from left) indicate the regions of interest, where green fluorescence was quantified. **(B)** Quantification of green fluorescence in the cells indicated by the numbers in A. **(C)** Quantification of green fluorescence in the bile canaliculus indicated by the arrow in A (bottom right panel). **(D)** Stills from a sandwich culture after repeated addition of CMFDA (four times) to the culture medium. The numbers indicate regions of interest, where green fluorescence was quantified. **(E)** Quantification in hepatocytes and **(F)** a bile canaliculus. (Taken from [80]).

3.2.4 CMFDA kinetics in primary human hepatocytes

After the in vivo in vitro comparison in mice showed that the cultivation of cells in a sheet format is more appropriate for the CMFDA assay, 5-CMF secretion in both sheet formats (monolayer and sandwich) was tested with primary human hepatocytes. The monolayer format, in which the hepatocytes attach to collagen-coated plates, is easy to handle, whereas the sandwich format, in which the hepatocytes are cultured between two layers of collagen, is more complex and, for example, favors the formation of bile canaliculi.

To compare the excretion kinetics of 5-CMF, cryopreserved human hepatocytes were incubated with CMFDA one day after seeding. Following the addition of CMFDA to the culture medium, the 5-CMF associated signal showed a transient increase in the cytoplasm of the hepatocytes for both monolayer and sandwich (**Figure 15**A). For the monolayer, an increase in intracellular fluorescence was observed immediately after the addition of CMFDA, followed by a decrease in intracellular fluorescence. The fluorescence in the bile canaliculi-like structures remained detectable until the end of the imaging period (60 minutes). In contrast, it took 15 minutes before the maximum intracellular intensity was observed in the sandwich culture. A possible explanation for this may be the delayed passage of the CMFDA to the hepatocytes caused by the upper collagen layer. Nevertheless, the canaliculi were already visible at 5 minutes, most likely due to the high affinity of export carriers to 5-CMF that facilitated its enrichment in the canaliculi at already low intracellular concentrations which were present 5 minutes after the addition of CMFDA.

Quantification of cytoplasmic fluorescence over time confirmed that both the increase and decrease of cytoplasmic 5-CMF-associated fluorescence occurred earlier in monolayer than in sandwich culture (**Figure 15**B). Moreover, the half-life of 5-CMF was shorter in ML (8 minutes) compared to SC (16 minutes). Thus, although both sandwich culture and monolayer successfully cleared 5-CMF from hepatocytes, supporting their suitability for the export inhibition assay, we nevertheless selected the monolayer culture for subsequent studies, primarily because they are easier to handle and standardize. A major challenge faced with using sandwich culture is the layer of collagen on top of the hepatocytes that influences clearance kinetics. Consequently, it is not sufficient to only standardize its thickness, but also to control the individual collagen gel batches with respect to their capacity to bind CMFDA and 5-CMF.

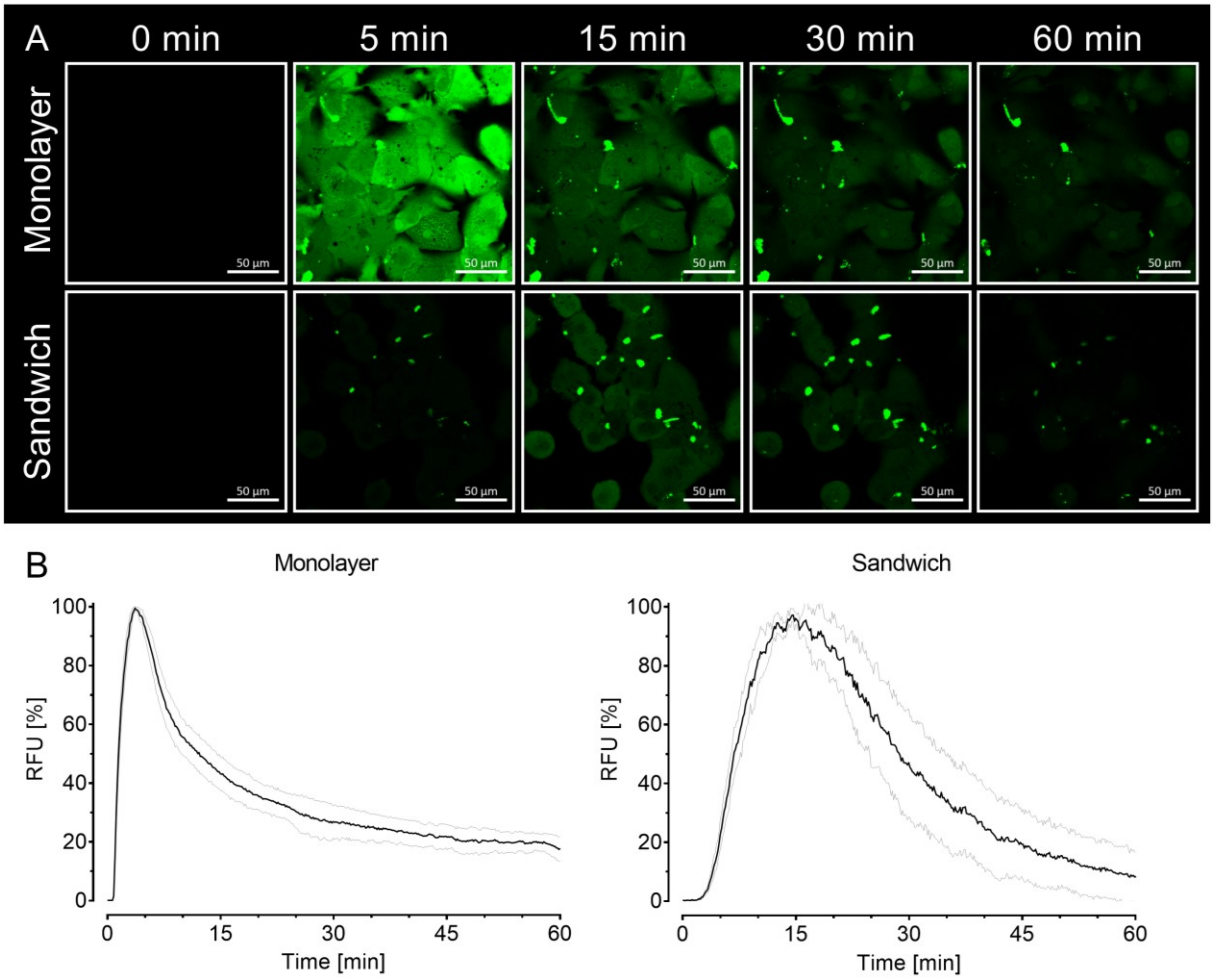

Figure 15: Optimization of the CMFDA assay in human hepatocytes. (A) Human hepatocytes cultivated as collagen sandwiches or monolayer cultures in the presence of CMFDA. Scale bar: 50 µm. **(B)** Fluorescence (excitation: 488 nm; emission band: 503-558 nm) in sandwich culture and monolayer were detected by laser scanning microscopy (LSM880). The three lines of the plots represent mean values and standard deviations of 5 regions of interest from each condition. Maximum fluorescence was set as 100% for each condition. (Taken from [80]).

Since the assay was intended for a 96-well format using fluorescence measured with a spectrophotometer as the quantifiable endpoint, we next studied the reproducibility of the assay using hepatocytes from three donors plated in collagen-coated 96-well plates. Measurement with the spectrophotometer lead to a peak of intracellular fluorescence at approximately 10 minutes after the addition of CMFDA followed by a decrease with relatively small inter-individual differences (**Figure 16**). Since the degree of clearance obtained with the 96-well fluorescence reader was similar to that observed with the confocal microscope, and the results were reproducible among the different donors, subsequent experiments were performed using the 96-well format.

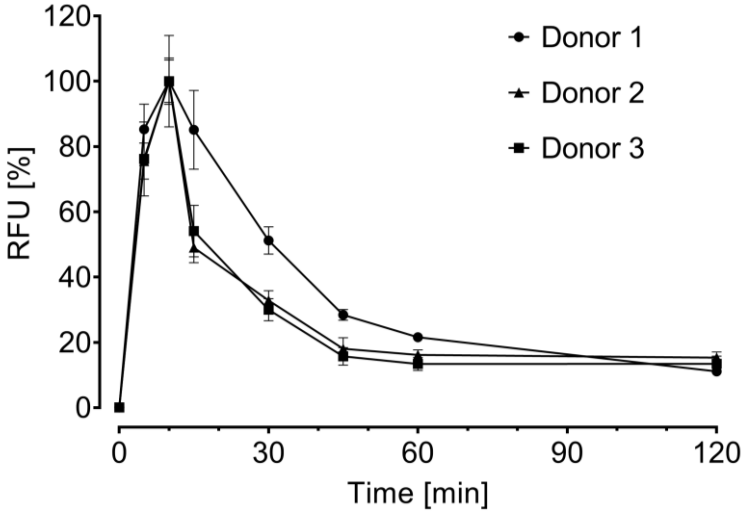

Figure 16: Intracellular fluorescence of primary human hepatocytes cultured in collagen-coated 96-well plates from three donors after addition of CMFDA to the culture medium detected with a spectrophotometer. (Excitation: 485; emission: 520). Data is expressed as mean±SD with 6 technical replicates per donor. Maximum fluorescence was set as 100% for each donor individually. (Taken from [80]).

3.2.5 Transport carrier expression in primary human hepatocytes

Since previous studies with rodent hepatocytes showed a rapid loss of export carriers in monolayer culture [104], [105], we investigated the gene expression of two important export carriers (BSEP and MRP2).

Primary human hepatocytes were harvested directly after thawing (d0) and one day after seeding (d1). Subsequent gene expression analysis showed that there were inter-individual differences between the three donors but in total MRP2 was still expressed after one day of cultivation, whereas BSEP expression was almost absent after 24 hours (**Figure 17**).

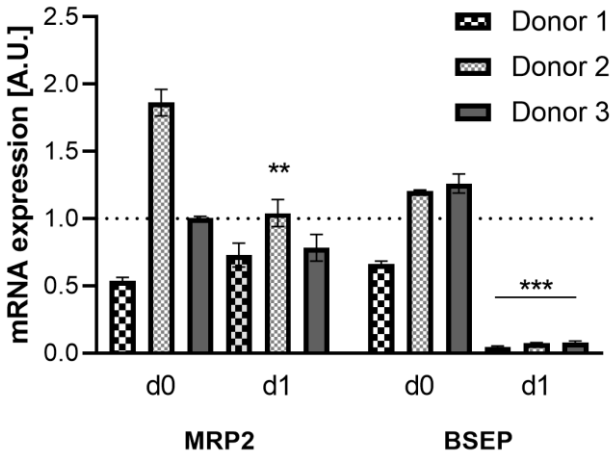

Figure 17: Gene expression of MRP2 and BSEP in primary human hepatocytes after thawing and one day after seeding. Three different human donors were tested. Data is expressed as mean±SD from 3 technical replicates per donor. ** indicates $p < 0.01$, *** indicates $p < 0.001$ compared to d0 of the respective donor.

Since RNA can be degraded quite quickly, but the protein can have a much longer half-life, we investigated BSEP expression via immunostaining and confocal microscopy in monolayer cultured primary human hepatocytes one day after seeding. We observed a relatively large fraction of BSEP in the cytoplasm and cytoplasmic vesicles; however, the carrier was also located at the cell membrane (**Figure 18**), which corresponds to the observed export activity. These results suggested the use of an early time point (≤ 1 day) for the CMFDA assay.

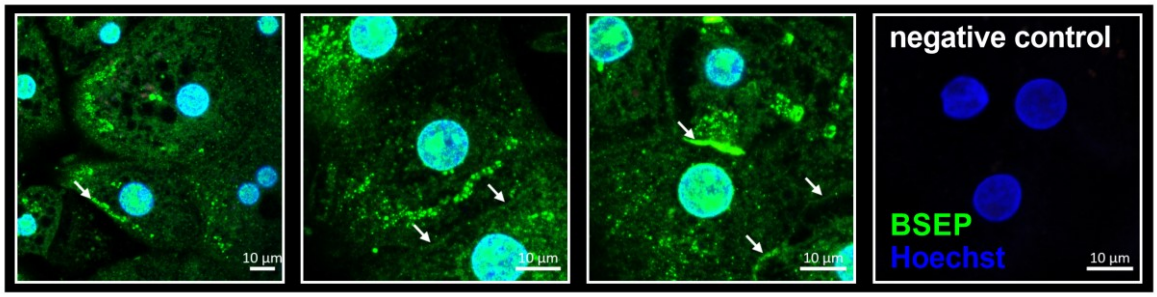

Figure 18: Visualization of the export transporter BSEP by immunostaining and confocal microscopy in monolayer cultured, cryopreserved human hepatocytes. BSEP = green, Hoechst = blue. Membrane localization is indicated by the white arrow. Scale bar: 10 µm. (Taken and adapted from [80]).

3.2.6 Influence of glutathione levels on the CMFDA kinetic

5-CMF is exported from hepatocytes as either itself or as a glutathione (GSH) conjugate (**Figure 12**), and to our knowledge, the export kinetics of either has not yet been quantified in human hepatocytes. In order to test the robustness of the assay, we investigated whether glutathione depletion or oxidation – relatively frequent mechanisms of hepatotoxic compounds, may influence the results. Thus, if 5-CMF and its GSH conjugate are exported at different rates, then compounds that alter cytoplasmic GSH levels, for example, by conjugating to GSH, may influence the results of the CMFDA assay. Therefore, we used two compounds that have been reported to alter intracellular GSH levels, DL-buthionine-sulfoximine (BSO), an inhibitor of gamma-glutamylcysteine synthetase [106], the rate-limiting enzyme in GSH synthesis, and the NRF2 activator tert-butylhydroquinone (tBHQ) [107]. Incubations with BSO and tBHQ were performed for 48 h before the CMFDA assay. BSO reduced both GSH and GSSG (**Figure 19**A), while tBHQ decreased GSH and increased GSSG (**Figure 19**B). However, at non-cytotoxic concentrations neither BSO nor tBHQ influenced the results of the CMFDA assay (**Figure 19**). Only at concentrations where cytotoxicity occurred (> 10 µM), we observed a decrease in 5-CMF associated fluorescence. In conclusion, these experiments show that neither decreased intracellular glutathione levels with BSO nor GSH oxidation with tBHQ at non-cytotoxic test compound concentrations influenced the results of the CMFDA assay.

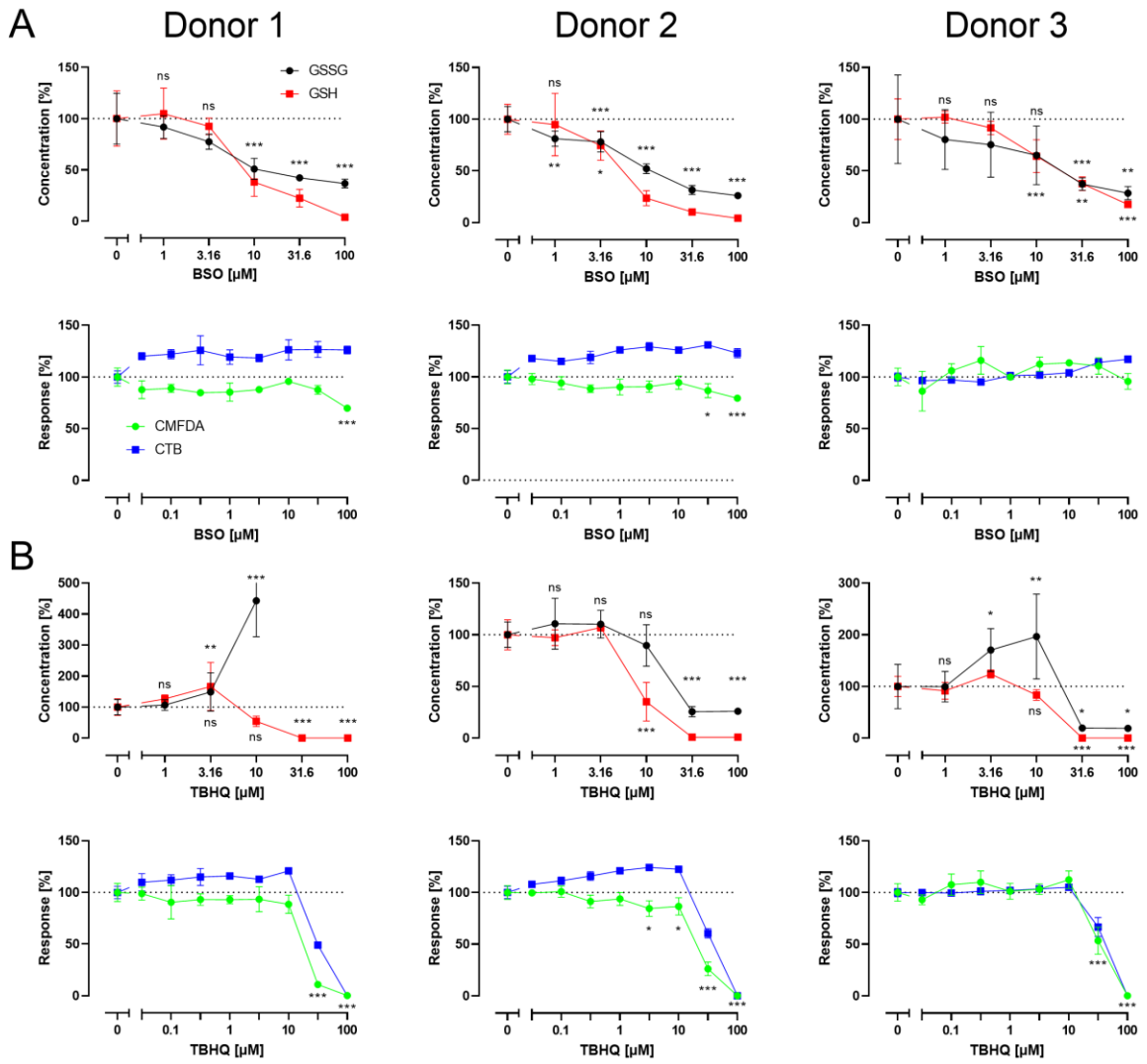

Figure 19: Influence of the glutathione content on the CMFDA assay. Cultivated human hepatocytes (monolayers) were concentration-dependently incubated with BSO **(A)** or tBHQ **(B)** for 48 hours. Intracellular concentrations of reduced (GSH) and oxidized (GSSH) glutathione, the fluorescence of 5-CMF in hepatocytes after exposure to CMFDA, and cytotoxicity (CTB) are shown. Data is given as mean±SD for at least 3 technical replicates. * indicates $p < 0.05$, ** indicates $p < 0.01$, *** indicates $p < 0.001$, ns indicates no significant changes compared to control. For the CTB assay only a significant decrease in response is given. (Taken from [80]).

3.2.7 Graphical SOP and exemplary curves of the CMFDA assay

Based on these preliminary experiments, we defined all relevant experimental conditions in a standard operating procedure (SOP) with the following main steps: (1) Thawing and plating of cryopreserved hepatocytes on day -1; (2) test compound exposure for one hour on day 0, followed by 20 minutes incubation with CMFDA (in the presence of test compound); (3) analysis of fluorescence in the cell culture supernatant; and (4) analysis of intracellular fluorescence after washing cells with PBS (**Figure 20**A).

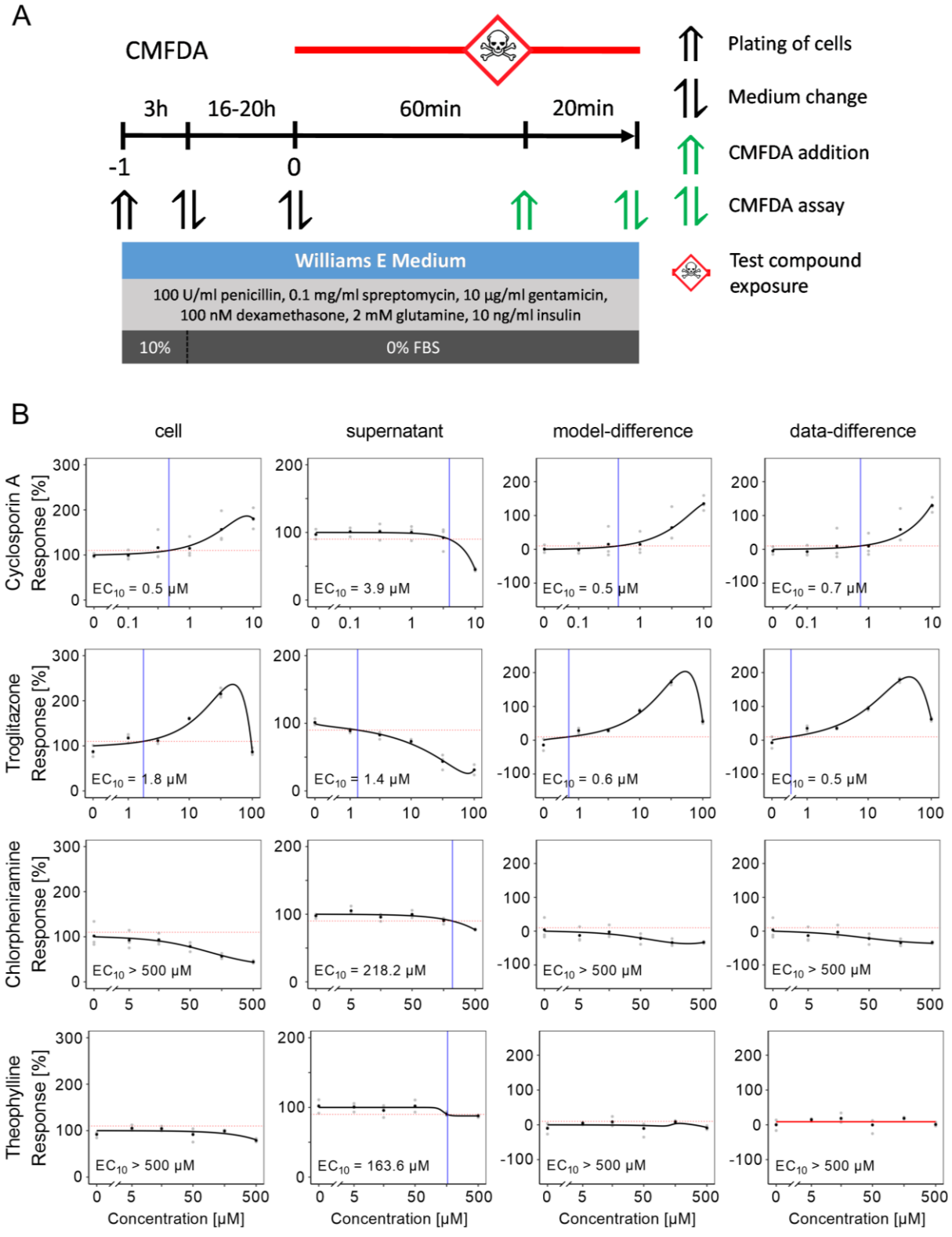

Figure 20: Experimental schedule (A) and results of the CMFDA assay of four test compounds (B). The indicated protocol was applied to primary human hepatocytes and concentration-response curves were determined. Exemplary curves are shown representing the median of 3 donors. Grey dots represent the results of three technical replicates, black dots denote the concentration-wise mean. The blue and red lines mark the EC_{10}. (Taken from [80]).

Results

We next analyzed different concentrations of 36 test compounds with the CMFDA assay using hepatocytes from at least three human donors (**Table 19**). The test compounds were chosen based on their known capacity to induce human hepatotoxicity and to inhibit BSEP and MRP2. An increased risk of human hepatotoxicity has been documented for 18 compounds based on a specific treatment regimen; whereas, 17 compounds are not known to cause an increased risk of hepatotoxicity. Acetaminophen (APAP) was also included among the test compounds because of its dose-dependent hepatotoxicity, i.e.- a C_{max} of up to 1.09×10^{-1} mM does not induce hepatotoxicity, while a C_{max} of 1.21 mM or higher is associated with an increased risk of human hepatotoxicity. For the other selected compounds, it is not possible to make such a differentiation because information on whether the risk of hepatotoxicity increases with dose is only reliably documented for the therapeutic regimen. Twenty of the 36 test compounds are known to inhibit BSEP and/or MRP2 (**Table 19**).

In principle, a test compound can interact with 5-CMF and alter its fluorescence which would compromise the results of the CMFDA assay. To control for such effects, fluorescein was incubated with all test compounds using the concentration range of the CMFDA assay without the presence of cells (Appendix Table 24). None of the test compounds caused a change of the fluorescence intensity that exceeded 10%, demonstrating that interaction of the tested chemicals with the fluorophore did not compromise the results of the CMFDA assay.

To illustrate representative results of the CMFDA assay (**Figure 20**A), two examples with expected positive (cyclosporine A and troglitazone) and two with expected negative results (chlorpheniramine and theophylline) are shown (**Figure 20**B). Data from the complete set of compounds are available in the Electronic supplement. Cyclosporine A caused a concentration-dependent increase in fluorescence in the hepatocytes, while the fluorescence signal decreased in the corresponding culture medium supernatants (**Figure 20**B), a scenario that fits to the inhibition of 5-CMF export. However, fluorescence in the cell and the supernatant were not just an inverse of each other, but rather the intracellular increase in signal occurred at lower concentrations compared to decreased extracellular fluorescence. The reasons for this deviation may be manifold, e.g. dilution of 5-CMF in the volume of the supernatant, or compound-specific mechanisms not specifically addressed in this study. Troglitazone, another hepatotoxic compound and known BSEP inhibitor, caused a concentration-dependent increase in intracellular fluorescence values, and a concurrent decrease in the supernatant - a similar scenario as seen for cyclosporine A (**Figure 20**B). However, the dramatic decrease in fluorescence values observed at the highest tested concentration of troglitazone (100 µM) was due to cytotoxicity. In contrast, the non-hepatotoxic compounds, chlorpheniramine and theophylline (both known not to inhibit BSEP or MRP2) did not cause any statistically significant increase in fluorescence inside the cells

nor a decrease in the supernatant (**Figure 20**B). The decrease in intracellular fluorescence observed for the three highest concentrations of chlorpheniramine is probably due to cytotoxicity.

3.2.8 Graphical SOP and exemplary curves of the CTB assay

Cytotoxicity was tested by the CTB assay (**Figure 21**), where primary human hepatocytes were cultivated under the same conditions as for the CMFDA assay, analyzing at least three donors per compound. The same test compounds are illustrated in **Figure 22** as for the CMFDA assay (**Figure 20**B), with data from all others summarized in the Electronic supplement. The comparison of the CTB (**Figure 22**) and the CMFDA (**Figure 20**B) assays shows that cyclosporine A and troglitazone inhibited export carriers at non-cytotoxic concentrations; whereas, non-cytotoxic concentrations of chlorpheniramine and theophylline did not block the export of 5-CMF.

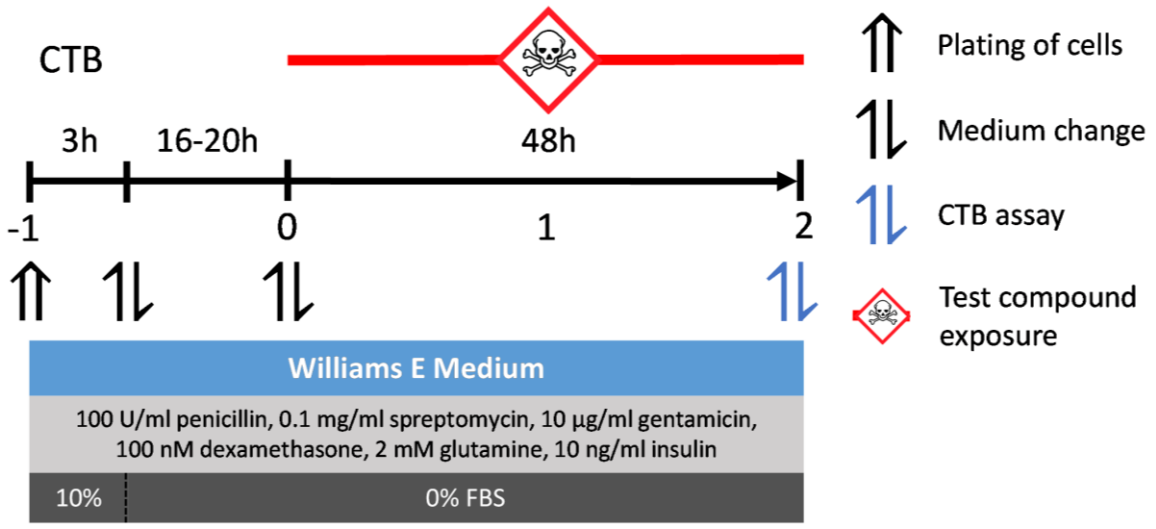

Figure 21: Experimental schedule of the CTB assay. CTB: Cell-Titer Blue, FBS: fetal bovine serum. (Taken from [80]).

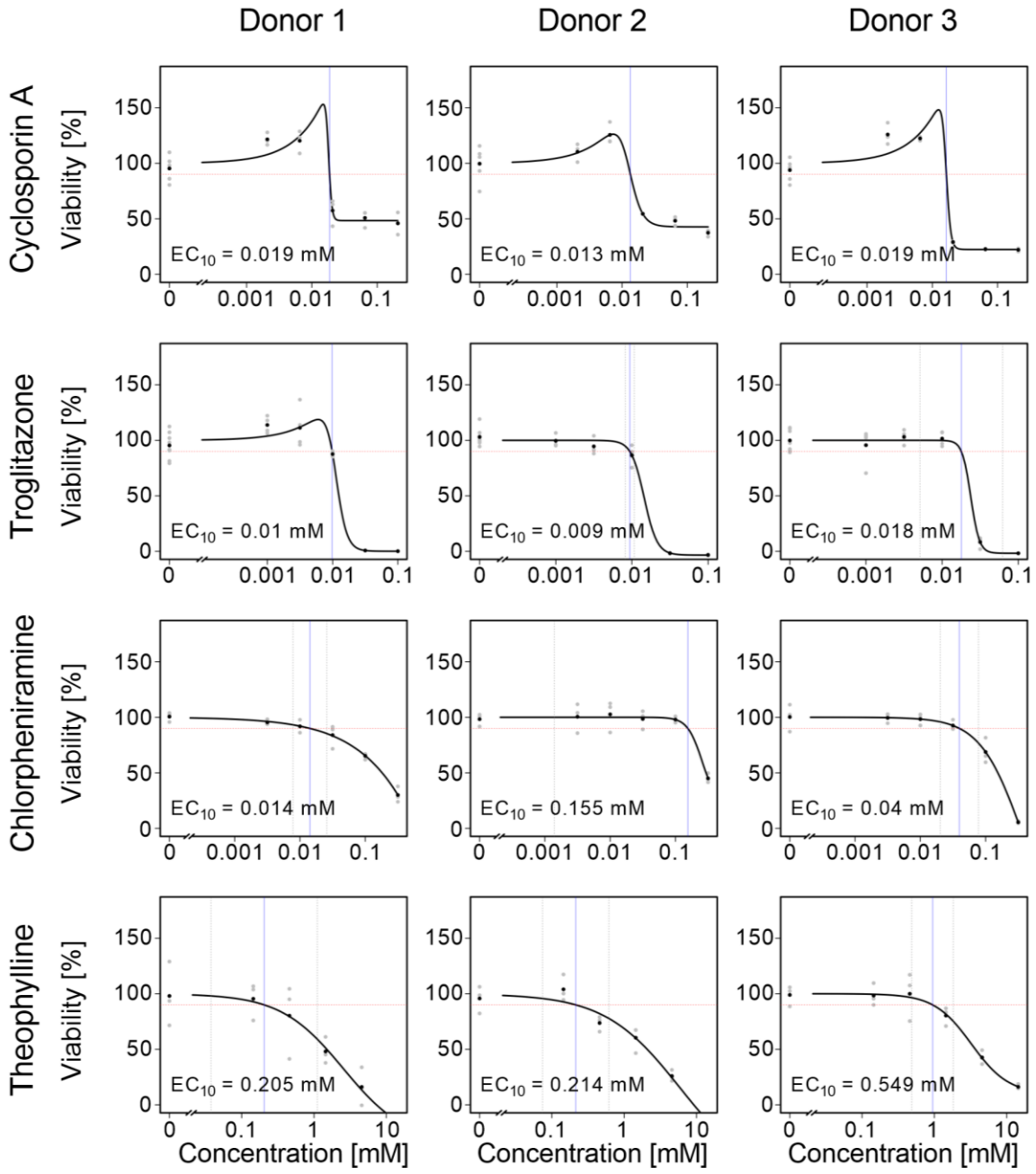

Figure 22: Exemplary cytotoxicity curves from the CMFDA assay compound set. The CTB assay was utilized with primary human hepatocytes after 48 h compound exposure. Shown concentration-response curves represent the median of at least 3 biological replicates. Grey dots represent the results of three to four technical replicates, black dots denote the concentration-wise mean. The blue and red lines mark the EC_{10}. (Taken from [80]).

Table 19: Summary of the results of the cytotoxicity tests, CMFDA assay, and pharmacokinetic modeling of the test compounds. In vitro values were calculated from at least 3 biological replicates. The in vivo concentration is given as the 95% percentile of the peak total systemic blood concentration modeled for a specific dose. All generated data including the raw data can be found in the supplement. Inhibition of hepatocellular carriers was indicated as "yes" if documented in at least one previous study together with an IC_{50}-value. "#" indicates that contradicting information has been reported, "N/A" indicates that no information could be identified. (Taken from [80]).

Compound	Abbre-viation	Hepato-toxicity reported	In vivo C_{max} whole blood 95% total [mM]	In vitro cytotoxicity EC_{10} [mM] median [min/max]	In vitro CMFDA model-difference EC_{10} [mM] median [min/max]	Inhibition of hepato-cellular export [BSEP/MRP2]	
Acetaminophen	APAP	no/yes	1.09×10^{-01} $1.21\times10^{+00}$	1.403 [0.500/2.833]	>0.5 [>0.5/>0.5]	no	no
Atorvastatin	AVS	yes	5.38×10^{-06}	2.238 [0.074/>3.16]	>1 [>1/>1]	yes	yes
Atropine	ATRO	no	1.50×10^{-05}	0.138 [0.065/0.208]	0.001 [0.001/0.017]	no	yes
Benzbromarone	BZB	yes	1.79×10^{-02}	0.010 [0.010/0.012]	0.001 [0.001/0.001]	yes	yes
Benztropine	BZT	no	1.23×10^{-05}	0.011 [0.007/0.038]	>0.5 [>0.5/>0.5]	N/A	N/A
Bosentan	BOS	yes	2.81×10^{-03}	0.018 [0.003/0.055]	0.042 [0.021/>0.1]	yes	no#
Chlorpheniramine	CHL	no	6.49×10^{-05}	0.044 [0.014/0.155]	>0.5 [>0.5/>0.5]	no	no
Codeine	COD	no	2.33×10^{-04}	0.956 [0.536/1.058]	>0.5 [>0.5/>0.5]	N/A	N/A
Cyclosporin A	CSA	yes	7.34×10^{-03}	0.014 [0.008/ 0.031]	0.0006 [0.0004/ 0.0049]	yes	yes
Diphenhydramine	DPH	no	5.90×10^{-04}	0.122 [0.056/0.143]	>0.5 [>0.5/>0.5]	no	no
Entacapone	ETC	yes	9.94×10^{-03}	0.020 [0.017/0.034]	0.005 [0.003/0.043]	yes#	no
Hydroxyzine	HYZ	no	4.94×10^{-04}	0.079 [0.045/0.094]	0.014 [0.010/0.036]	yes	N/A
Indomethacin	INDO	yes	3.48×10^{-03}	>0.245 [0.081/ >0.245]	0.019 [0.019/ >0.1]	yes	yes#
Isosorbide dinitrate	ISS	no	1.03×10^{-04}	0.108 [0.098/0.135]	>0.5 [>0.5/>0.5]	N/A	N/A
Ketoconazole	KC	yes	1.62×10^{-02}	0.026 [0.008/0.100]	0.003 [0.002/0.003]	yes	yes
Lovastatin	LO	yes	8.48×10^{-06}	>0.245 [0.024/ >0.245]	0.017 [0.010/ >0.1]	yes	yes
Melatonin	MEL	no	2.70×10^{-05}	0.921 [0.077/>5]	>0.5 [0.402/>0.5]	no	no
N-Acetylcysteine	NAC	no	3.19×10^{-03}	>10 [0.242/>10]	>0.5 [>0.5/>0.5]	N/A	N/A

Results

Compound	Abbre-viation	Hepato-toxicity reported	In vivo C_{max} whole blood 95% total [mM]	In vitro cytotoxicity EC_{10} [mM] median [min/max]	In vitro CMFDA model-difference EC_{10} [mM] median [min/max]	Inhibition of hepato-cellular export [BSEP/MRP2]	
Nifedipine	NDP	yes	1.16×10^{-03}	>0.433 [>0.433/ >0.433]	0.003 [0.0001/ 0.004]	yes	no
Oxycodone	OXC	no	9.84×10^{-05}	1.149 [0.546/6.337]	>0.5 [0.0667/>0.5]	N/A	N/A
Oxymorphone	OXM	no	1.13×10^{-05}	0.028 [0.024/0.043]	0.033 [0.003/>0.5]	N/A	N/A
Pazopanib	PZB	yes	6.20×10^{-02}	>0.189 [>0.189/ >0.189]	>0.1 [0.094/ >0.1]	yes	no
Pindolol	PIN	no	1.71×10^{-04}	>0.5 [>0.5/>0.5]	>0.5 [>0.5/>0.5]	no	no
Pioglitazone	PIO	yes	5.33×10^{-03}	0.009 [0.008/0.080]	>0.1 [0.0001/>0.1]	yes	no
Pyridoxine	PDX	no	7.04×10^{-05}	1.023 [0.106/5.082]	>0.5 [0.467/>0.5]	N/A	N/A
Rifampicin	RIF	yes	2.01×10^{-02}	0.262 [0.121/0.424]	0.004 [0.003/0.018]	yes	yes
Rosiglitazone	RGZ	yes	5.99×10^{-04}	0.036 [0.034/0.047]	0.028 [0.016/>0.1]	yes	yes#
Rosuvastatin	ROS	yes	9.78×10^{-06}	0.028 [0.026/0.028]	>0.1 [0.003/>0.1]	yes	yes
Simvastatin	SIM	yes	2.15×10^{-05}	0.020 [0.013/0.046]	0.004 [0.001/0.006]	yes	yes
Sitaxentan	SXS	yes	1.73×10^{-02}	0.132 [0.086/0.184]	0.002 [0.001/0.002]	yes	yes#
4-Phenylbutyrate	SPB	no	9.11×10^{-01}	1.969 [0.192/>10]	>0.5 [>0.5/>0.5]	N/A	N/A
Theophylline	THE	no	6.10×10^{-02}	0.214 [0.205/0.945]	>0.5 [0.055/>0.5]	no	no
Tolcapone	TOLC	yes	1.06×10^{-02}	0.028 [0.020/0.031]	0.002 [0.001/0.006]	yes	no
Triprolidine	TPL	no	3.16×10^{-05}	0.161 [0.122/>1.6]	>0.5 [>0.5/>0.5]	yes	N/A
Troglitazone	TROG	yes	2.21×10^{-03}	0.011 [0.009/0.022]	0.001 [0.001/0.002]	yes	yes#
Zaleplon	ZAL	no	1.94×10^{-04}	0.097 [0.016/>0.5]	>0.5 [0.268/>0.5]	no	no

3.2.9 Evaluation of the CMFDA assay

To determine if the CTB or the CMFDA assay is more sensitive, we calculated $\log_2$ ratios of the EC_{10} values obtained from each assay for each of the 36 tested compounds, using the 'model-difference' for the CMFDA assay (**Figure 20**). A $\log_2$ ratio above zero indicates that the CMFDA assay is more sensitive. Interestingly, 14 of the tested compounds had a $\log_2$ ratio higher than two, while six compounds had ratios even higher than five, revealing that for these compounds the CMFDA assay was more sensitive (**Figure 23**). Conversely, the CMFDA assay was negative up to the highest tested concentration for 19 compounds, which was not surprising since no inhibition of export carriers was reported for the set of non-hepatotoxic compounds.

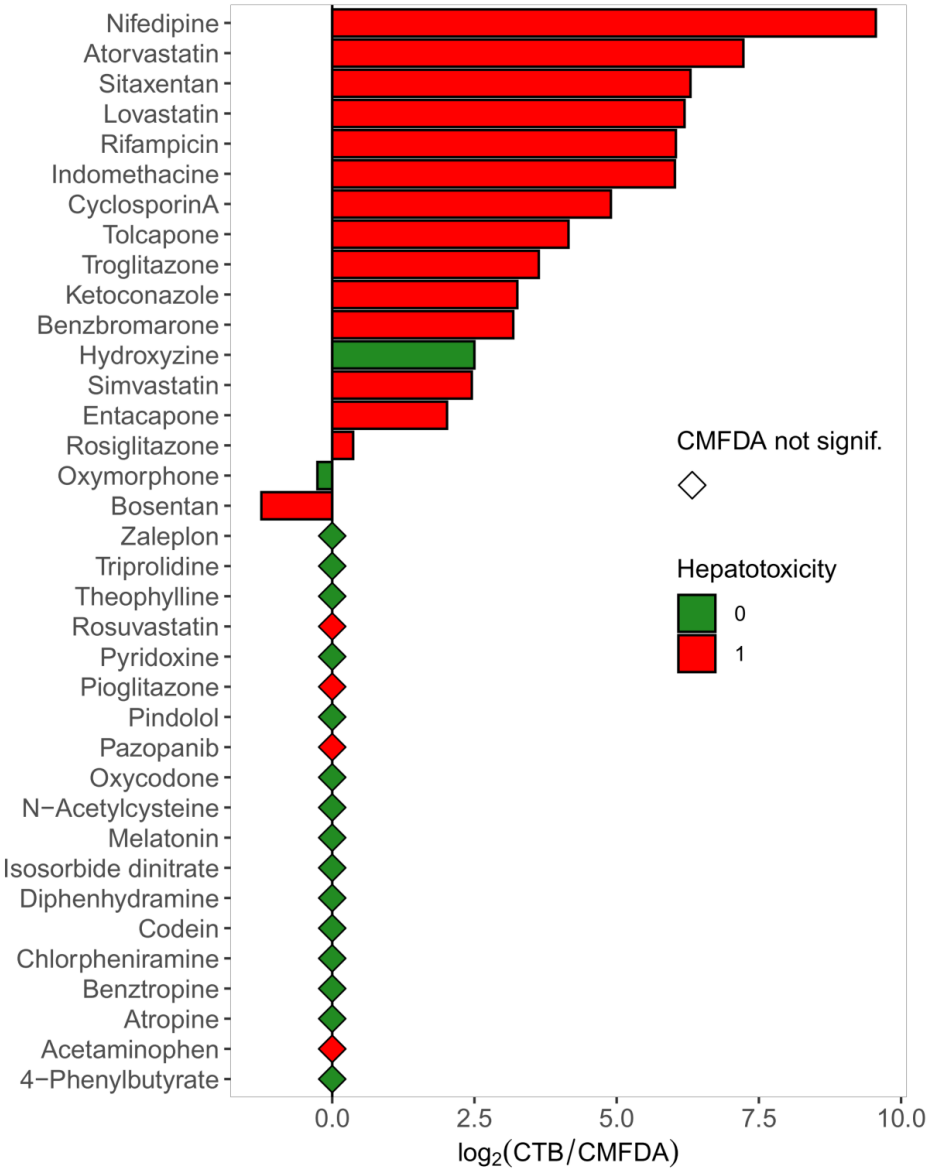

Figure 23: Ratio plot comparing cytotoxicity and fluorescein export inhibition. Ratios were calculated by dividing the EC_{10} (median) values measured with the CTB assay by those obtained with the CMFDA assay and $\log_2$ values of the respective ratios are shown. 1: hepatotoxic; 0: non-hepatotoxic compounds. Diamond indicates that up to the highest tested concentration no EC value could be determined for the CMFDA assay. (Taken from [80]).

Results

To compare the performance of our in vitro test system when using export carrier inhibition (CMFDA assay) as an endpoint compared to the cytotoxicity (CTB assay) - or a combination of both - we calculated the TSI, a measure of how well hepatotoxic and non-hepatotoxic compounds can be differentiated for a given set of compounds, and TEI, which informs how well a hepatotoxic C_{max} in vivo can be determined for these three options. Determining the EC_{10} based on the CTB assay alone led to a TSI of 0.77 and a TEI of 0.69 (**Table 20**A). The CMFDA assay resulted in a consistently higher TSI and TEI compared to the CTB test, regardless of whether the intra- or extracellular fluorescence values or the modeling-based results were used. The best performance (highest TSI and TEI) was achieved using the 'model-difference' for CMFDA (**Table 20**A). Next, the data of the CTB and the CMFDA assay were combined so that the lower EC_{10} of the respective assay was used. The combination of the CTB and CMFDA assay resulted in a higher TSI and TEI compared to the CTB assay alone (**Figure 24**A). The in vitro - in vivo extrapolation plots of the CTB (**Figure 24**A), CMFDA (**Figure 24**B) and combined CTB-CMFDA data (**Figure 24**C) illustrate that considering export kinetics in addition to cytotoxicity allows for better differentiation of hepatotoxic and non-hepatotoxic compounds in relation to the maximal whole blood concentration compared to using cytotoxicity alone.

Table 20: Toxicity separation index (TSI) and toxicity estimation index (TEI) for the CTB and CMFDA assays alone and in combination. (Taken from [80]).

A TSI and TEI are based on the EC_{10} values of the CTB and/or CMFDA assay and median values of three donors.

Assay	EC_{10} median	TSI	TEI
CTB	-	0.77	0.69
CMFDA	cell	0.86	0.72
	supernatant	0.80	0.74
	data-difference	0.86	0.76
	model-difference	0.89	0.80
Combination	CTB & cell	0.83	0.78
	CTB & supernatant	0.83	0.81
	CTB & data-difference	0.86	0.80
	CTB & model-difference	0.89	0.83

B TSI and TEI for all possible parameter combinations considering EC_{10}, EC_{20}, …, EC_{90} as well as median, minimum and maximum values. The parameters resulting in the highest TSI are given for both assays alone and in combination.

Assay / EC value	TSI	TEI
CTB / EC_{20} max	0.84	0.63
CMFDA / EC_{10} min model-difference	0.91	0.87
CTB / EC_{20} max CMFDA / EC_{10} min model-difference	0.93	0.87
CTB / EC_{40} max CMFDA / EC_{10} min model-difference	0.93	0.87

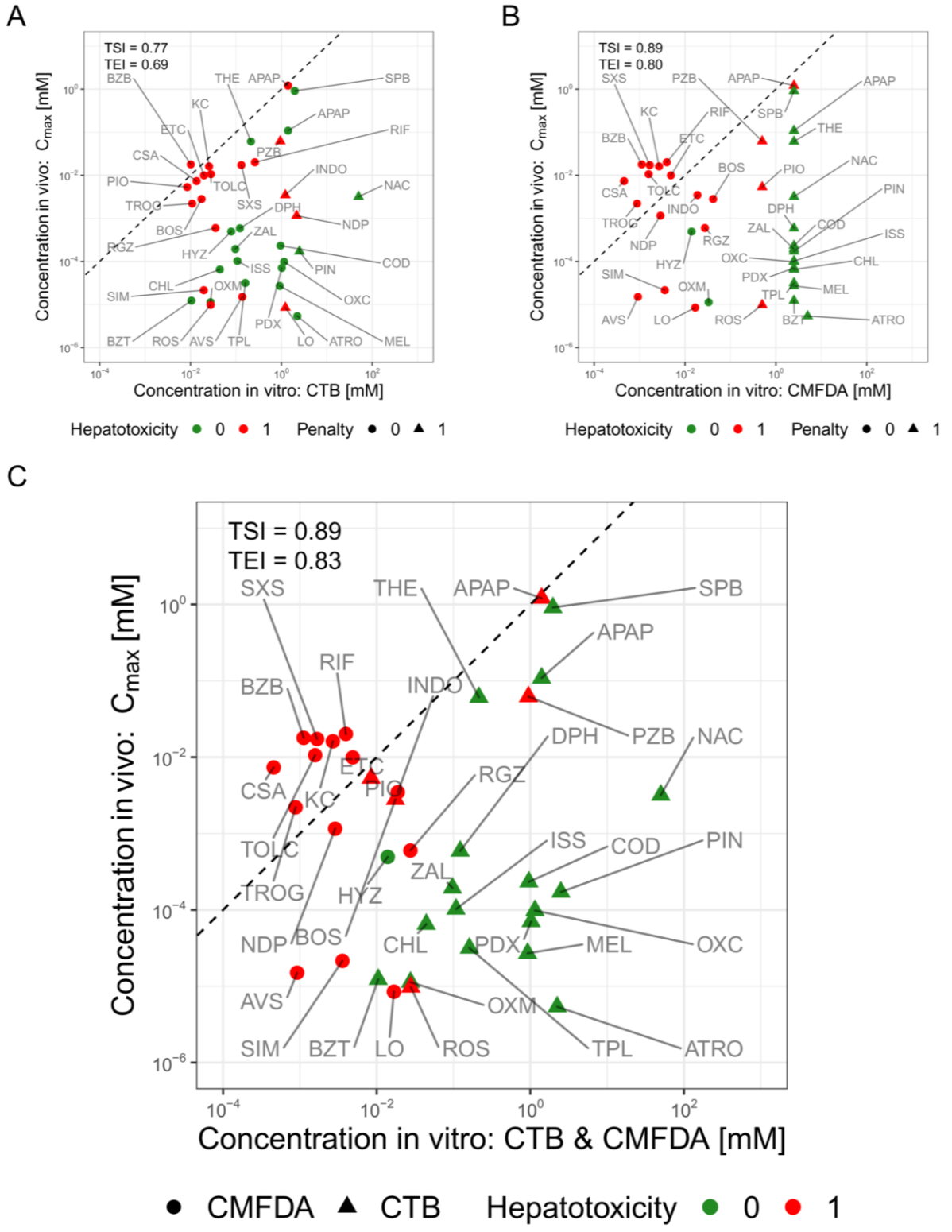

Figure 24: Evaluation of the CMFDA assay. Extrapolation plots **(A)** based on cytotoxicity data alone using the EC_{10} median values of the cytotoxicity test (x-axis) and the C_{max} (total concentration in the blood; 95% percentile); **(B)** based on the export assay (CMFDA assay using model-differences) and **(C)** based on the lower value of either the CTB test or the CMFDA assay (x-axis). Red indicates hepatotoxic compounds (1) and green indicates non-hepatotoxic compounds (0). For (A/B) a triangle indicates that up to the highest tested concentration no EC value was reached and a penalty factor (x5) was applied. For (C) the circle and triangle indicate if the CTB or CMFDA assay resulted in a lower EC_{10} values, respectively. (Taken from [80]).

3.2.10 Prediction of export inhibition using classification models

Finally, we investigated whether it was necessary to test all compounds with the CMFDA assay for export inhibition, or if it is possible to identify a subset of compounds with a high probability of a negative experimental result using an in silico method. Recently, a web service including classification models of different transporters was established that allows for the prediction of whether small molecules inhibit export carriers of hepatocytes [91]. In the present study, the web service was used to predict the inhibitory capacity of all test compounds (**Table 21**). Using these classification models on our set of selected compounds, a good agreement with the experimental data was obtained. If a score ≥0.65 [91] is used for the three carriers (BSEP, MRP3, and MRP4), 21 of the 36 compounds were predicted as positive. Experimentally, 17 out of the 36 compounds were positive in the CMFDA assay (**Figure 23**, **Table 19**). If one considers the result of the export assay (CMFDA assay) as true positives or negatives, the classification resulted in a sensitivity, specificity, accuracy, negative prediction value (NPV), and positive prediction value (PPV) of 0.86, 0.85, 0.85, 0.92 and 0.75, respectively. Thus, the here-applied web service may indeed contribute towards reducing experimental effort in the future once the performance metrics presented here are confirmed with higher numbers of test compounds.

Table 21: Compound classification based on the CMFDA assay[1] and a web service based classification model[2] (2.2.14). Green indicates values < 0.65 for all predictions or no observable inhibition for the CMFDA assay. Red indicates observable inhibition in the CMFDA assay or predicted inhibition (value > 0.65 for at least one of the three export carriers). (Taken from [80]).

Compound	BSEP Inhibition	MRP3 Inhibition	MRP4 Inhibition	Experiment[1]	Prediction[2]
Acetaminophen	0	0	0		
Atropine	0	0	1		
Benztropine	0	0	1		
Chlorpheniramine	0	0	0		
Codeine	0	0	0		
Diphenhydramine	0	0	0		
Hydroxyzine	0.02	0.96	1		
Isosorbide dinitrate	0	0	0		
Melatonin	0	0	0		
N-Acetylcysteine	0	0	0		
Oxycodone	0	0	0		
Oxymorphone	0	0	0		

Compound	BSEP Inhibition	MRP3 Inhibition	MRP4 Inhibition	Experiment[1]	Prediction[2]
Pindolol	0	0	0		
Pyridoxine	0	0	0		
4-Phenylbutyrate	0	0	0		
Theophylline	0	0	0		
Triprolidine	0	0	0		
Zaleplon	0	0	0.01		
Atorvastatin	1	1	1		
Benzbromarone	0	1	1		
Bosentan	1	1	1		
Cyclosporin A	1	1	0		
Entacapone	0	0	1		
Indometacin	0	0.96	1		
Ketoconazole	1	1	1		
Lovastatin	1	1	1		
Nifedipine	0	0	1		
Pazopanib	1	1	1		
Pioglitazone	0	0	1		
Rifampicin	1	1	1		
Rosiglitazone	0	0	1		
Rosuvastatin	1	1	1		
Simvastatin	1	1	1		
Sitaxentan	1	1	1		
Troglitazone	1	1	1		
Tolcapone	0	0	1		

3.3 AdipoRed assay

3.3.1 Introduction and graphical concept

After demonstrating that the study of bile acid transport inhibition by the CMFDA assay and its addition to the cytotoxicity test led to an improvement in TSI and TEI, an additional assay was evaluated. We aimed to extend our in vitro test battery by developing a concept to detect steatosis-inducing drugs. Steatosis is the abnormal accumulation of lipids inside the cells. It can be attributed to overeating, metabolic disorders, diabetes mellitus, and excessive alcohol consumption [108]. Likewise, drugs can lead to steatosis by interfering for example with mitochondrial functions, ATP production, or the lipid metabolism [109].

We assumed that there are three different scenarios of how increasing concentrations of a compound can act on the cell in terms of the relationship between cytotoxicity and lipid accumulation (**Figure 25**). In the first scenario, lipid accumulation already begins at non-cytotoxic concentrations. In this case the inclusion of an assay that detects lipid droplets into the in vitro test battery could lead to improved separation and estimation and thus DILI prediction, provided that the earlier lipid accumulation is observed only or predominantly in hepatotoxic compounds compared to non-hepatotoxic ones. In the second scenario, lipid accumulation and cytotoxicity occur simultaneously. In this case, lipid droplet detection would give a positive result in form of effective concentrations, but the inclusion of lipid droplet detection would not improve the test system as both readouts result in similar EC values. In the third scenario, cytotoxicity occurs with increasing drug concentrations, but no lipid accumulation is observed inside the cell. For this case, the detection of intracellular lipid droplets would lead to no positive test result and no EC values could be determined. With the following study, we aimed to investigate whether one or more of the three scenarios are present and whether the detection of lipid accumulation improves our test system.

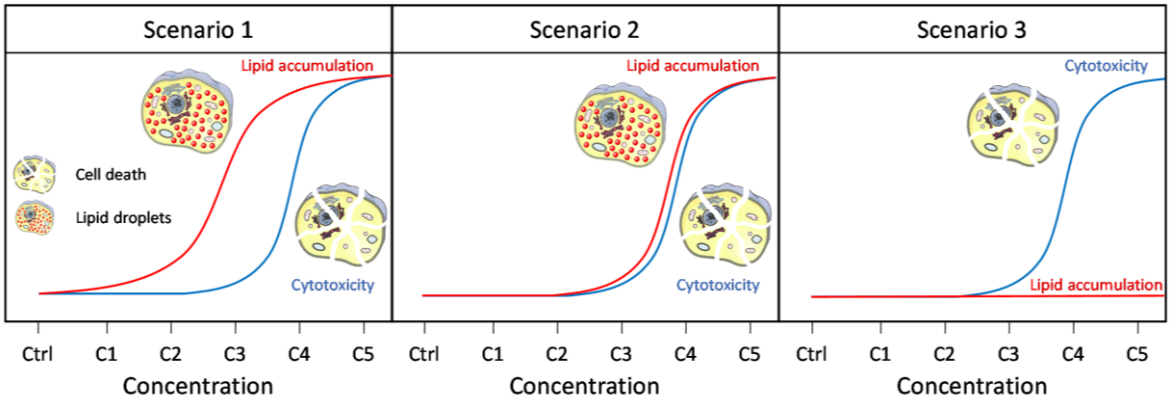

Figure 25: Possible scenarios of lipid accumulation in comparison to cytotoxicity under increasing drug concentrations. Graphical elements were taken from Servier Medical Art by Servier.

As already described by other researchers, intracellular lipid droplet accumulation can be induced in vitro by adding free fatty acids (FFA) to the cell culture medium [110]. For detection, lipid droplets can be stained with commercially available fluorophores followed by fluorescence measurement via a microscope or a plate reader. For our approach, we adapted an established protocol from cooperation partners using a defined mix of two fatty acids and HepG2 cells [111], [112].

3.3.2 Influence of free fatty acids on HepG2 cells

First, we wanted to investigate how the cells react to free fatty acids to verify whether they are suitable cell model for lipid accumulation and, if so, under which conditions. For this purpose, HepG2 cells were incubated with increasing concentrations of free fatty acids for 48 hours, stained with AdipoRed (AR) for visualization of intracellular lipids, and observed under a fluorescence microscope. A clear concentration-dependent increase in lipid droplets was visible after 48 hours exposure (**Figure 26**A). Additionally, cells were incubated with increasing concentrations of free fatty acids for 48 hours and stained with AdipoRed and markers for cell viability (Hoechst = cell number, CTB = metabolic activity, TMRE = mitochondrial membrane potential) flowed by fluorescence detection with a plate reader. The microscopically visible accumulation of lipid droplets was confirmed by the results of the fluorescence plate reader, which simultaneously demonstrated the practicability for a higher-throughput method (**Figure 26**B). Up to a concentration of 248 µM, the intracellular lipid content increased and decreased sharply thereafter, which was accompanied by cytotoxicity (**Figure 26**C).

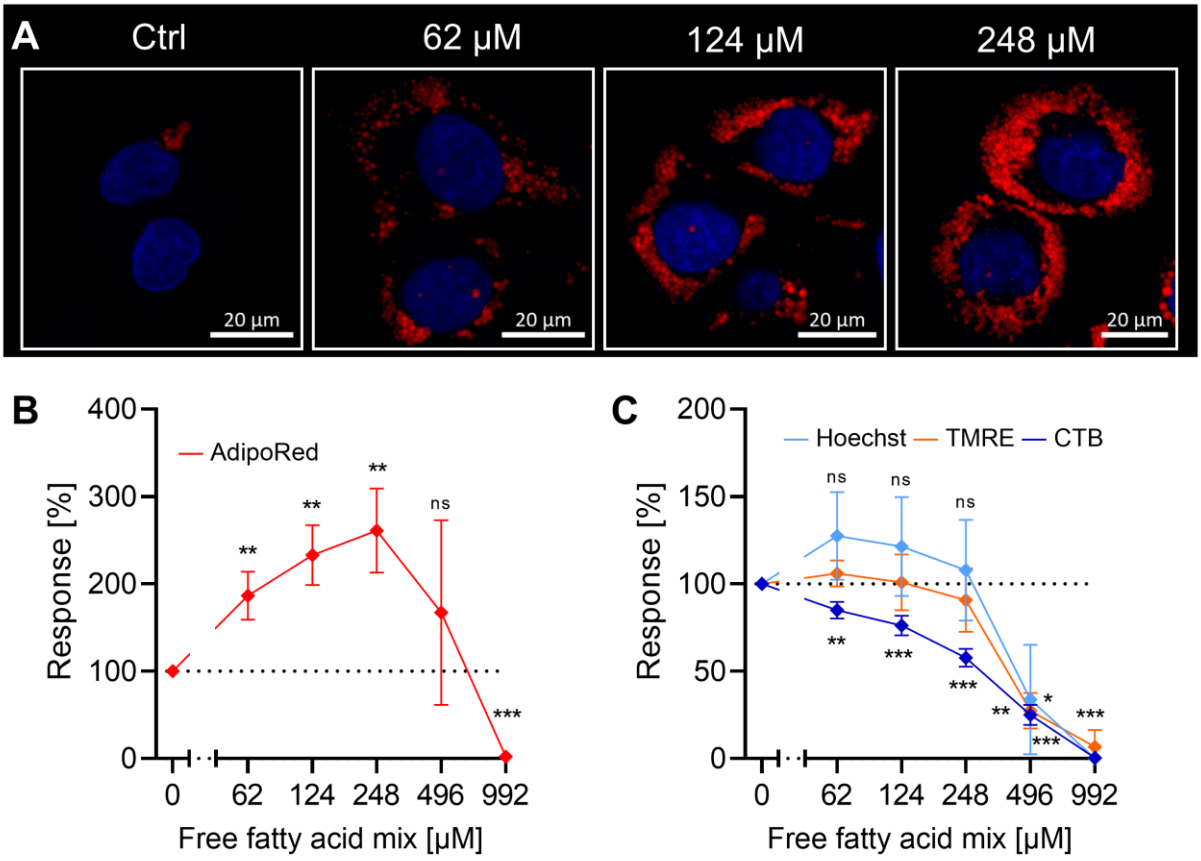

Figure 26: Influence of 48 hours free fatty acid exposure on HepG2 cells. (A) Microscopic pictures of cells stained with AdipoRed (red, lipid droplets) and Hoechst (blue, cell nuclei). Scale bar = 20 µM. **(B)** Measurement of AdipoRed signal in a fluorescence plate reader. **(C)** Measurement of cell vitality markers with a fluorescence plate reader. Data is given as mean±SD from at least 3 biological replicates. * indicates $p < 0.05$, ** indicates $p < 0.01$, *** indicates $p < 0.001$, ns indicates no significant changes compared to control.

After confirming that lipid accumulation can be artificially induced in HepG2 cells by the addition of free fatty acids, the next question was which exposure duration and concentration would be most appropriate. For this purpose, HepG2 cells were incubated with five different concentrations of FFA for 24 hours, 48 hours, and 72 hours, respectively. Subsequently, the cells were stained with AdipoRed, Hoechst, and TMRE followed by fluorescence detection with a plate reader. Furthermore, a CTB assay was performed.

There were no major differences between the individual time points (**Figure 27**). The intracellular lipid content almost doubled at 62 µM FFA and then increased up to 248 µM, where the maximum was reached (**Figure 27**A). At 496 µM, the AdipoRed signal was already reduced and eventually resulted in 0% at 992 µM. The Hoechst signal and thus the cell count was slightly higher in the lower three concentrations compared to the control (**Figure 27**B). The cell number was reduced by more than 50% with 496 µM FFA exposure and yielded near 0% at 992 µM for all time points. Interestingly, metabolic activity measured by the CTB assay decreased continuously from 62 µM to 992 µM (**Figure 27**C). In

contrast, the mitochondrial membrane potential remained quite constant and decreased markedly with 496 µM (**Figure 27**D).

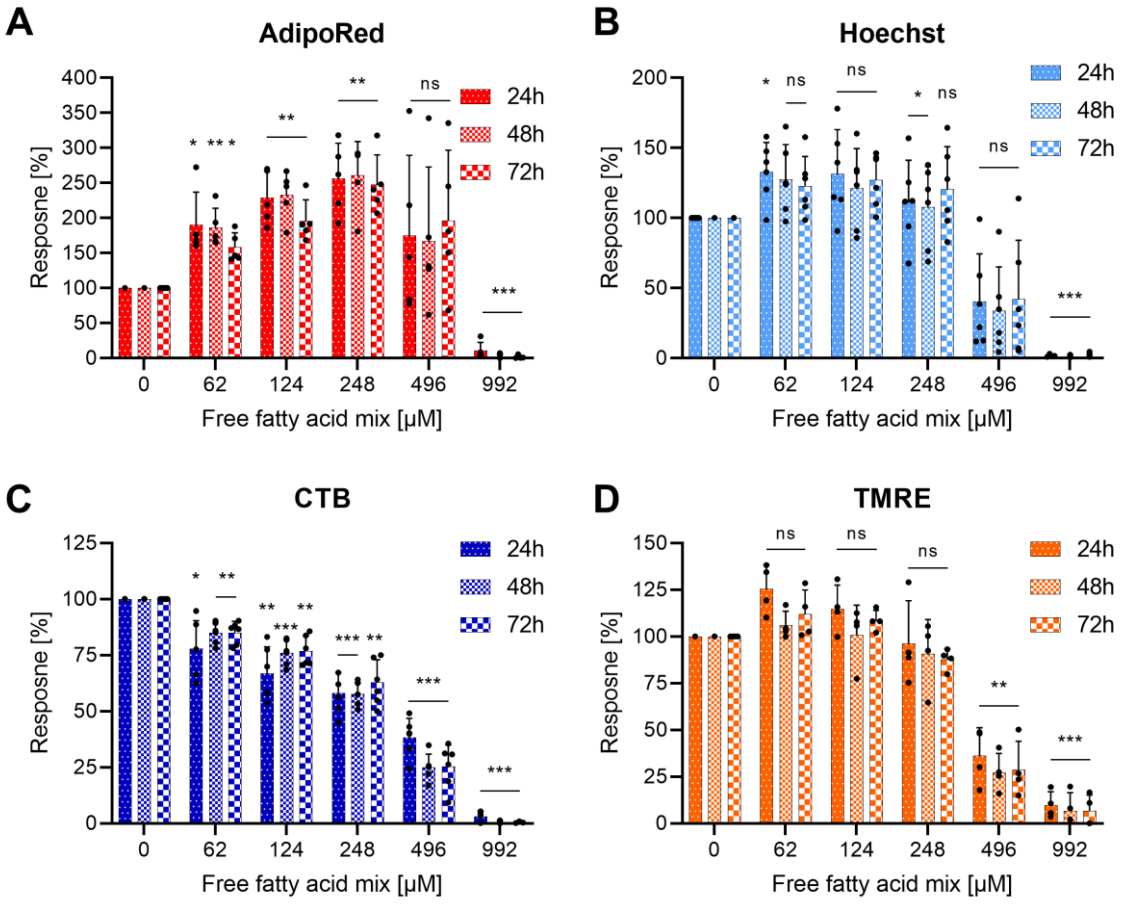

Figure 27: Influence of free fatty acid exposure time on HepG2 cells. HepG2 cells were exposed to FFA and stained with **(A)** AdipoRed for lipid accumulation, **(B)** Hoechst for cell nuclei/cell number, **(C)** CellTiter-Blue for metabolic activity, and **(D)** Tetramethylrhodamine for mitochondrial membrane potential. Fluorescence was measured with a fluorescence plate reader. Data is given as mean±SD from at least 3 biological replicates after normalization to the corresponding control. * indicates $p < 0.05$, ** indicates $p < 0.01$, *** indicates $p < 0.001$, ns indicates no significant changes compared to control.

In the absence of major differences regarding the influence of FFA incubation time, an exposure period of 48 hours was selected for greater comparability to the cytotoxicity assay and because of the results of a previous study were 48 hours incubation time led to the best separation of hepatotoxic and non-hepatotoxic compounds compared to 24 hours or 96 hours [79]. Furthermore, 62 µM was selected as an appropriate FFA concentration because increased lipid accumulation was already present while simultaneously only minor changes in cell vitality occurred.

After selecting an incubation time of 48 hours and a concentration of 62 µM FFA, the question arose whether the treatment scheme could be improved. In the protocol adapted from collaborators, cells were first exposed to FFA followed by incubation with the test compound in the absence of FFA. Permanent exposure of the cells to FFA and a test compound seemed potentially superior, so we tested

different scenarios. As a test compound valproic acid (VPA), a known hepatotoxic and steatosis-inducing drug, was used.

After 24 hours of FFA incubation followed by exposure to 1.25 mM VPA, the intracellular lipid content increased by 14% compared to the control without VPA (**Figure 28**). Incubation of the cells with FFA and VPA simultaneously for 48 hours increased the lipid content by 57%. Interestingly, exposure of cells with VPA alone for 48 hours without FFA produced similar results. It was shown that longer and simultaneous incubation of FFA and a test compound is beneficial for increased lipid accumulation compared to the original treatment scheme, although the question arose whether FFA are needed at all. Nevertheless, 48 hours of incubation with FFA and the test compound was chosen as the treatment schedule for the so-called AdipoRed assay.

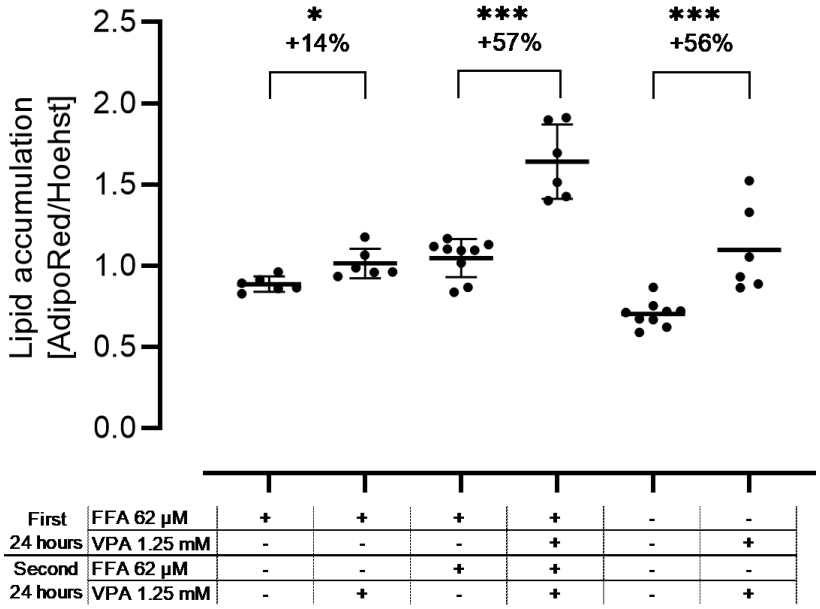

Figure 28: Free fatty acid treatment schedule. Fluorescence was detected with a fluorescence plate reader. Data is given as mean±SD from at least 6 biological replicates. VPA: Valproic acid. FFA: free fatty acids. * indicates $p < 0.05$. *** indicates $p < 0.001$.

3.3.3 Graphical SOP and exemplary curves of lipid accumulation and cytotoxicity

The previous experiments led to the following protocol for the AdipoRed assay in which HepG2 cells are plated on day -1 and incubated with a mix of free fatty acids and a test compound on day 0 for 48 hours one day after plating. Subsequently, on day 2 the cells are stained with AdipoRed and Hoechst and the fluorescence is measured with a plate reader (**Figure 29**A).

In order to investigate the influence of test compounds on the lipid accumulation in HepG2 cells and subsequently to verify whether the new assay is a useful addition to the in vitro test battery, a test set with a total number of 60 compounds was prepared for which AdipoRed and CTB assays were

performed. Since this assay was performed in the HepG2 cell line, unlike the previous ones, cytotoxicity (CTB assay) in HepG2 cells was also considered.

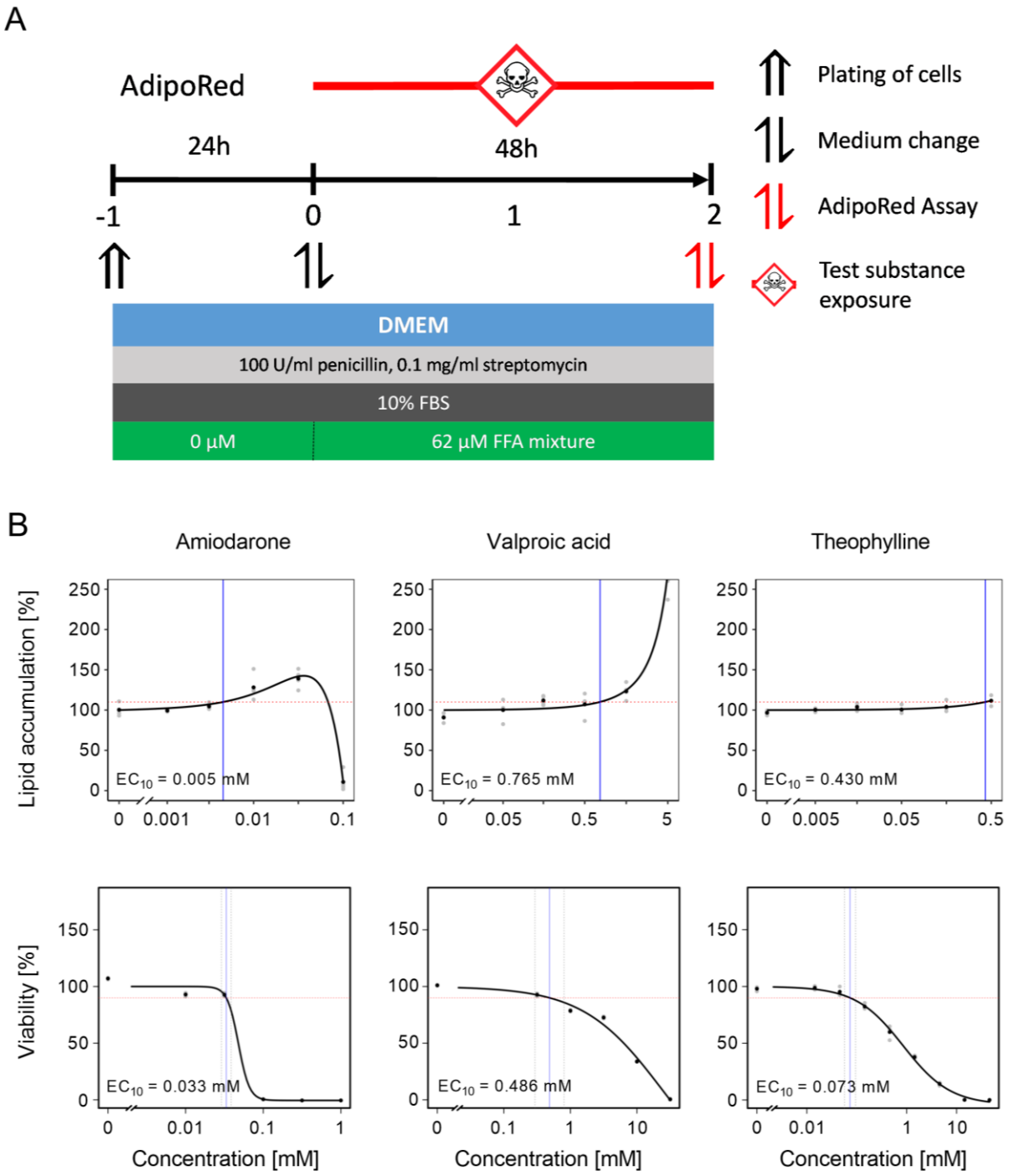

Figure 29: Experimental schedule and exemplary curves of the AdipoRed assay. (A) Graphical experimental schedule. DMEM: Dulbecco's modified eagles medium, FBS: fetal bovine serum, FFA: free fatty acid. **(B)** Exemplary curves with EC_{10} median values of the AdipoRed and CellTiter-Blue assay in HepG2 cells. Grey dots represent the results of three to four technical replicates, black dots denote the concentration-wise mean. Blue and red lines mark the EC_{10} value, grey dotted line the 95% confidence interval.

Results

The compound set consisted of 29 non-hepatotoxic and 29 hepatotoxic compounds for which the blood concentration for a specific, mostly therapeutic, dose was determined. In addition, acetaminophen and ethanol, for which both a hepatotoxic and a non-hepatotoxic treatment scenario was known, were tested. Among the compounds were also a number of those known to induce steatosis in vivo for example amiodarone, methotrexate, and valproic acid. For the majority of the compounds, an EC_{10} value could be determined according to the present protocol of the AdipoRed assay. The initially proposed scenarios (3.3.1) could all be observed, which is illustrated by the exemplary curves (**Figure 29**).

Amiodarone is a hepatotoxic compound that induces steatosis in vivo and is an example for scenario one (**Figure 25**). The EC_{10} for the lipid accumulation is more than a factor 6 below the EC_{10} resulting from the CTB assay. Valproic acid is an anticonvulsant with hepatotoxic side effects at therapeutic doses and is also known to cause steatosis in vivo. The EC_{10} values for lipid accumulation (0.765 mM) and cytotoxicity (0.486 mM) are close together and represent an example of scenario 2. Theophylline is a non-hepatotoxic compound and shows no noticeable lipid accumulation beyond the onset of cytotoxicity (EC_{10} = 0.073 mM).

In total, the CTB assay in PHH and HepG2 cells, as well as the AdipoRed assay in HepG2 cells were performed for 60 compounds. The EC_{10} values, in vivo concentrations, and the toxicity status that was defined for this study are listed in **Table 22**.

Table 22: Summary results of the in vitro test, toxicity status, and in vivo concentration. Minimum, median, and maximum EC_{10} values of the cytotoxicity test in PHH and HepG2 cells are given as well as of the AdipoRed assay in HepG2 cells. For all experiments at least 3 biological replicates were utilized. The in vivo concentration is the 95% percentile of the peak total systemic blood concentration modeled for a specific dose. Raw and processed data is given in the Electronic supplement.

Compound	Abbre-viation	Hepato-toxicity reported	In vivo C_{max} whole blood 95% total [mM]	In vitro cyto-toxicity HepG2 EC_{10} [mM] median [min/max]	In vitro lipid accumulation EC_{10} [mM] median [min/max]	In vitro cyto-toxicity PHH EC_{10} [mM] median [min/max]
Acetaminophen	APAP	no	1.09×10^{-01}	1.576 [1.172/1.962]	0.561 [0.259/0.997]	1.403 [0.5/2.833]
Acetaminophen	APAP	yes	$1.21\times10^{+00}$	1.576 [1.172/1.962]	0.561 [0.259/0.997]	1.403 [0.5/2.833]
Amiodarone	AMIO	yes	3.70×10^{-04}	0.034 [0.033/0.035]	0.005 [0.004/0.008]	>1 [>1/>1]
Aspirin	ASP	yes	2.40×10^{-01}	4.089 [1.752/4.146]	2.132 [1.044/4.774]	4.115 [0.335/>10]
Atorvastatin	AVS	yes	1.50×10^{-05}	0.013 [0.008/0.113]	0.045 [0.029/>0.1]	0.138 [0.065/0.208]
Atropine	ATRO	no	5.38×10^{-06}	0.966 [0.539/1.105]	0.111 [0.107/0.188]	2.238 [0.074/>3.16]

Compound	Abbre-viation	Hepato-toxicity reported	In vivo C_{max} whole blood 95% total [mM]	In vitro cyto-toxicity HepG2 EC_{10} [mM] median [min/max]	In vitro lipid accumulation EC_{10} [mM] median [min/max]	In vitro cyto-toxicity PHH EC_{10} [mM] median [min/max]
Benzbromarone	BZB	yes	1.79×10^{-02}	0.015 [0.011/0.038]	0.037 [0.037/0.038]	0.010 [0.010/0.012]
Benztropine	BZT	no	1.23×10^{-05}	0.024 [0.024/0.045]	0.002 [0.002/0.002]	0.011 [0.007/0.038]
Bosentan	BOS	yes	2.81×10^{-03}	0.028 [0.006/0.350]	0.027 [0.015/0.028]	0.018 [0.003/0.055]
Buspirone	BPR	no	2.90×10^{-05}	0.258 [0.176/0.258]	0.016 [0.015/0.020]	0.013 [0.009/0.026]
Carbamazepine	CBZ	yes	1.81×10^{-02}	0.254 [0.204/>3.16]	0.076 [0.064/0.090]	0.009 [0.002/0.020]
Chlorpheniramine	CHL	no	6.49×10^{-05}	0.081 [0.068/0.087]	0.007 [0.007/0.013]	0.044 [0.014/0.155]
Clofibrate	CLFI	yes	1.47×10^{-05}	>1 [0.023/>1]	0.167 [0.166/>1]	>1 [>1/>1]
Clonidine	CLON	no	9.40×10^{-06}	0.379 [0.060/0.850]	0.124 [0.119/0.229]	0.317 [0.057/0.555]
Codeine	COD	no	2.33×10^{-04}	0.442 [0.409/0.800]	0.082 [0.052/0.223]	0.956 [0.536/1.058]
Cyclosporin A	CSA	yes	7.34×10^{-03}	0.026 [0.026/0.027]	0.003 [0.002/0.007]	0.014 [0.008/0.031]
Diclofenac	DFN	yes	5.42×10^{-03}	0.147 [0.039/0.647]	0.076 [0.067/0.115]	0.115 [0.036/0.143]
Digoxin	DIGI	no	2.15×10^{-06}	0.000029 [0.000016/ 0.000282]	0.000083 [0.000026/ >0.000316]	0.000066 [0.000046/ 0.000136]
Diphenhydramine	DPH	no	5.90×10^{-04}	0.088 [0.086/0.104]	0.008 [0.007/0.012]	0.122 [0.056/0.143]
Dimethyl sulfoxide	DMSO	no	1.08×10^{-01}	134.61 [25.73/ >1400]	379.19 [124.13/ 747.93]	>1400 [21.47/ >1400]
Entacapone	ETC	yes	9.94×10^{-03}	0.001 [0.005/0.017]	0.037 [0.031/0.038]	0.020 [0.017/0.034]
Ethanol	ETOH	no	5.76×10^{-03}	125.77 [62.40/ 128.87]	274.70 [65.90/ >1000]	10.22 [2.05/ 170.50]
Ethanol	ETOH	yes	$1.01\times10^{+01}$	125.77 [62.40/ 128.87]	274.70 [65.90/ >1000]	10.22 [2.05/ 170.50]
Glucose	GLC	no	$7.15\times10^{+00}$	98.54 [86.25/ 141.87]	19.45 [16.36/ 79.22]	119.71 [71.94/ >316]
Hydroxyzine	HYZ	no	4.94×10^{-04}	0.067 [0.032/ 0.097]	>0.5 [>0.5 />0.5]	0.079 [0.045/ 0.094]

Results

Compound	Abbre-viation	Hepato-toxicity reported	In vivo C_{max} whole blood 95% total [mM]	In vitro cyto-toxicity HepG2 EC_{10} [mM] median [min/max]	In vitro lipid accumulation EC_{10} [mM] median [min/max]	In vitro cyto-toxicity PHH EC_{10} [mM] median [min/max]
Ibuprofen	IBU	yes	2.53×10^{-01}	1.133 [0.913/2.530]	0.411 [0.226/0.426]	1.992 [0.948/2.056]
Indomethacin	INDO	yes	3.48×10^{-03}	0.057 [0.035/ 0.117]	0.077 [0.038/ >0.1]	>0.245 [0.081/ >0.245]
Isosorbide dinitrate	ISS	no	1.03×10^{-04}	>0.614 [>0.614/ >0.614]	0.192 [0.083/ 0.262]	0.108 [0.098/ 0.135]
Ketoconazole	KC	yes	1.62×10^{-02}	0.017 [0.002/0.109]	0.002 [0.002/0.019]	0.026 [0.008/0.100]
Lovastatin	LO	yes	8.48×10^{-06}	0.032 [0.002/ 0.069]	0.034 [0.018/ >0.316]	>0.245 [0.024/ >0.245]
Melatonin	MEL	no	2.70×10^{-05}	1.608 [0.995/>10]	0.801 [0.327/1.021]	0.687 [0.040/>5]
Methotrexate	MTX	yes	1.03×10^{-03}	0.00001 [0.000004/ 0.00001]	0.00003 [0.00003/ 0.00003]	>0.033 [>0.033/ >0.033]
N-Acetylcysteine	NAC	no	3.19×10^{-03}	>10 [>10/>10]	2.06 [0.388/6.221]	>10 [0.243/>10]
Nifedipine	NDP	yes	1.16×10^{-03}	0.033 [0.019/ 0.044]	0.012 [0.008/ 0.012]	>0.432 [>0.432/ >0.432]
Oxycodone	OXC	no	9.84×10^{-05}	0.692 [0.155/0.869]	0.177 [0.139/0.221]	1.149 [0.546/6.337]
Oxymorphone	OXM	no	1.13×10^{-05}	>1.997 [>1.997/ >1.997]	1.021 [0.338/ 1.315]	0.028 [0.024/ 0.043]
Pazopanib	PZB	yes	6.20×10^{-02}	>0.189 [>0.189/ >0.189]	0.008 [0.007/ 0.009]	>0.189 [>0.189/ >0.189]
Perhexiline	PRX	yes	8.69×10^{-01}	0.002 [0.002/0.002]	>0.05 [>0.05/>0.05]	0.004 [0.003/0.006]
Pindolol	PIN	no	1.71×10^{-04}	0.163 [0.033/>0.5]	0.062 [0.049/0.129]	>0.5 [>0.5/>0.5]
Pioglitazone	PIO	yes	5.33×10^{-03}	0.112 [0.093/0.161]	0.036 [0.002/0.047]	0.009 [0.008/0.08]
Primaquine	PRIMA	no	6.63×10^{-04}	0.034 [0.018/0.061]	0.022 [0.009/0.026]	0.001 [0.001/0.027]
Primidone	PRI	no	5.48×10^{-02}	>0.5 [>0.5/>0.5]	>0.5 [0.0859/>0.5]	>0.5 [>0.5/>0.5]
Promethazine	PMZ	no	3.27×10^{-05}	0.024 [0.018/0.031]	0.002 [0.002/0.002]	0.014 [0.004/0.032]

Compound	**Abbre-viation**	**Hepato-toxicity reported**	**In vivo C_{max} whole blood 95% total [mM]**	**In vitro cyto-toxicity HepG2 EC_{10} [mM] median [min/max]**	**In vitro lipid accumulation EC_{10} [mM] median [min/max]**	**In vitro cyto-toxicity PHH EC_{10} [mM] median [min/max]**
Propranolol	PPL	no	2.35×10^{-04}	0.043 [0.041/0.053]	>0.316 [0.01/>0.316]	0.021 [0.003/0.080]
Pyridoxine	PDX	no	7.04×10^{-05}	1.998 [1.117/>10]	>3.16 [>3.16/>3.16]	1.023 [0.106/5.082]
Rifampicin	RIF	yes	2.01×10^{-02}	0.508 [0.022/0.941]	0.033 [0.020/0.046]	0.262 [0.121/0.424]
Rosiglitazone	RGZ	yes	5.99×10^{-04}	0.014 [0.013/0.017]	0.003 [0.003/0.092]	0.036 [0.034/0.047]
Rosuvastatin	ROS	yes	9.78×10^{-06}	0.042 [0.002/0.113]	0.001 [0.00/0.002]	0.028 [0.026/0.028]
Simvastatin	SIM	yes	2.15×10^{-05}	0.039 [0.019/0.063]	>0.5 [>0.5/>0.5]	0.020 [0.013/0.046]
Sitaxentan	SXS	yes	1.73×10^{-02}	>0.419 [0.159/ >0.419]	0.054 [0.034/ 0.077]	0.132 [0.086/ 0.184]
4-Phenylbutyrate	SPB	no	9.11×10^{-01}	6.376 [3.125/7.047]	1.044 [0.757/1.442]	1.969 [0.192/>10]
Stavudine	STAVU	yes	2.41×10^{-03}	1.293 [0.765/3.375]	0.869 [0.830/>10]	0.920 [0.913/1.911]
Tetracycline	TC	yes	1.55×10^{-02}	0.114 [0.056/0.700]	0.088 [0.060/0.102]	0.397 [0.397/>1]
Theophylline	THE	no	6.10×10^{-02}	0.073 [0.050/0.178]	0.430 [0.204/>0.5]	0.214 [0.205/0.945]
Tolcapone	TOLC	yes	1.06×10^{-02}	0.014 [0.011/0.022]	0.029 [0.008/0.039]	0.028 [0.02/0.031]
Tolterodine	TTD	no	1.55×10^{-05}	0.072 [0.024/0.116]	0.004 [0.003/0.008]	0.035 [0.025/0.128]
Triclosan	TSN	no	2.60×10^{-04}	0.002 [0.002/ 0.005]	>0.0316 [0.007/ >0.0316]	0.136 [0.047/ 0.250]
Triprolidine	TPL	no	3.16×10^{-05}	0.109 [0.107/0.124]	0.011 [0.010/0.013]	0.161 [0.122/>1.6]
Troglitazone	TROG	yes	2.21×10^{-03}	0.067 [0.035/>0.1]	>1 [>1/>1]	0.011 [0.010/0.022]
Valproic acid	VPA	yes	5.69×10^{-01}	0.486 [0.373/0.756]	0.765 [0.393/2.259]	10.13 [8.46/22.13]
Vitamin C	VITC	no	6.98×10^{-03}	1.094 [0.960/1.629]	2.877 [0.731/>3.16]	3.701 [0.283/>31.6]
Zaleplon	ZAL	no	1.94×10^{-04}	0.088 [0.076/0.154]	0.115 [0.077/0.366]	0.097 [0.016/>0.5]

3.3.4 Evaluation of the AdipoRed assay and comparison of both cell systems

For a detailed analysis which assay is more sensitive for each compound, we calculated log_2 ratios of the EC_{10} median values obtained from the CTB assay in PHH and the AR assay in HepG2 cells. In order to additionally verify which cell system is more sensitive for which compound, also the log_2 ratios of the EC_{10} median values from the CTB assay in PHH and HepG2 were calculated. A log_2 ratio below zero indicates that the CTB assay in PHH is more sensitive, vice versa a ratio above zero suggests that the AR or CTB assay in HepG2 cells is more sensitive.

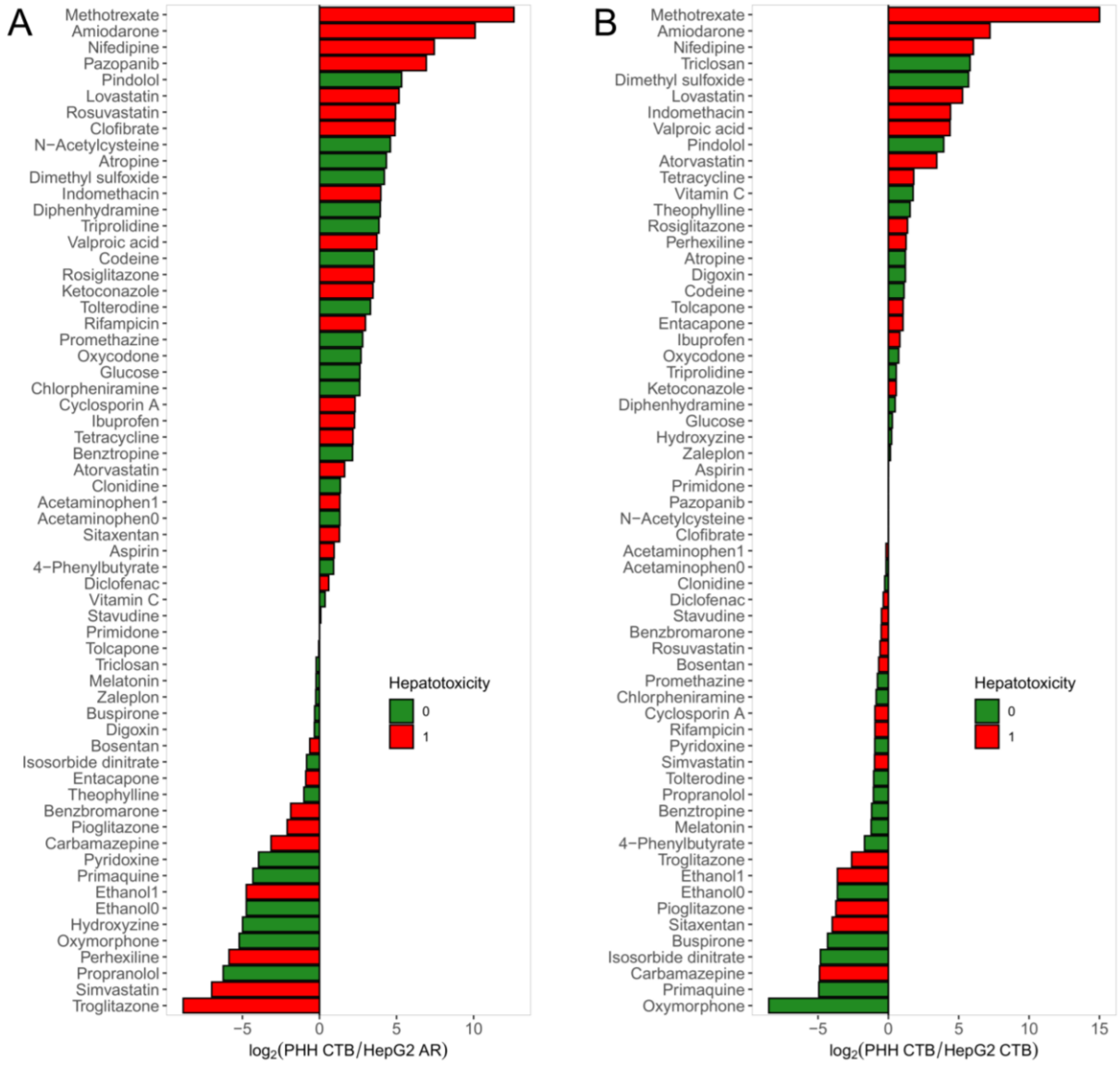

Figure 30: Ratio plots comparing cytotoxicity in PHH to the in vitro assays in HepG2 cells. (A) log_2 values of the EC_{10} median values from the CTB assay in PHH and the AR assay in HepG2 cells. **(B)** log_2 values of the EC_{10} median values from the CTB assay in PHH and the CTB assay in HepG2 cells. Red indicates hepatotoxic compounds/scenarios (1) and green indicates non-hepatotoxic compounds/scenarios (0).

In total, 37 of the tested substances had a log_2 ratio higher than 0, of which approximately 60% were hepatotoxic (**Figure 30**A). Conversely, 22 substances had a log_2 ratio lower than 0. For one substance,

primidone, the same EC value was determined in both assays which resulted in a ratio of 0. In conclusion, the AdipoRed assay in HepG2 cells was more sensitive than the CTB assay in PHH. No increased sensitivity was observed when comparing the cytotoxicity of the two cell systems (PHH vs. HepG2). (**Figure 30**B). Overall, 28 compounds had a log_2 ratio higher and 27 lower than 0, respectively. For 5 compounds no cytotoxicity was observed up to the highest tested concentration in both systems which resulted in a log_2 ratio of 0. Interestingly, the highest ratios were obtained for methotrexate, amiodarone, and nifedipine for both assays in HepG2 cells.

To evaluate whether the detection of lipid accumulation in HepG2 cells would improve our test system and whether the AdipoRed assay should be included in the in vitro test battery, a comprehensive TSI/TEI analysis was performed. Since the test system is based on cytotoxicity in primary human hepatocytes, but the AdipoRed assay was performed in HepG2 cells, the CTB assay in both cell systems and the AdipoRed assay were considered separately and in combination (**Figure 31**).

As in previous studies, the 95% percentile whole blood total concentration was used as in vivo input parameter and for the in vitro parameter the EC_{10} median values of the different assays was utilized. Analysis of the 60 compounds resulted in a TSI of 0.74 and a TEI of 0.67 for cytotoxicity in PHH (**Figure 31**A). The AdipoRed assay alone achieved a TSI of 0.78 and a TEI of 0.74 (**Figure 31**B). When both assays were combined using the respective minimum of both EC_{10} median values, both indices were improved to 0.80 and 0.81 for TSI and TEI, respectively (**Figure 31**D). After determining that the addition of the lipid accumulation data to cytotoxicity improved the indices, the performance of cytotoxicity in HepG2 cells was also considered. This assay alone resulted in TSI and TEI of 0.79 and 0.71 (**Figure 31**C). The combination of both cytotoxicity assays also increased TSI (0.74 → 0.79) and TEI (0.67 → 0.76) compared to PHH alone (**Figure 31**E). A combination of all three assays resulted in a TSI value of 0.80 and thus performed not better compared to the combination of cytotoxicity in PHH and lipid accumulation in HepG2 cells. Overall, it was shown that the addition of cytotoxicity or lipid accumulation in HepG2 to cytotoxicity in PHH resulted in improved separation of the test compounds, while the AdipoRed assay performed slightly better (**Table 23**).

Table 23: TSI and TEI values of the in vitro assays alone and in combination.

	Assay	EC cutoff	TSI	TEI
Single assay	PHH CTB	EC_{10} median	0.74	0.67
	HepG2 AR	EC_{10} median	0.78	0.74
	HepG2 CTB	EC_{10} median	0.79	0.72
Combination	PHH CTB + HepG2 AR	EC_{10} median	0.80	0.81
	PHH CTB + HepG2 CTB	EC_{10} median	0.79	0.76

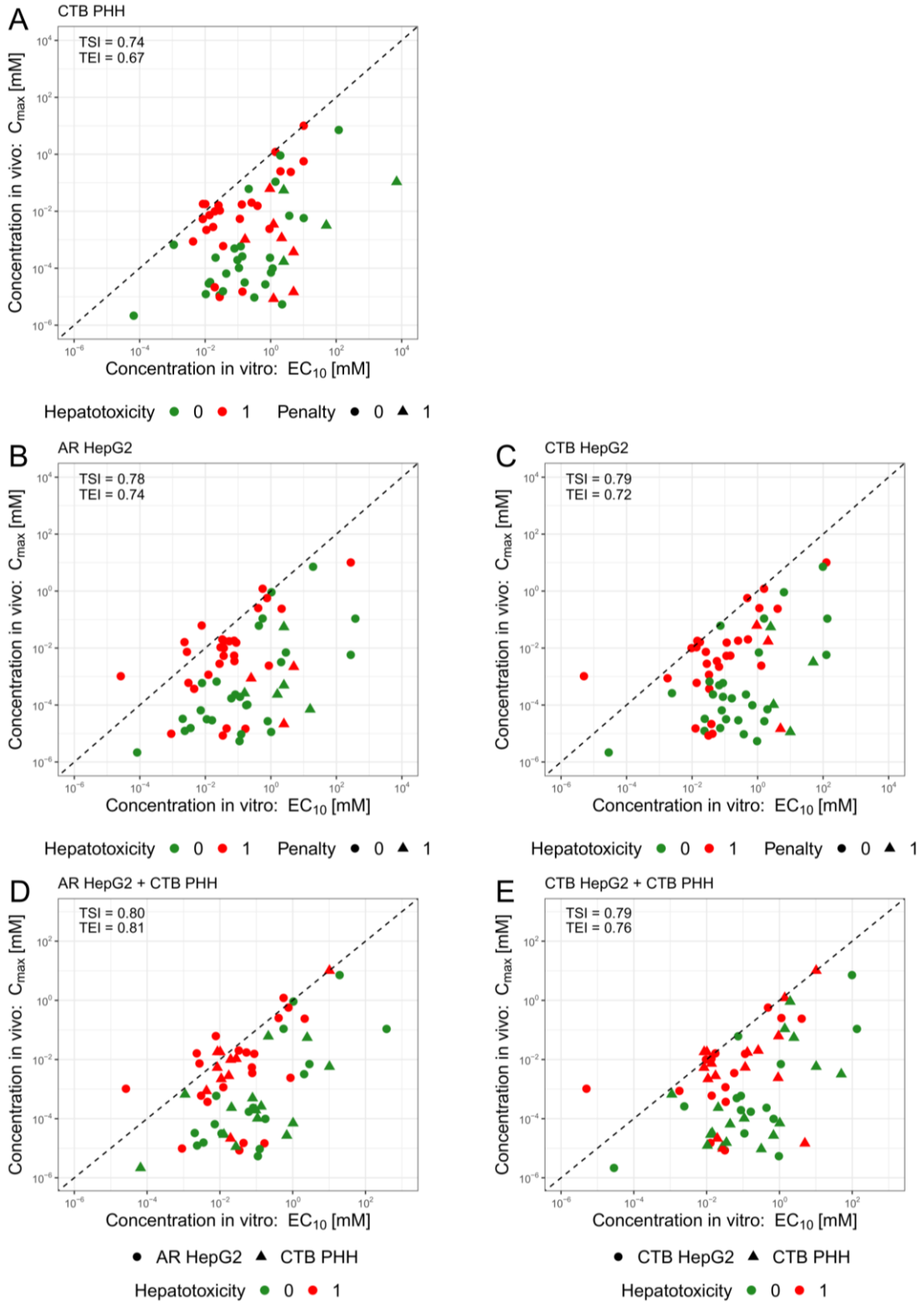

Figure 31: Evaluation of the in vitro assays. Extrapolation plots **(A)** based on cytotoxicity data alone using the EC_{10} median values of the cytotoxicity test in PHH (x-axis) and the C_{max} (total concentration in the blood; 95% percentile); **(B)** based on the AdipoRed assay in HepG2 cells; **(C)** based on the cytotoxicity test in HepG2 cells; **(D)** based on the lower value of either the CTB assay in PHH or the AdipoRed assay in HepG2 cells; **(E)** based on the lower values of either the CTB assay in PHH or HepG2 cells. Red indicates hepatotoxic compounds (1) and green indicates non-hepatotoxic compounds (0). For (A/B/C) a triangle indicates that up to the highest tested concentration no EC values was reached and a penalty factor (x5) was used. For (D/E) the circle and triangle indicate if the CTB in PHH or the other assay resulted in a lower EC_{10} value.

4 Discussion

4.1 Bile acid mix assay

The prediction of drug-induced liver injury by measuring cytotoxicity in primary human hepatocytes has been shown to be suitable in our test system for a selected compound set. In drug-induced cholestatic liver disease, bile acids accumulate in hepatocytes when their excretion is inhibited, leading to cytotoxicity [113]. Therefore, it was previously unclear if it is sufficient to use cytotoxicity as an in vitro readout for DILI analysis, or if inhibition of export carriers as an additional assay was of advantage. One reason that supports conducting both assays arises from the differences in the exposure of hepatocytes to bile acids in vitro and in vivo. In vivo, hepatocytes are constantly exposed to bile acids that are absorbed from the intestine and drained into the liver via the blood of the portal vein [60], [114]. Moreover, cultivated hepatocytes express low levels of Cyp7A1, a key enzyme of bile acid synthesis [104]. Therefore, bile acid accumulation due to export inhibition may result in less toxicity in cultivated hepatocytes than in hepatocytes in vivo. An approach to investigate this is to add bile acids to the culture medium to compensate for the decreased synthesis and exposure via the portal bloodstream. Importantly, this approach has already been performed [83], [115], but not yet analyzed if it improves the differentiation of hepatotoxic and non-hepatotoxic compounds based on quantitative metrics and under other cultivation conditions. Therefore, we studied the susceptibility of cultured human hepatocytes in the presence and absence of a bile acid mix containing the most abundant human bile acids at physiological ratios. If bile acid export carriers are inhibited by a test compound, accumulation of intracellular bile acids can be expected, which may exceed cytotoxic thresholds. In this case, cytotoxicity in the presence of bile acids in the culture medium should occur at lower test compound concentrations compared to the situation without added bile acids.

In contrast to our hypothesis, the addition of a bile acid mix did not improve the separation of hepatotoxic and non-hepatotoxic compounds as quantified by the TSI, nor did it improve the estimation of hepatotoxic blood concentrations. The reason for the negative result is that the bile acid mix did not only increase the susceptibility to hepatotoxic, but also to non-hepatotoxic compounds as well. The hepatotoxic compounds rifampicin, cyclosporin A and ketoconazole are well-known BSEP and MRP2 inhibitors. The addition of bile acids notably increased their cytotoxicity, which agrees with our hypothesis. The hepatotoxic compounds acetaminophen and ethanol act by mechanisms other than bile acid export inhibition and their cytotoxicity was not enhanced by the addition of the bile acid mix, which also supports this approach. In fact, the cytotoxicity of ethanol and acetaminophen was even reduced by the addition of bile acids, which agrees with previous studies [116]–[118]. However, the

major drawback was that the bile acid mix increased the cytotoxicity of three non-hepatotoxic compounds, with glucose showing the strongest enhancement. Glucose is not a known inhibitor of BSEP or MRP2; therefore, other mechanisms not analyzed in this study must be responsible.

The influence of bile acids on the susceptibility of hepatocytes seems to be complex since, in addition to the above described increased susceptibility to the cytotoxic effects of some test chemicals, it also increased resistance to other compounds, with chlorpheniramine, melatonin, and ethanol showing the strongest effects. Bile acids influence hepatocyte physiology by numerous mechanisms, for example via the well-characterized activation of the nuclear receptor FXR [113]. Besides the negative feedback inhibition of bile acid biosynthesis and modification of metabolic functions, FXR activation may also influence susceptibility to chemicals [119]. For example, it has been reported that bile acids are protective against hepatotoxicity due to APAP overdose in mice [120]. Furthermore, the depletion of bile acids by a 2% cholestyramine-containing diet for one week was reported to increase the extent of liver damage and delay regeneration. Conversely, dietary supplementation with cholic acid (0.2%) was shown to ameliorate the damage and support regeneration [120]. Although several open questions still remain from their study, for example, if the cholic acid diet itself induced some damage and regeneration, the results suggest an influence of bile acids on APAP susceptibility. Moreover, FXR has been reported to contribute to the antioxidative capacity by for instance increasing the expression of metallothionein [121] and upregulating chemoresistance genes [122].

It is important to consider that the total bile acid concentration of 0.5 mM added to the culture medium of the hepatocytes is relatively high and is only reached in the blood of mice or patients in the event of severe cholestasis [123], [124]. This high concentration corresponded to approximately 50% of the EC_{10} of the cultivated hepatocytes and was thus chosen in order to reach intracellular bile acid concentrations that were close to cytotoxic levels to be able to detect the cytotoxic consequences of inhibition. This mechanism would be less relevant at much lower concentrations, such as in the range of blood concentrations found in healthy individuals (< 2 µM).

In addition, it should be noted that a total cultivation time of 3 days can lead to the absence or loss of function of the necessary transporters, for example, BSEP and MRP2. Gene expression analysis showed a rapid decrease of BSEP mRNA already after 24 hours of cultivation time (**Figure 17**) and immunofluorescence staining showed that protein was still present, but mainly in the cytoplasm (**Figure 18**). This is a possible reason why transport inhibitors did not specifically increase cytotoxicity in this approach. Furthermore, it is possible that the added bile acids, which were incubated at the same time as the test compound, reacted with it. This is another factor and it cannot be excluded that effects have occurred which do not originate from the pure compound. As a possible optimization

attempt, human bile could be used instead of an artificial bile mix to increase the similarity to the in vivo situation. Although this does not seem suitable for a high-throughput assay and would result in further donor differences.

In conclusion, the effect of the addition of bile acids to the culture medium of cultivated human hepatocytes has complex effects and may significantly enhance or reduce the susceptibility of the cells depending on the individual compound. The addition of bile acids did not improve the in vitro evaluation of hepatotoxicity, because susceptibility to both hepatotoxic and non-hepatotoxic compounds was influenced without any preference to the hepatotoxic compounds in the here evaluated set of compounds.

4.2 CMFDA assay

Since the bile acid mix assay approach was not suitable to specifically detect bile salt transporter inhibition and did not markedly improve neither TSI nor TEI, we further investigated whether we can improve the differentiation of hepatotoxic from non-hepatotoxic compounds, as evaluated by the TSI, by including inhibition of export carriers as a functional in vitro readout in addition to cytotoxicity. Therefore, we established an assay that quantifies the ability of test compounds to inhibit the export of 5-CMF from human hepatocytes. The fluorophore 5-CMF is a substrate of several carriers, including BSEP and MRP2 [101]; therefore, delayed clearance of 5-CMF-associated fluorescence from hepatocytes after exposure to a test compound indicates inhibition of these export carriers. Our results reveal that integration of this inhibition assay with the cytotoxicity assay indeed allowed for a better separation of hepatotoxic and non-hepatotoxic compounds quantified by the TSI. Moreover, it also improved the estimation of hepatotoxic blood concentrations by the TEI.

With regard to the in vitro in vivo differences in bile acid concentrations discussed earlier, one advantage of the CMFDA assay presented here is the quantification of the inhibition of 5-CMF secretion, and thus an accumulation of bile acids up to cytotoxic levels due to this export inhibition is not required. Therefore, the results of the CMFDA assay will not be compromised if bile acid homeostasis of the cultivated hepatocytes deviates from the in vivo situation, because the export inhibiting concentrations of the test compounds are based on an exogenously administered fluorophore.

A further alternative to the here-established export assay and the bile acid mix assay is a technique based on artificial membrane vesicles that contain proteins, e.g. BSEP. This assay has been reported to detect BSEP inhibition at relatively low concentrations [125]. For example, an inhibitory concentration (IC_{50}) of 0.5 µM for BSEP and 14.5 µM for MRP2 was reported for cyclosporine A [125]. These values

are similar to those obtained by the CMFDA assay in the present study (0.6 µM). An advantage of the vesicle assay is that it provides specific information, which carrier is inhibited, which is not easily possible by the hepatocyte export assay, since CMFDA/5-CMF in addition to being a substrate for the canalicular exporters MRP2 and BSEP, also appear to be transported by BCRP and MDR1/P-GP [126]. This does not invalidate the concept of the CMFDA assay but complicates the mechanistic explanation of toxicity for a certain compound if non bile acid efflux transporters are involved. For example, entacapone may be a more potent inhibitor of BCRP [127] than BSEP. On the other hand, the present CMFDA assay is performed in human hepatocytes with drug-metabolizing capacity that would not be provided by the vesicle assay. Thus, future work should compare the here-established CMFDA assay to the vesicle assay with respect to the TSI and TEI in the same set of compounds.

An important aspect in test development is the choice of adequate culture conditions. First, we asked, if mouse hepatocytes cultivated as a spheroid or as a sheet of cells are more suitable. Because of the reproducible kinetics we decided to continue with hepatocytes cultivated as sheets, either as sandwich or monolayer cultures; in contrast, individual cells in the spheroids showed a high degree of variability which was not observed in vivo. It has been reported that SC may allow for better long-term maintenance of differentiated hepatocellular functions than conventional cell cultures, but on the other hand, they also require greater experimental effort [60]. Our results do not indicate that the sandwich culture of human hepatocytes has an advantage over the monolayer culture concerning export kinetics. This may be because the here-established method represents a short-term assay with only one hour of test compound incubation followed by 20 min of substrate (CMFDA) exposure. Further advantages of the monolayer culture include the rapid and homogeneous uptake of CMFDA into all cultivated hepatocytes, the reproducible export kinetics, and that the technique is easy to standardize.

To minimize the experimental workload, we investigated if it was necessary to test all compounds in the CMFDA assay for export inhibition, or if we could use an in silico method to identify a subset of compounds with a high probability of a negative experimental result so that these negatively predicted compounds would not require testing with the CMFDA assay. The here-applied machine learning approach for BSEP, MRP3 and MRP4 inhibition [91] identified 16 of 17 compounds that inhibited 5-CMF export in hepatocytes. Thus, the in silico technique may indeed reduce the experimentally required effort, but a higher number of compounds must be studied before a recommendation for routine application is possible. Furthermore, the addition of MRP2 inhibition, for which there is currently no model available, could improve the prediction. Compounds identified as export inhibitors by the in silico tool still require experimental testing, because the EC_{10} cannot be obtained in silico.

A limitation of the established CMFDA assay is that the set of tested hepatotoxic compounds consisted mostly of known BSEP and/or MRP2 inhibitors. Although the analysis of 'gold standard compounds' represents an essential first step in test system development [128], the method must next be tested on a large, representative set of hepatotoxic and non-hepatotoxic compounds. Our selection of hepatotoxic compounds that act as export carrier inhibitors may also explain the very high TSI based on the CMFDA assay alone. Such a high TSI may decrease in a representative set of hepatotoxic compounds for which mechanisms other than export inhibition are relevant. However, good separation may still be possible by including cytotoxicity assays, and eventually other functional tests.

In conclusion, a short-term in vitro test has been established that allows for the detection of bile acid export carrier inhibition in cultivated human hepatocytes. When used in combination with a cytotoxicity test, this method improves the identification of DILI compounds compared to cytotoxicity analysis alone in a set of compounds where export carrier inhibition is relevant for hepatotoxicity.

4.3 AdipoRed assay

In order to provide another assay for the in vitro test battery and thus to better predict DILI, the AdipoRed assay was developed. In this assay, compound-induced lipid accumulation in HepG2 cells is determined. Lipid accumulation and degradation is a natural cellular process in the liver and is used for maintaining the energy homeostasis. If these natural processes are disturbed, for example by stress, excess lipid accumulation may occur inside the cell. Abnormal lipid accumulation, also known as steatosis, is a mild and usually reversible form of liver damage. However, if the underlying causes are not addressed, steatohepatitis and fibrosis may follow.

To investigate the lipid accumulation in vitro, HepG2 cells were incubated simultaneous with free fatty acids and the test compound. Intracellular lipids were stained with AdipoRed, a commercially available dye for triglycerides, and subsequently fluorescence was detected via a plate reader. Quantitative analysis with the TSI and TEI showed that integration of the AdipoRed assay in HepG2 cells to cytotoxicity in PHH led to improved separation of hepatotoxic and non-hepatotoxic compounds. Furthermore, it also improved the estimation of hepatotoxic blood concentrations measured by the TEI.

It was shown by several other researchers that the addition of free fatty acids to the culture medium of HepG2 cells increases lipid accumulation and therefore this culture system is utilized as a simple steatosis cell model [110]. To confirm this, we investigated how HepG2 cells respond to increasing concentrations of FFA. The concentration-dependent increase shown here and the irrelevance of incubation time are consistent with other studies [111], [129], [130]. However, there were differences

in the FFA concentrations used. For example, in a study by Gomez-Lechon et al. [111], cells tolerated concentrations of at least 1 mM of the FFA mix, whereas in this study, the cells showed strong changes in the monitored viability markers already at a concentration of 0.5 mM. This may be due to several reasons, such as the different medium which was used, the different serum concentration, or the cell number that was seeded.

After showing that lipid accumulation can be induced in HepG2 cells, we investigated whether the original lipid accumulation protocol could be improved. Simultaneous and prolonged incubation of the test substance and FFA increased the intracellular lipid content. However, it was observed that a similar degree of lipid accumulation was also caused by the test substance only. Further tests are required to determine whether this is substance-specific or a general effect. By omitting FFA, the protocol could be simplified. In addition, there would be one less influencing factor. It should be noted that FFA binds to albumin and thus decreases the free protein concentration in the culture medium [131]. This has an impact on the actual effective test compound concentration. Furthermore, test compounds can influence the binding of FFA to albumin or bind to FFA directly which might also influence the lipid accumulation and processes inside the cell [131]–[133].

Contrary to our expectations, the AdipoRed assay produced a positive result (finite EC value) for the majority of compounds (52/60). This suggests that lipid accumulation is not a very specific effect, limited to a small fraction of compounds like the export inhibition of the CMFDA assay. An explanation might be that altered mitochondrial functions and ER stress which are caused by a majority of drugs, are leading mechanisms for excess lipid accumulation which results finally in cell death. Therefore, lipid accumulation could be seen as an upstream marker for cytotoxicity which means that most drugs would lead to steatosis at a certain concentration. To test this theory it would be interesting to investigate whether the compounds that are not considered to induce steatosis in vivo would lead to steatosis at doses higher than their therapeutic one.

However, there were also differences between cytotoxicity and lipid accumulation. For 6 substances that resulted in effective concentrations in the AdipoRed assay, no cytotoxicity was detected up to the highest concentration tested. Similarly, 7 substances showed no increased lipid accumulation up to the highest concentration tested, which was cytotoxic. The reasons for this may be the substances themselves or the assay design. In order to be able to recognize a clear pattern, more compounds have to be tested. Only one compound, Primidone, was not detected by either assay; which might be due to the solubility limit of 0.5 mM.

In addition to lipid accumulation, the measured cytotoxicity in HepG2 was also able to improve both test parameters (TSI & TEI) compared to cytotoxicity in PHH alone. One possible reason could be that

the transporter functions in HepG2 cells are altered and thus toxins cannot be transported out of the cell or can only be exported slowly. In addition, the cells have the ability to proliferate. If a compound interferes with this process, the usage of HepG2 cells may provide an advantage compared to PHH.

In summary, the AdipoRed assay allows the measurement of lipid accumulation in HepG2 cells and a combination with the CTB assay in PHH leads to an improvement in the separation of hepatotoxic and non-hepatotoxic compounds, as well as a better estimation of in vivo blood concentrations. Similarly, it has been shown that the inclusion of cytotoxicity in HepG2 leads to better performance.

4.4 Considerations for developing in vitro assays

Many factors need to be considered when establishing a test system based on in vitro methods, such as the cell type, the culture format, the choice of test compounds, and, of course, the test method.

Primary cells and cell lines may possess similar functions and properties in the cell culture dish as they had in their original organ, for example, primary hepatocytes are known for their metabolic activity and the expression of liver-specific transporters such as BSEP [134]. Primary cells usually have a greater similarity to the in vivo situation. Compared to primary human hepatocytes, HepG2 cells have a lower expression of CYP-enzymes and bile salt transporters, which are important for detoxification [64], [135]. Studies showed that the lack of transporter activity in HepG2 cells argues for the use of PHH for the investigation of bile salt transport. In the case of lipid metabolism, it was shown that HepG2 cells are suitable as an in vitro model and represent a cost-effective yet efficient alternative to the 'gold standard' PHH [111]. Similarly, the consideration of cytotoxicity in HepG2 cells resulted in higher TSI and TEI values compared to PHH. This shows that the use of supposedly simpler cell systems can indeed be suitable for certain questions.

Cell properties and functions such as cell metabolism, gene expression, or the formation of bile canaliculi can be enhanced or influenced by specific culture formats. For example, the cultivation of primary human hepatocytes between extracellular matrix layers leads to polarization and the formation of bile canalicular structures, which is the preferred method for studying bile salt transport [81]. In this thesis, however, it was shown that transport kinetics can also be studied in a monolayer format. This allows, for example, the use of fluorescence plate readers, which cannot distinguish between intracellular and canalicular fluorescence. A major focus is also on the use of spheroids, in which cells are cultured in spherical shape as small organoids. This has the advantage that the cells can be cultured for longer periods and thus longer exposure studies can be performed [70], [136]. Whether this is necessary for the prediction of hepatotoxicity has not yet been determined. We were able to show that longer cultivation and exposure (7 days) was worse in separating hepatotoxic and non-

hepatotoxic compounds compared to two days, at least in the monolayer format [79]. Similarly, spheroids do not resemble cell morphology in vivo. In vivo, hepatocytes are present in layers (**Figure 13**) and not as a cell sphere. In addition, quantification is more complicated compared to the sandwich or monolayer format (**Figure 14**). In summary, each culture format has its advantages and disadvantages, the choice depends on the specific question and the mechanism to be investigated.

Another aspect in addition to the choice of a cell system and culture format is the cell type. Since an organ does not consist of only one cell type, efforts are being made to develop more in vivo similar systems using co-cultures of several cell types, for example, by co-culturing hepatocytes and NPCs [137], [138]. The interactions of both cell types with each other again influence the properties and functions. There are also major interactions not only between different cell types but also between the individual organs in the body. For example, the liver interacts strongly with the digestive system by secreting bile and subsequently recycling bile acids and nutrients from the intestine. Furthermore, it is assumed that the gut microbiota plays a role in some liver diseases [139], [140]. In order to investigate interactions of different organs in vitro, so-called 'organ or bodies on a chip' are created, in which several organ-like cell systems can interact with one another [141]–[143].

The choice of test compounds for a test set is essential for the establishment of a test system. It is particularly important that the effects in vivo are known, for example for this test system the toxicity status for a certain exposure scenario and certain properties such as the inhibition of the bile salt transporters [128]. Only if the developed tests detect the known drugs, there is a chance that one can predict with high probability the effect/impact of unknown compounds. It should be kept in mind that the performance of a selected set such as the CMFDA assay is quite high and is likely to decrease if the test set is extended.

In addition to the limitations just discussed, other limitations must be considered when selecting a compound. One important aspect is the solubility of the test compound. It is of interest to achieve cytotoxic concentrations, which is not always possible due to the low solubility of the test compound. In addition, pH changes may occur due to the test compound, making it impossible to increase the concentration. In order to achieve higher concentrations of a test compound, solvents such as DMSO and EtOH can be used, whereby an appropriate solvent control must always be included in order to exclude cytotoxic effects due to the solvent. In addition, it is possible to use salts of the corresponding test compounds, as these usually have a higher solubility in water. Another point to consider is the availability of the test compounds. Regulatory issues such as the ‘Betäubungsmittelgesetz’ or other reasons like the withdrawal of drugs years ago can influence the compound selection. Further limitations come from the availability of in vivo information of the test compounds. Since in vivo

modeling by itself only gives estimates, the underlying data must be as precise as possible. In addition, a specific exposure scenario is needed to validate a model. This is a particular problem for compounds that have not been tested in clinical studies. In summary, one should always establish an assay with a smaller set of well-known compounds and then expand the test set for validation.

When selecting the test method, there are many different possibilities, such as the fluorescence measurement of certain compounds with a microscope or a plate reader, gene expression measurement of certain marker genes, or the staining of intracellular components. For easy handling, possible automatization, and thus testing of many compounds, the use of a fluorescence plate reader is particularly suitable, which is why all three assays were developed and adapted for it. Fluorescence measurement with microscope images is more sensitive and allows the differentiation of, for example, extracellular and canalicular fluorescence, as well as other parameters such as the displacement or morphology of cellular compartments. However, this requires more effort, takes longer, and requires the establishment of automated detection software. All in all, there are many different possibilities and options. This has great potential, but can also be detrimental if the wrong choice is made. Therefore, it is essential to quantify the performance of a test system and the individual assays as in this thesis by the TSI and TEI. This allows us to determine directly whether the addition of a test makes sense and which is the most suitable parameter.

4.5 Conclusion

The aim of this work was to extend the in vitro battery of the test system of Albrecht et al. 2019 [79] by implementing new assays to achieve a better separation between hepatotoxic and non-hepatotoxic compounds and thus allow a more reliable prediction of DILI. This was targeted with functional readouts investigating mechanisms of clinical liver diseases. First, cholestasis, which is characterized by impaired bile production and secretion, and second, steatosis, which is characterized by abnormal lipid accumulation in the cells. For the first one, two assays (BAM and CMFDA) were developed, which target the inhibition of bile acid transport, and for the second one (AdipoRed), which targets compound-induced lipid accumulation. The performance of the different assays was evaluated with the toxicity separation index and the toxicity estimation index. Application of the BAM assay alone did not increase the TSI or TEI and a combination with the cytotoxicity assay also did not lead to a noticeable improvement. The subsequently developed CMFDA assay was able to specifically detect bile acid inhibitors at non-cytotoxic concentrations and the combination with the cytotoxicity assay resulted in a distinct increase of both indices. Likewise, the AdipoRed assay resulted in a higher TSI and TEI in combination with the cytotoxicity assay. Our recommendation is therefore to use the cytotoxicity

assay in PHH, the CMFDA assay in PHH, and the AdipoRed assay in HepG2 cells combined in an in vitro test battery (**Figure 32**).

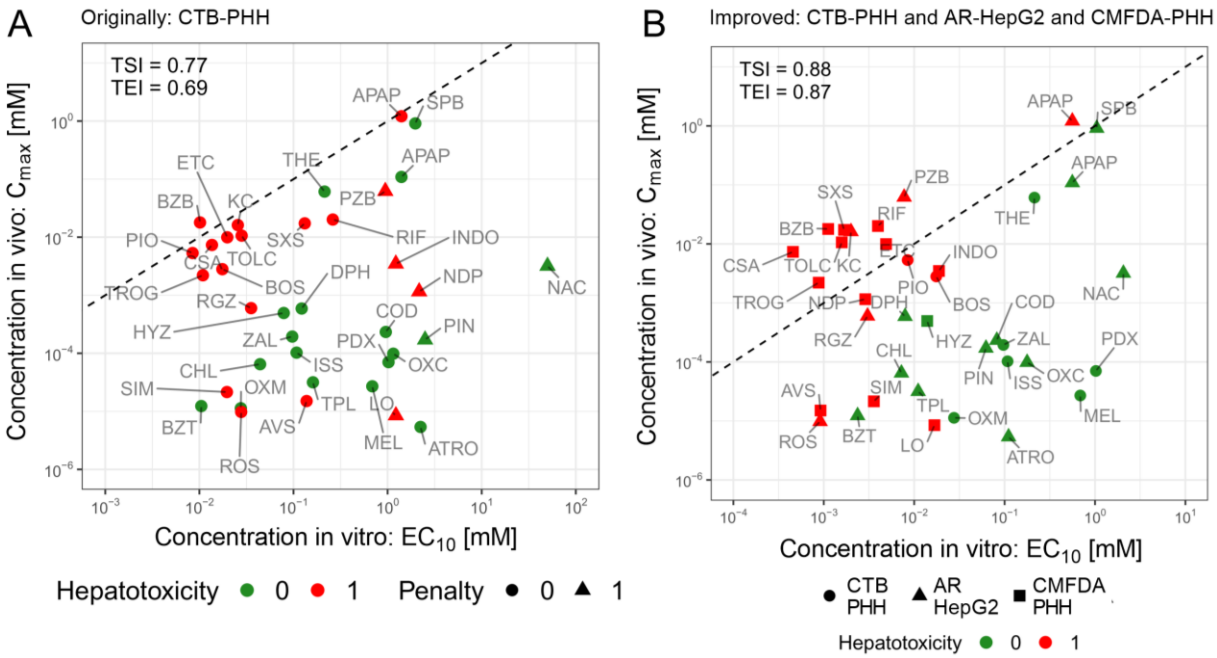

Figure 32: Comparison of the originally and improved in vitro test battery results. (A) Extrapolation plot based on cytotoxicity data using the EC_{10} median values of the cytotoxicity test in PHH (x-axis) and the C_{max} (total concentration in the blood; 95%-CI); **(B)** based on the lower EC_{10} median value of the CTB assay in PHH, AdipoRed assay in HepG2 and the CMFDA assay in PHH. The dotted line represents the iso-line at which the in vivo and in vitro concentration is the same. Red indicates hepatotoxic compounds (1) and green indicates non-hepatotoxic compounds (0). For (A) a triangle indicates that up to the highest tested concentration no EC value was reached and a penalty factor (x5) was used. For (B) the circle, triangle, and square indicate if the CTB assay in PHH, AdipoRed assay in HepG2 or the CMFDA assay in PHH resulted in a lower EC_{10} value, respectively.

The aim of this work was to improve the in silico/in vitro test system for the prediction of DILI by including additional in vitro tests addressing DILI relevant mechanisms. This was achieved with the development and subsequent validation of the CMFDA assay and the AdipoRed assay. In addition, interesting information was obtained through the work on the bile acid mix assay. As discussed before, the results of this thesis need to be validated with a larger and representative set of compounds. This set should consist of at least 100 substances which cover the different DILI relevant mechanisms. Subsequent validation will identify potential shortcomings and help to improve the test system. The successfully developed test system can finally be used in the preclinical phase to identify potentially harmful drug candidates and to perform risk assessment for already existing compounds.

5 References

[1] E. Trefts, M. Gannon, and D. H. Wasserman, “The liver,” *Current Biology*, vol. 27, no. 21. pp. R1147–R1151, 2017, doi: 10.1016/j.cub.2017.09.019.

[2] A. Kalra, E. Yetiskul, C. J. Wehrle, and F. Tuma, *Physiology, Liver*. Central Michigan University College of Medicine: StatPearls Publishing, Treasure Island (FL), 2020.

[3] M. M. Adeva-Andany, N. Pérez-Felpete, C. Fernández-Fernández, C. Donapetry-García, and C. Pazos-García, “Liver glucose metabolism in humans,” *Biosci. Rep.*, vol. 36, no. 6, p. 416, 2016, doi: 10.1042/BSR20160385.

[4] M. Enjoji, M. Kohjima, and M. Nakamuta, “Lipid metabolism and the liver,” in *The Liver in Systemic Diseases*, 2016, pp. 105–122.

[5] C. L. Wu, S. P. Zhao, and B. L. Yu, “Intracellular role of exchangeable apolipoproteins in energy homeostasis, obesity and non-alcoholic fatty liver disease,” *Biol. Rev.*, vol. 90, no. 2, pp. 367–376, May 2015, doi: 10.1111/brv.12116.

[6] P. Nguyen *et al.*, “Liver lipid metabolism,” *J. Anim. Physiol. Anim. Nutr. (Berl).*, vol. 92, no. 3, pp. 272–283, Jun. 2008, doi: 10.1111/j.1439-0396.2007.00752.x.

[7] Y. Wen, J. Lambrecht, C. Ju, and F. Tacke, “Hepatic macrophages in liver homeostasis and diseases-diversity, plasticity and therapeutic opportunities,” *Cellular and Molecular Immunology*, vol. 18, no. 1. Nature Publishing Group, pp. 45–56, Oct. 12, 2021, doi: 10.1038/s41423-020-00558-8.

[8] D. P. Bogdanos, B. Gao, and M. E. Gershwin, “Liver immunology,” *Compr. Physiol.*, vol. 3, no. 2, pp. 567–598, 2013, doi: 10.1002/cphy.c120011.

[9] M. Hundt and S. John, “Physiology, Bile Secretion,” *StatPearls*, Oct. 2018, Accessed: Aug. 18, 2021. [Online]. Available: http://www.ncbi.nlm.nih.gov/pubmed/29262229.

[10] D. M. Grant, “Detoxification Pathways in the Liver,” in *Journal of Inherited Metabolic Disease*, Springer, Dordrecht, 1991, pp. 421–430.

[11] D. A. J. Liska, “The detoxification enzyme systems,” *Altern. Med. Rev.*, vol. 3, no. 3, pp. 187–198, 1998.

[12] U. M. Zanger, M. Turpeinen, K. Klein, and M. Schwab, “Functional pharmacogenetics/genomics of human cytochromes P450 involved in drug biotransformation,” *Anal. Bioanal. Chem.*, vol. 392, no. 6, pp. 1093–1108, Aug. 2008, doi: 10.1007/s00216-008-2291-6.

[13] B. Meunier, S. P. de Visser, and S. Shaik, “Mechanism of oxidation reactions catalyzed by cytochrome P450 enzymes,” *Chem. Rev.*, vol. 104, no. 9, pp. 3947–3980, Sep. 2004, doi: 10.1021/cr020443g.

[14] P. Jancova, P. Anzenbacher, and E. Anzenbacherova, “Phase II drug metabolizing enzymes,” *Biomed. Pap.*, vol. 154, no. 2, pp. 103–116, 2010, doi: 10.5507/bp.2010.017.

[15] U. Apte and P. Krishnamurthy, “Detoxification Functions of the Liver,” pp. 147–163, 2011, doi: 10.1007/978-1-4419-7107-4_11.

[16] D. E. Amacher, “The primary role of hepatic metabolism in idiosyncratic drug-induced liver injury,” *Expert Opin. Drug Metab. Toxicol.*, vol. 8, no. 3, pp. 335–347, Mar. 2012, doi:

10.1517/17425255.2012.658041.

[17] S. Phang-Lyn and V. A. Llerena, “Biochemistry, Biotransformation,” *StatPearls*, Sep. 2020, Accessed: Aug. 20, 2021. [Online]. Available: http://www.ncbi.nlm.nih.gov/pubmed/31335073.

[18] H. Orhan, “Extrahepatic Targets and Cellular Reactivity of Drug Metabolites,” *Curr. Med. Chem.*, vol. 22, no. 4, pp. 408–437, 2015, doi: 10.2174/0929867321666140826113716.

[19] B. L. Woolbright, C. D. Williams, M. R. McGill, and H. Jaeschke, “Liver Toxicity,” *Ref. Modul. Biomed. Sci.*, Jan. 2014, doi: 10.1016/b978-0-12-801238-3.00205-1.

[20] X. Chu *et al.*, “Intracellular drug concentrations and transporters: Measurement, modeling, and implications for the liver,” *Clin. Pharmacol. Ther.*, vol. 94, no. 1, pp. 126–141, Jul. 2013, doi: 10.1038/clpt.2013.78.

[21] N. Kaplowitz, “Drug-Induced Liver Injury,” *Clin. Infect. Dis.*, vol. 38, no. SUPPL. 2, pp. S44–S48, Mar. 2004, doi: 10.1086/381446.

[22] D. Larrey and G.-P. Pageaux, “Drug-induced acute liver failure,” *Eur. J. Gastroenterol. Hepatol.*, vol. 17, no. 2, 2005, [Online]. Available: https://journals.lww.com/eurojgh/Fulltext/2005/02000/Drug_induced_acute_liver_failure.2.aspx.

[23] W. M. Lee, “Drug-Induced Hepatotoxicity,” *http://dx.doi.org/10.1056/NEJMra021844*, vol. 349, no. 5, pp. 474–485, Oct. 2009, doi: 10.1056/NEJMRA021844.

[24] R. J. Andrade *et al.*, “Drug-induced liver injury: An analysis of 461 incidences submitted to the Spanish registry over a 10-year period,” *Gastroenterology*, vol. 129, no. 2, pp. 512–521, 2005, doi: 10.1016/j.gastro.2005.05.006.

[25] N. Chalasani *et al.*, “Causes, Clinical Features, and Outcomes From a Prospective Study of Drug-Induced Liver Injury in the United States,” *Gastroenterology*, vol. 135, no. 6, 2008, doi: 10.1053/j.gastro.2008.09.011.

[26] B. Bégaud, K. Martin, F. Haramburu, and N. Moore, “Rates of spontaneous reporting of adverse drug reactions in France [3],” *J. Am. Med. Assoc.*, vol. 288, no. 13, p. 1588, Oct. 2002, doi: 10.1001/jama.288.13.1588.

[27] E. S. Björnsson, O. M. Bergmann, H. K. Björnsson, R. B. Kvaran, and S. Olafsson, “Incidence, presentation, and outcomes in patients with drug-induced liver injury in the general population of iceland,” *Gastroenterology*, vol. 144, no. 7, 2013, doi: 10.1053/j.gastro.2013.02.006.

[28] E. S. Björnsson, “Incidence and outcomes of DILI in Western patients,” *Clin. Liver Dis.*, vol. 4, no. 1, pp. 9–11, 2014, doi: 10.1002/cld.368.

[29] W. M. Lee, “Acetaminophen (APAP) hepatotoxicity—Isn’t it time for APAP to go away?,” *J. Hepatol.*, vol. 67, no. 6, pp. 1324–1331, Dec. 2017, doi: 10.1016/j.jhep.2017.07.005.

[30] B. H. Norman, “Drug Induced Liver Injury (DILI). Mechanisms and Medicinal Chemistry Avoidance/Mitigation Strategies,” *J. Med. Chem.*, vol. 63, no. 20, pp. 11397–11419, Oct. 2020, doi: 10.1021/acs.jmedchem.0c00524.

[31] S. Russmann, G. Kullak-Ublick, and I. Grattagliano, “Current Concepts of Mechanisms in Drug-Induced Hepatotoxicity,” *Curr. Med. Chem.*, vol. 16, no. 23, pp. 3041–3053, Jul. 2009, doi: 10.2174/092986709788803097.

[32] N. Noureddin and N. Kaplowitz, “Overview of mechanisms of drug-induced liver injury (DILI) and key challenges in DILI research,” *Methods Pharmacol. Toxicol.*, no. 9781493976768, pp. 3–18, 2018, doi: 10.1007/978-1-4939-7677-5_1.

[33] I. Grattagliano, L. Bonfrate, C. V. Diogo, H. H. Wang, D. Q. H. Wang, and P. Portincasa, “Biochemical mechanisms in drug-induced liver injury: Certainties and doubts,” *World J. Gastroenterol.*, vol. 15, no. 39, pp. 4865–4876, 2009, doi: 10.3748/wjg.15.4865.

[34] M. D. Aleo, Y. Luo, R. Swiss, P. D. Bonin, D. M. Potter, and Y. Will, “Human drug-induced liver injury severity is highly associated with dual inhibition of liver mitochondrial function and bile salt export pump,” *Hepatology*, vol. 60, no. 3, pp. 1015–1022, Sep. 2014, doi: 10.1002/hep.27206.

[35] M. Vairetti, L. G. Di Pasqua, M. Cagna, P. Richelmi, A. Ferrigno, and C. Berardo, “Changes in glutathione content in liver diseases: An update,” *Antioxidants*, vol. 10, no. 3, pp. 1–39, Mar. 2021, doi: 10.3390/antiox10030364.

[36] Y. Wei, R. S. Rector, J. P. Thyfault, and J. A. Ibdah, “Nonalcoholic fatty liver disease and mitochondrial dysfunction,” *World J. Gastroenterol.*, vol. 14, no. 2, pp. 193–199, Jan. 2008, doi: 10.3748/wjg.14.193.

[37] D. Pessayre and B. Fromenty, “NASH: A mitochondrial disease,” *J. Hepatol.*, vol. 42, no. 6, pp. 928–940, Jun. 2005, doi: 10.1016/j.jhep.2005.03.004.

[38] R. J. Weaver *et al.*, “Managing the challenge of drug-induced liver injury: a roadmap for the development and deployment of preclinical predictive models,” *Nat. Rev. Drug Discov.*, vol. 19, no. 2, pp. 131–148, 2020, doi: 10.1038/s41573-019-0048-x.

[39] T. M. Šarenac and M. Mikov, “Bile acid synthesis: From nature to the chemical modification and synthesis and their applications as drugs and nutrients,” *Front. Pharmacol.*, vol. 9, no. SEP, p. 939, Sep. 2018, doi: 10.3389/fphar.2018.00939.

[40] M. Schonewille, J. F. De Boer, and A. K. Groen, “Bile salts in control of lipid metabolism,” *Curr. Opin. Lipidol.*, vol. 27, no. 3, pp. 295–301, 2016, doi: 10.1097/MOL.0000000000000303.

[41] I. A. Brownlee, D. J. Forster, M. D. Wilcox, P. W. Dettmar, C. J. Seal, and J. P. Pearson, “Physiological parameters governing the action of pancreatic lipase,” *Nutr. Res. Rev.*, vol. 23, no. 1, pp. 146–154, 2010, doi: 10.1017/S0954422410000028.

[42] G. R. Thompson, “Absorption of fat-soluble vitamins and sterols,” *J. Clin. Pathol.*, vol. S3-5, no. 1, pp. 85–89, 1971, doi: 10.1136/jcp.s3-5.1.85.

[43] J. L. Boyer, “Bile formation and secretion,” *Compr. Physiol.*, vol. 3, no. 3, pp. 1035–1078, 2013, doi: 10.1002/cphy.c120027.

[44] H. M. Cheng, K. K. Mah, and K. Seluakumaran, “Recycling of Bile Salts: Enterohepatic Circulation (EHC),” *Defin. Physiol. Princ. Themes, Concepts. Vol. 2*, pp. 43–45, 2020, doi: 10.1007/978-3-030-62285-5_12.

[45] C. J. Soroka, J. M. Lee, F. Azzaroli, and J. L. Boyer, “Cellular localization and up-regulation of multidrug resistance-associated protein 3 in hepatocytes and cholangiocytes during obstructive cholestasis in rat liver,” *Hepatology*, vol. 33, no. 4, pp. 783–791, 2001, doi: 10.1053/jhep.2001.23501.

[46] G. U. Denk, C. J. Soroka, Y. Takeyama, W. S. Chen, J. D. Schuetz, and J. L. Boyer, “Multidrug resistance-associated protein 4 is up-regulated in liver but down-regulated in kidney in obstructive cholestasis in the rat,” *J. Hepatol.*, vol. 40, no. 4, pp. 585–591, Apr. 2004, doi:

10.1016/j.jhep.2003.12.001.

[47] M. Wagner, G. Zollner, and M. Trauner, “New molecular insights into the mechanisms of cholestasis,” *J. Hepatol.*, vol. 51, no. 3, pp. 565–580, Sep. 2009, doi: 10.1016/j.jhep.2009.05.012.

[48] R. J. Andrade *et al.*, “EASL Clinical Practice Guidelines: Drug-induced liver injury,” *J. Hepatol.*, vol. 70, no. 6, pp. 1222–1261, 2019, doi: 10.1016/j.jhep.2019.02.014.

[49] T. H. Lee, W. R. Kim, and J. J. Poterucha, “Evaluation of Elevated Liver Enzymes,” *Clin. Liver Dis.*, vol. 16, no. 2, pp. 183–198, May 2012, doi: 10.1016/j.cld.2012.03.006.

[50] G. M. Hirschfield, “Genetic Determinants of Cholestasis,” *Clin. Liver Dis.*, vol. 17, no. 2, pp. 147–159, May 2013, doi: 10.1016/j.cld.2012.12.002.

[51] M. J. Harris, D. G. Le Gouteur, and I. M. Arias, “Progressive familial intrahepatic cholestasis: Genetic disorders of biliary transporters,” *J. Gastroenterol. Hepatol.*, vol. 20, no. 6, pp. 807–817, Jun. 2005, doi: 10.1111/j.1440-1746.2005.03743.x.

[52] J. G. Kenna *et al.*, “Can Bile Salt Export Pump Inhibition Testing in Drug Discovery and Development Reduce Liver Injury Risk? An International Transporter Consortium Perspective,” *Clin. Pharmacol. Ther.*, vol. 104, no. 5, pp. 916–932, Nov. 2018, doi: 10.1002/cpt.1222.

[53] H. Liu and J. Sahi, “Role of Hepatic Drug Transporters in Drug Development,” *J. Clin. Pharmacol.*, vol. 56, no. S7, pp. S11–S22, 2016, doi: 10.1002/jcph.703.

[54] S. Robinson *et al.*, “A European pharmaceutical company initiative challenging the regulatory requirement for acute toxicity studies in pharmaceutical drug development,” *Regul. Toxicol. Pharmacol.*, vol. 50, no. 3, pp. 345–352, Apr. 2008, doi: 10.1016/j.yrtph.2007.11.009.

[55] S. M. Barlow *et al.*, “Hazard identification by methods of animal-based toxicology,” *Food Chem. Toxicol.*, vol. 40, no. 2–3, pp. 145–191, Feb. 2002, doi: 10.1016/S0278-6915(01)00117-X.

[56] S. Garattini, “Toxic effects of chemicals: Difficulties in extrapolating data from animals to man,” *Crit. Rev. Toxicol.*, vol. 16, no. 1, pp. 1–29, 1985, doi: 10.3109/10408448509041323.

[57] G. R. Langley, G. Langley, M. A. Phd, and M. Cbiol, “WellBeing International WellBeing International WBI Studies Repository WBI Studies Repository Acute Toxicity Testing Without Animals: More Scientific and Less Acute Toxicity Testing Without Animals: More Scientific and Less of a Gamble of a Gamble Acute T,” 2005, Accessed: Aug. 05, 2021. [Online]. Available: https://www.wellbeingintlstudiesrepository.org/appamet.

[58] S. Morgan, P. Grootendorst, J. Lexchin, C. Cunningham, and D. Greyson, “The cost of drug development: A systematic review,” *Health Policy (New. York).*, vol. 100, no. 1, pp. 4–17, Apr. 2011, doi: 10.1016/j.healthpol.2010.12.002.

[59] H. Ishibashi, M. Nakamura, A. Komori, K. Migita, and S. Shimoda, “Liver architecture, cell function, and disease,” *Semin. Immunopathol.*, vol. 31, no. 3, pp. 399–409, 2009, doi: 10.1007/s00281-009-0155-6.

[60] P. Godoy *et al.*, “Recent advances in 2D and 3D in vitro systems using primary hepatocytes, alternative hepatocyte sources and non-parenchymal liver cells and their use in investigating mechanisms of hepatotoxicity, cell signaling and ADME,” *Archives of Toxicology*, vol. 87, no. 8. Springer, pp. 1315–1530, Aug. 23, 2013, doi: 10.1007/s00204-013-1078-5.

[61] B. Bulutoglu *et al.*, “A comparison of hepato-cellular in vitro platforms to study CYP3A4 induction,” *PLoS One*, vol. 15, no. 2, p. e0229106, 2020, doi: 10.1371/journal.pone.0229106.

[62] N. Dianat, C. Steichen, L. Vallier, A. Weber, and A. Dubart-Kupperschmitt, “Human Pluripotent Stem Cells for Modelling Human Liver Diseases and Cell Therapy,” *Curr. Gene Ther.*, vol. 13, no. 2, pp. 120–132, Mar. 2013, doi: 10.2174/1566523211313020006.

[63] J. A. Heslop *et al.*, “Donor-dependent and other nondefined factors have greater influence on the hepatic phenotype than the starting cell type in induced pluripotent stem cell derived hepatocyte-like cells,” *Stem Cells Transl. Med.*, vol. 6, no. 5, pp. 1321–1331, May 2017, doi: 10.1002/sctm.16-0029.

[64] S. Wilkening, F. Stahl, and A. Bader, “Comparison of primary human hepatocytes and hepatoma cell line HepG2 with regard to their biotransformation properties,” *Drug Metab. Dispos.*, vol. 31, no. 8, pp. 1035–1042, 2003, doi: 10.1124/dmd.31.8.1035.

[65] L. Guo *et al.*, “Similarities and differences in the expression of drug-metabolizing enzymes between human hepatic cell lines and primary human hepatocytes,” *Drug Metab. Dispos.*, vol. 39, no. 3, pp. 528–538, Mar. 2011, doi: 10.1124/dmd.110.035873.

[66] M. Ölander, J. R. Wiśniewski, I. Flörkemeier, N. Handin, J. Urdzik, and P. Artursson, “A simple approach for restoration of differentiation and function in cryopreserved human hepatocytes,” *Arch. Toxicol.*, vol. 93, no. 3, pp. 819–829, Dec. 2019, doi: 10.1007/s00204-018-2375-9.

[67] A. P. Li *et al.*, “Cryopreserved human hepatocytes: Characterization of drug-metabolizing activities and applications in higher throughput screening assays for hepatotoxicity, metabolic stability, and drug-drug interaction potential,” *Chem. Biol. Interact.*, vol. 121, no. 1, pp. 17–35, Jun. 1999, doi: 10.1016/S0009-2797(99)00088-5.

[68] M. J. Gómez-Lechón, J. V. Castell, and M. T. Donato, “Hepatocytes-the choice to investigate drug metabolism and toxicity in man: In vitro variability as a reflection of in vivo,” *Chem. Biol. Interact.*, vol. 168, no. 1, pp. 30–50, May 2007, doi: 10.1016/j.cbi.2006.10.013.

[69] M. Ruoß *et al.*, “Towards improved hepatocyte cultures: Progress and limitations,” *Food Chem. Toxicol.*, vol. 138, Apr. 2020, doi: 10.1016/j.fct.2020.111188.

[70] C. C. Bell *et al.*, “Comparison of hepatic 2D sandwich cultures and 3d spheroids for long-term toxicity applications: A multicenter study,” *Toxicol. Sci.*, vol. 162, no. 2, pp. 655–666, Apr. 2018, doi: 10.1093/toxsci/kfx289.

[71] J. Li, R. S. Settivari, M. J. Lebaron, and M. S. Marty, “Functional Comparison of HepaRG Cells and Primary Human Hepatocytes in Sandwich and Spheroid Culture as Repeated-Exposure Models for Hepatotoxicity,” *Appl. Vitr. Toxicol.*, vol. 5, no. 4, pp. 187–195, Dec. 2019, doi: 10.1089/aivt.2019.0008.

[72] E. L. LeCluyse *et al.*, “Isolation and culture of primary human hepatocytes.,” *Methods Mol. Biol.*, vol. 290, pp. 207–229, 2005, doi: 10.1385/1-59259-838-2:207.

[73] A. Baze *et al.*, “Three-Dimensional Spheroid Primary Human Hepatocytes in Monoculture and Coculture with Nonparenchymal Cells,” *Tissue Eng. - Part C Methods*, vol. 24, no. 9, pp. 534–545, Sep. 2018, doi: 10.1089/ten.tec.2018.0134.

[74] E. Fitzpatrick *et al.*, “Coculture with mesenchymal stem cells results in improved viability and function of human hepatocytes,” *Cell Transplant.*, vol. 24, no. 1, pp. 73–83, Jan. 2015, doi: 10.3727/096368913X674080.

[75] A. Burkard *et al.*, “Generation of proliferating human hepatocytes using upcyte® technology: Characterisation and applications in induction and cytotoxicity assays,” *Xenobiotica*, vol. 42, no. 10, pp. 939–956, Oct. 2012, doi: 10.3109/00498254.2012.675093.

[76] S. R. Khetani *et al.*, “Use of micropatterned cocultures to detect compounds that cause drug-induced liver injury in humans,” *Toxicol. Sci.*, vol. 132, no. 1, pp. 107–117, Mar. 2013, doi: 10.1093/toxsci/kfs326.

[77] W. R. Proctor *et al.*, “Utility of spherical human liver microtissues for prediction of clinical drug-induced liver injury,” *Arch. Toxicol.*, vol. 91, no. 8, pp. 2849–2863, Jun. 2017, doi: 10.1007/s00204-017-2002-1.

[78] J. J. Xu, P. V. Henstock, M. C. Dunn, A. R. Smith, J. R. Chabot, and D. de Graaf, “Cellular imaging predictions of clinical drug-induced liver injury,” *Toxicol. Sci.*, vol. 105, no. 1, pp. 97–105, 2008, doi: 10.1093/toxsci/kfn109.

[79] W. Albrecht *et al.*, “Prediction of human drug-induced liver injury (DILI) in relation to oral doses and blood concentrations,” *Arch. Toxicol.*, vol. 93, no. 6, pp. 1609–1637, 2019, doi: 10.1007/s00204-019-02492-9.

[80] T. Brecklinghaus *et al.*, “The hepatocyte export carrier inhibition assay improves the separation of hepatotoxic from non-hepatotoxic compounds,” *Chem. Biol. Interact.*, p. 109728, Oct. 2021, doi: 10.1016/j.cbi.2021.109728.

[81] P. Godoy *et al.*, “Recent advances in 2D and 3D in vitro systems using primary hepatocytes, alternative hepatocyte sources and non-parenchymal liver cells and their use in investigating mechanisms of hepatotoxicity, cell signaling and ADME,” *Arch. Toxicol.*, vol. 87, no. 8, pp. 1315–1530, Aug. 2013, doi: 10.1007/s00204-013-1078-5.

[82] Promega Cooperation, “CellTiter-Blue Assay Protocol, TB317,” *Tech. Bull.*, p. 16, 2016.

[83] S. Chatterjee, L. Richert, P. Augustijns, and P. Annaert, “Hepatocyte-based in vitro model for assessment of drug-induced cholestasis,” *Toxicol. Appl. Pharmacol.*, vol. 274, no. 1, pp. 124–136, Jan. 2014, doi: 10.1016/j.taap.2013.10.032.

[84] L. S. New and E. C. Y. Chan, “Evaluation of BEH C18, BEH HILIC, and HSS T3 (C18) column chemistries for the UPLC-MS-MS analysis of glutathione, glutathione disulfide, and ophthalmic acid in mouse liver and human plasma,” *J. Chromatogr. Sci.*, vol. 46, no. 3, pp. 209–214, 2008, doi: 10.1093/chromsci/46.3.209.

[85] B. MacLean *et al.*, “Skyline: An open source document editor for creating and analyzing targeted proteomics experiments,” *Bioinformatics*, vol. 26, no. 7, pp. 966–968, Feb. 2010, doi: 10.1093/bioinformatics/btq054.

[86] K. J. Livak and T. D. Schmittgen, “Analysis of relative gene expression data using real-time quantitative PCR and the 2-ΔΔCT method,” *Methods*, vol. 25, no. 4, pp. 402–408, Dec. 2001, doi: 10.1006/meth.2001.1262.

[87] S. Köppert *et al.*, “Cellular clearance and biological activity of calciprotein particles depend on their maturation state and crystallinity,” *Front. Immunol.*, vol. 9, no. SEP, p. 1991, Sep. 2018, doi: 10.3389/fimmu.2018.01991.

[88] R. Reif *et al.*, “In vivo imaging of systemic transport and elimination of xenobiotics and endogenous molecules in mice,” *Arch. Toxicol.*, vol. 91, no. 3, pp. 1335–1352, Mar. 2017, doi: 10.1007/s00204-016-1906-5.

[89] J. Verma, V. Khedkar, and E. Coutinho, “3D-QSAR in Drug Design - A Review,” *Curr. Top. Med. Chem.*, vol. 10, no. 1, pp. 95–115, Jan. 2010, doi: 10.2174/156802610790232260.

[90] M. Karelson, V. S. Lobanov, and A. R. Katritzky, “Quantum-chemical descriptors in QSAR/QSPR studies,” *Chem. Rev.*, vol. 96, no. 3, pp. 1027–1043, 1996, doi: 10.1021/cr950202r.

[91] F. Montanari *et al.*, "Vienna LiverTox Workspace—A Set of Machine Learning Models for Prediction of Interactions Profiles of Small Molecules With Transporters Relevant for Regulatory Agencies," *Front. Chem.*, vol. 7, p. 899, Jan. 2020, doi: 10.3389/fchem.2019.00899.

[92] A. Wilson and N. Norden, "The R Project for Statistical Computing The R Project for Statistical Computing," *URL: http://www. r-project. org/254*, 2015. https://www.r-project.org/ (accessed May 10, 2021).

[93] C. Ritz, F. Baty, J. C. Streibig, and D. Gerhard, "Dose-response analysis using R," *PLoS One*, vol. 10, no. 12, p. e0146021, Dec. 2015, doi: 10.1371/journal.pone.0146021.

[94] P. BRAIN and R. COUSENS, "An equation to describe dose responses where there is stimulation of growth at low doses," *Weed Res.*, vol. 29, no. 2, pp. 93–96, Apr. 1989, doi: 10.1111/j.1365-3180.1989.tb00845.x.

[95] H. Akaike, "Akaike's Information Criterion," in *International Encyclopedia of Statistical Science*, Springer Berlin Heidelberg, 2011, pp. 25–25.

[96] D. A. Elashoff, "Statistical analysis of gene expression data," 2006.

[97] F. Bretz, J. C. Pinheiro, and M. Branson, "Combining multiple comparisons and modeling techniques in dose-response studies," *Biometrics*, vol. 61, no. 3, pp. 738–748, 2005, doi: 10.1111/j.1541-0420.2005.00344.x.

[98] B. Bornkamp, "DoseFinding: Planning and Analyzing Dose Finding Experiments. R package version 0.9-17," 2019, doi: 10.1002/sim.6052.

[99] X. Robin *et al.*, "pROC: An open-source package for R and S+ to analyze and compare ROC curves," *BMC Bioinformatics*, vol. 12, no. 1, pp. 1–8, Mar. 2011, doi: 10.1186/1471-2105-12-77.

[100] L. Kuepfer *et al.*, "Applied Concepts in PBPK Modeling: How to Build a PBPK/PD Model," *CPT Pharmacometrics Syst. Pharmacol.*, vol. 5, no. 10, pp. 516–531, Oct. 2016, doi: 10.1002/psp4.12134.

[101] L. Qiu *et al.*, "High-Content Imaging in Human and Rat Hepatocytes Using the Fluorescent Dyes CLF and CMFDA Is Not Specific Enough to Assess BSEP/Bsep and/or MRP2/Mrp2 Inhibition by Cholestatic Drugs," *Appl. Vitr. Toxicol.*, vol. 1, no. 3, pp. 198–212, Sep. 2015, doi: 10.1089/aivt.2015.0014.

[102] R. Reif *et al.*, "In vivo imaging of systemic transport and elimination of xenobiotics and endogenous molecules in mice," *Arch. Toxicol.*, vol. 91, no. 3, pp. 1335–1352, Mar. 2017, doi: 10.1007/s00204-016-1906-5.

[103] A. Ghallab *et al.*, "Bile Microinfarcts in Cholestasis Are Initiated by Rupture of the Apical Hepatocyte Membrane and Cause Shunting of Bile to Sinusoidal Blood," *Hepatology*, vol. 69, no. 2, pp. 666–683, Feb. 2019, doi: 10.1002/hep.30213.

[104] P. Godoy *et al.*, "Gene network activity in cultivated primary hepatocytes is highly similar to diseased mammalian liver tissue," *Arch. Toxicol.*, vol. 90, no. 10, pp. 2513–2529, Oct. 2016, doi: 10.1007/s00204-016-1761-4.

[105] G. Campos *et al.*, "Inflammation-associated suppression of metabolic gene networks in acute and chronic liver disease," *Arch. Toxicol.*, vol. 94, no. 1, pp. 205–217, Jan. 2020, doi: 10.1007/s00204-019-02630-3.

[106] F. J. Romero and H. Sies, "Subcellular glutathione contents in isolated hepatocytes treated with L-buthionine sulfoximine," *Biochem. Biophys. Res. Commun.*, vol. 123, no. 3, pp. 1116–

1121, Sep. 1984, doi: 10.1016/S0006-291X(84)80248-X.

[107] R. Li, P. Zhang, C. Li, W. Yang, Y. Yin, and K. Tao, "Tert-butylhydroquinone mitigates carbon tetrachloride induced hepatic injury in mice," *Int. J. Med. Sci.*, vol. 17, no. 14, pp. 2095–2103, 2020, doi: 10.7150/ijms.45842.

[108] M. Benedict and X. Zhang, "Non-alcoholic fatty liver disease: An expanded review," *World J. Hepatol.*, vol. 9, no. 16, pp. 715–732, Jun. 2017, doi: 10.4254/wjh.v9.i16.715.

[109] L. Rabinowich and O. Shibolet, "Drug induced steatohepatitis: An uncommon culprit of a common disease," *Biomed Res. Int.*, vol. 2015, 2015, doi: 10.1155/2015/168905.

[110] F. A. Müller and S. J. Sturla, "Human in vitro models of nonalcoholic fatty liver disease," *Curr. Opin. Toxicol.*, vol. 16, pp. 9–16, Aug. 2019, doi: 10.1016/j.cotox.2019.03.001.

[111] M. J. Gómez-Lechón, M. T. Donato, A. Martínez-Romero, N. Jiménez, J. V. Castell, and J. E. O'Connor, "A human hepatocellular in vitro model to investigate steatosis," *Chem. Biol. Interact.*, vol. 165, no. 2, pp. 106–116, Jan. 2007, doi: 10.1016/j.cbi.2006.11.004.

[112] M. T. Donato, L. Tolosa, N. Jiménez, J. V. Castell, and M. J. Gómez-Lechón, "High-content imaging technology for the evaluation of drug-induced steatosis using a multiparametric cell-based assay," *J. Biomol. Screen.*, vol. 17, no. 3, pp. 394–400, Mar. 2012, doi: 10.1177/1087057111427586.

[113] P. L. M. Jansen *et al.*, "The ascending pathophysiology of cholestatic liver disease," *Hepatology*, vol. 65, no. 2. John Wiley and Sons Inc., pp. 722–738, Feb. 01, 2017, doi: 10.1002/hep.28965.

[114] N. Vartak *et al.*, "Intravital Dynamic and Correlative Imaging of Mouse Livers Reveals Diffusion-Dominated Canalicular and Flow-Augmented Ductular Bile Flux," *Hepatology*, vol. 73, no. 4, pp. 1531–1550, Apr. 2021, doi: 10.1002/hep.31422.

[115] J. P. Jackson, K. M. Freeman, R. L. St Claire, C. B. Black, and K. R. Brouwer, "Cholestatic Drug Induced Liver Injury: A Function of Bile Salt Export Pump Inhibition and Farnesoid X Receptor Antagonism," *Appl. Vitr. Toxicol.*, vol. 4, no. 3, pp. 265–279, Sep. 2018, doi: 10.1089/aivt.2018.0011.

[116] A. M. Montet, L. Oliva, F. Beaugé, and J. C. Montet, "Bile salts modulate chronic ethanol-induced hepatotoxicity," *Alcohol Alcohol.*, vol. 37, no. 1, pp. 25–29, Jan. 2002, doi: 10.1093/alcalc/37.1.25.

[117] M. G. Neuman, N. H. Shear, S. Bellentani, and C. Tiribelli, "Role of cytokines in ethanol-induced cytotoxicity in vitro in Hep G2 cells," *Gastroenterology*, vol. 115, no. 1, pp. 157–166, 1998, doi: 10.1016/S0016-5085(98)70377-4.

[118] B. Bhushan *et al.*, "Bile acid depletion increases susceptibility to acetaminophen-induced hepatotoxicity in mice," *FASEB J.*, vol. 27, no. S1, pp. 387.1-387.1, Apr. 2013, doi: 10.1096/fasebj.27.1_supplement.387.1.

[119] F. Y. Lee, H. Lee, M. L. Hubbert, P. A. Edwards, and Y. Zhang, "FXR, a multipurpose nuclear receptor," *Trends Biochem. Sci.*, vol. 31, no. 10, pp. 572–580, Oct. 2006, doi: 10.1016/j.tibs.2006.08.002.

[120] B. Bhushan *et al.*, "Role of bile acids in liver injury and regeneration following acetaminophen overdose," *Am. J. Pathol.*, vol. 183, no. 5, pp. 1518–1526, Nov. 2013, doi: 10.1016/j.ajpath.2013.07.012.

[121] B. Wang *et al.*, "Farnesoid X receptor (FXR) activation induces the antioxidant protein

metallothionein 1 expression in mouse liver," *Exp. Cell Res.*, vol. 390, no. 1, May 2020, doi: 10.1016/j.yexcr.2020.111949.

[122] J. Vaquero, O. Briz, E. Herraez, J. Muntané, and J. J. G. Marin, "Activation of the nuclear receptor FXR enhances hepatocyte chemoprotection and liver tumor chemoresistance against genotoxic compounds," *Biochim. Biophys. Acta - Mol. Cell Res.*, vol. 1833, no. 10, pp. 2212–2219, Oct. 2013, doi: 10.1016/j.bbamcr.2013.05.006.

[123] S. Fischer, U. Beuers, U. Spengler, F. M. Zwiebel, and H. G. Koebe, "Hepatic levels of bile acids in end-stage chronic cholestatic liver disease," *Clin. Chim. Acta*, vol. 251, no. 2, pp. 173–186, Jul. 1996, doi: 10.1016/0009-8981(96)06305-X.

[124] S. Y. Cai *et al.*, "Bile acids initiate cholestatic liver injury by triggering a hepatocyte-specific inflammatory response," *J. Clin. Invest.*, vol. 2, no. 5, Mar. 2017, doi: 10.1172/jci.insight.90780.

[125] R. E. Morgan *et al.*, "A multifactorial approach to hepatobiliary transporter assessment enables improved therapeutic compound development," *Toxicol. Sci.*, vol. 136, no. 1, pp. 216–241, Nov. 2013, doi: 10.1093/toxsci/kft176.

[126] P. Caetano-Pinto, M. J. Janssen, L. Gijzen, L. Verscheijden, M. J. G. Wilmer, and R. Masereeuw, "Fluorescence-Based Transport Assays Revisited in a Human Renal Proximal Tubule Cell Line," *Mol. Pharm.*, vol. 13, no. 3, pp. 933–944, Mar. 2016, doi: 10.1021/acs.molpharmaceut.5b00821.

[127] J. Bicker, A. Fortuna, G. Alves, P. Soares-Da-Silva, and A. Falcão, "Elucidation of the impact of P-glycoprotein and breast cancer resistance protein on the brain distribution of catechol-O-methyltransferase inhibitors," *Drug Metab. Dispos.*, vol. 45, no. 12, pp. 1282–1291, Dec. 2017, doi: 10.1124/dmd.117.077883.

[128] A. Sachinidis *et al.*, "Road Map for Development of Stem Cell-Based Alternative Test Methods," *Trends in Molecular Medicine*, vol. 25, no. 6. Elsevier Ltd, pp. 470–481, Jun. 01, 2019, doi: 10.1016/j.molmed.2019.04.003.

[129] M. Ricchi *et al.*, "Differential effect of oleic and palmitic acid on lipid accumulation and apoptosis in cultured hepatocytes," *J. Gastroenterol. Hepatol.*, vol. 24, no. 5, pp. 830–840, May 2009, doi: 10.1111/j.1440-1746.2008.05733.x.

[130] W. Cui, S. L. Chen, and K. Q. Hu, "Quantification and mechanisms of oleic acid-induced steatosis in HepG2 cells," *Am. J. Transl. Res.*, vol. 2, no. 1, pp. 95–104, 2010, Accessed: Sep. 08, 2021. [Online]. Available: /pmc/articles/PMC2826826/.

[131] A. A. Spector, "Fatty acid binding to plasma albumin," *J. Lipid Res.*, vol. 16, no. 3, pp. 165–179, May 1975, doi: 10.1016/s0022-2275(20)36723-7.

[132] J. Anguizola, S. Basiaga, and D. Hage, "Effects of Fatty Acids and Glycation on Drug Interactions with Human Serum Albumin," *Curr. Metabolomics*, vol. 1, no. 3, pp. 241–252, Sep. 2013, doi: 10.2174/2213235x1130100005.

[133] K. Yamasaki *et al.*, "Long chain fatty acids alter the interactive binding of ligands to the two principal drug binding sites of human serum albumin," *PLoS One*, vol. 12, no. 6, p. e0180404, Jun. 2017, doi: 10.1371/journal.pone.0180404.

[134] S. Caddeo, M. Boffito, and S. Sartori, "Tissue engineering approaches in the design of healthy and pathological in vitro tissue models," *Front. Bioeng. Biotechnol.*, vol. 5, no. AUG, Jul. 2017, doi: 10.3389/fbioe.2017.00040.

[135] M. Le Vee, E. Jigorel, D. Glaise, P. Gripon, C. Guguen-Guillouzo, and O. Fardel, "Functional expression of sinusoidal and canalicular hepatic drug transporters in the differentiated human hepatoma HepaRG cell line," *Eur. J. Pharm. Sci.*, vol. 28, no. 1–2, pp. 109–117, May 2006, doi: 10.1016/j.ejps.2006.01.004.

[136] C. C. Bell *et al.*, "Characterization of primary human hepatocyte spheroids as a model system for drug-induced liver injury, liver function and disease," *Sci. Rep.*, vol. 6, no. 1, pp. 1–13, May 2016, doi: 10.1038/srep25187.

[137] G. Wang *et al.*, "Co-culture system of hepatocytes and endothelial cells: two in vitro approaches for enhancing liver-specific functions of hepatocytes," *Cytotechnology*, vol. 70, no. 4, pp. 1279–1290, Aug. 2018, doi: 10.1007/s10616-018-0219-3.

[138] S. S. Bale, S. Geerts, R. Jindal, and M. L. Yarmush, "Isolation and co-culture of rat parenchymal and non-parenchymal liver cells to evaluate cellular interactions and response," *Sci. Rep.*, vol. 6, May 2016, doi: 10.1038/srep25329.

[139] D. Compare *et al.*, "Gut-liver axis: The impact of gut microbiota on non alcoholic fatty liver disease," *Nutr. Metab. Cardiovasc. Dis.*, vol. 22, no. 6, pp. 471–476, Jun. 2012, doi: 10.1016/j.numecd.2012.02.007.

[140] H. Tilg, P. D. Cani, and E. A. Mayer, "Gut microbiome and liver diseases," *Gut*, vol. 65, no. 12, pp. 2035–2044, Dec. 2016, doi: 10.1136/gutjnl-2016-312729.

[141] M. B. Esch, G. J. Mahler, T. Stokol, and M. L. Shuler, "Body-on-a-chip simulation with gastrointestinal tract and liver tissues suggests that ingested nanoparticles have the potential to cause liver injury," *Lab Chip*, vol. 14, no. 16, pp. 3081–3092, Jul. 2014, doi: 10.1039/c4lc00371c.

[142] J. H. Sung *et al.*, "Recent Advances in Body-on-a-Chip Systems," *Anal. Chem.*, vol. 91, no. 1, pp. 330–351, Jan. 2019, doi: 10.1021/acs.analchem.8b05293.

[143] A. Skardal, T. Shupe, and A. Atala, "Organoid-on-a-chip and body-on-a-chip systems for drug screening and disease modeling," *Drug Discov. Today*, vol. 21, no. 9, pp. 1399–1411, Sep. 2016, doi: 10.1016/j.drudis.2016.07.003.

[144] B. Bornkamp, J. Pinheiro, and F. Bretz, "MCPMod: An R package for the design and analysis of Dose-Finding studies," *J. Stat. Softw.*, vol. 29, no. 7, pp. 1–23, Feb. 2009, doi: 10.18637/jss.v029.i07.

6 Appendix

Table 24: Normalized fluorescence values of 2',7'-Dichlorofluorescein and the corresponding test compounds. Fluorescence was normalized plate-wise to a control of PBS with 0.5% DMSO. The corresponding control for the additional tested DMSO was PBS (Phosphate buffered saline). The used concentrations correspond to the lowest, median, and highest concentrations used in the CMFDA assay.

Compound	Abbreviation	Normalized fluorescence		
		C1	C3	C5
Acetaminophen	APAP	1.01	1.03	1.02
Atorvastatin	AVS	1.02	1.03	1.04
Atropine	ATRO	0.99	1.02	1.01
Benzbromarone	BZB	1.00	0.99	1.00
Benztropine	BZT	1.06	1.08	1.06
Bosentan	BOS	1.04	1.04	1.04
Chlorpheniramine	CHL	0.98	0.97	0.98
Codeine	COD	1.03	1.03	1.03
Cyclosporin A	CSA	1.02	1.03	1.05
Diphenhydramine	DPH	0.98	1.05	1.04
Entacapone	ETC	0.96	0.97	0.96
Hydroxyzine	HYZ	1.03	1.05	1.01
Indomethacin	INDO	1.02	1.01	1.03
Isosorbide dinitrate	ISS	1.02	1.02	1.03
Ketoconazole	KC	1.04	1.02	1.03
Lovastatin	LO	1.04	1.04	1.04
Melatonin	MEL	1.00	1.00	1.01
N-acetylcysteine	NAC	0.95	0.98	0.96
Nifedipine	NDP	1.02	1.02	1.01
Oxycodone	OXC	1.05	1.04	1.02
Oxymorphone	OCM	1.00	1.01	1.04
Pazopanib	PZB	1.02	1.02	1.03
Pindolol	PIN	1.03	1.04	1.03
Pioglitazone	PIO	1.01	1.00	1.00
Pyridoxine	PDX	0.96	0.99	0.98
Rifampicin	RIF	0.92	0.92	0.92
Rosiglitazone	RGZ	1.03	1.02	1.01
Rosuvastatin	ROS	1.07	1.05	1.05
Simvastatin	SIM	1.06	1.08	1.10
Sitaxentan	SXS	1.05	1.04	1.04
4-Phenylbutyrate	SPB	1.03	1.01	1.01
Theophylline	THE	1.03	1.04	1.04
Tolcapone	TOLC	0.97	0.98	0.98
Triprolidine	TPL	1.03	1.03	1.03
Troglitazone	TROG	1.03	1.03	1.04
Zaleplon	ZAL	1.00	1.00	1.01

Dimethyl sulfoxide (DMSO)						
Concentration (v/v)	0.1%	0.2%	0.3%	0.4%	0.5%	1%
Normalized fluorescence	1.01	0.98	1.01	1.00	0.96	1.02

Table 25: Dose-response models implemented in the MCP-Mod package (from [144]).

Name	$f(d, \boldsymbol{\theta})$	$f^0(d, \boldsymbol{\theta}^*)$	(*)	(♯)
`linear`	$E_0 + \delta d$	d		
`linlog`	$E_0 + \delta \log(d + c)$	$\log(d + c)$		c
`quadratic`	$E_0 + \beta_1 d + \beta_2 d^2$	$d + \delta d^2$ if $\beta_2 < 0$	δ	
`emax`	$E_0 + E_{\max} d/(ED_{50} + d)$	$d/(ED_{50} + d)$	ED_{50}	
`logistic`	$E_0 + E_{\max}/\left\{1 + \exp\left[(ED_{50} - d)/\delta\right]\right\}$	$1/\left\{1 + \exp\left[(ED_{50} - d)/\delta\right]\right\}$	$(ED_{50}, \delta)^\top$	
`exponential`	$E_0 + E_1(\exp(d/\delta) - 1)$	$\exp(d/\delta) - 1$	δ	
`sigEmax`	$E_0 + E_{\max} d^h/(ED_{50}^h + d^h)$	$d^h/(ED_{50}^h + d^h)$	$(ED_{50}, h)^\top$	
`betaMod`	$E_0 + E_{\max} B(\delta_1, \delta_2)(d/D)^{\delta_1}(1 - d/D)^{\delta_2}$	$B(\delta_1, \delta_2)(d/D)^{\delta_1}(1 - d/D)^{\delta_2}$	$(\delta_1, \delta_2)^\top$	D

7 Electronic supplement

Supplement 1: General compound information (trivial name, CAS, MW, supplier and product number), hepatotoxicity information, donor data, and transporter data for all test compounds.

Supplement 2: In vivo data (exposure scenarios, input parameters, and modeled concentrations)

Supplement 3: Fitted concentration-response curves for all assays

Supplement 4: Raw and processed data of the BAM assay

Supplement 5: Raw and processed data of the CMFDA assay

Supplement 6: Raw and processed data of the AdipoRed assay

8 List of figures

9 List of tables

10 Publications

The hepatocyte export carrier inhibition assay improves the separation of hepatotoxic from non-hepatotoxic compounds. **Brecklinghaus T.** , Albrecht W. , Kappenberg F. , Duda J. , Vartak N. , Edlund K. , Marchan R. , Ghallab A. , Cadenas C. , Günther G. , Leist M. , Zhang M. , Gardner I. , Reinders J. , Russel F.GM. , Foster A.J. , Williams D.P. , Damle-Vartak A. , Grandits M. , Ecker G. , Kittana N. , Rahnenführer J. , Hengstler J.G. , (2021). Chem.Bio.Int., 351.

Prediction of human drug-induced liver injury (DILI) in relation to oral doses and blood concentrations. Albrecht W. , Kappenberg F. , **Brecklinghaus T.** , Stoeber R. , Marchan R. , Zhang M. , Ebbert K. , Kirschner H. , Grinberg M. , Leist M. , Moritz W. , Cadenas C. , Ghallab A. , Reinders J. , Vartak N. , van Thriel C. , Golka K. , Tolosa L. , Castell J. V. , Damm G. , Seehofer D. , Lampen A. , Braeuning A. , Buhrke T. , Behr A.C. , Oberemm A. , Gu X. , Kittana N. , van de Water B. , Kreiling R. , Fayyaz S. , van Aerts L. , Smedsrød B. , Ellinger-Ziegelbauer H. , Steger-Hartmann T. , Gundert-Remy U. , Zeigerer A. , Ullrich A. , Runge D. , Lee S.M.L. , Schiergens T.S. , Kuepfer L. , Aguayo-Orozco A. , Sachinidis A. , Edlund K. , Gardner I. , Rahnenführer J. , Hengstler J.G. , (2019). *Arch. Toxicol.*, 93, 1609–1637.

Relevance of the incubation period in cytotoxicity testing with primary human hepatocytes. Gu X. , Albrecht W. , Edlund K. , Kappenberg F. , Rahnenführer J. , Leist M. , Moritz W. , Godoy P. , Cadenas C. , Marchan R. , **Brecklinghaus T.** , Pardo L.T. , Castell J. V. , Gardner I. , Han B. , Hengstler J.G. , Stoeber R. , (2018). *Arch. Toxicol.*, 92, 3505–3515.

Comparing in vitro human liver models to in vivo human liver using RNA-Seq. Gupta R. , Schrooders Y. , Hauser D. , van Herwijnen M. , Albrecht W. , ter Braak B. , **Brecklinghaus T.** , Castell J. V. , Elenschneider L. , Escher S. , Guye P. , Hengstler J.G. , Ghallab A. , Hansen T. , Leist M. , Maclennan R. , Moritz W. , Tolosa L. , Tricot T. , Verfaillie C. , Walker P. , van de Water B. , Kleinjans J. , Caiment F. , (2021). *Arch. Toxicol.*, 95, 573–589.

Handling deviating control values in concentration-response curves. Kappenberg F. , **Brecklinghaus T.** , Albrecht W. , Blum J. , van der Wurp C. , Leist M. , Hengstler J.G. , Rahnenführer J. , (2020). *Arch. Toxicol.*, 94, 3787–3798.

Histone deacetylase 5 regulates interleukin 6 secretion and insulin action in skeletal muscle. Klymenko O. , **Brecklinghaus T.** , Dille M. , Springer C. , de Wendt C. , Altenhofen D. , Binsch C. , Knebel B. , Scheller J. , Hardt C. , Herwig R. , Chadt A. , Pfluger P.T. , Al-Hasani H. , Kabra D.G. , (2020). *Mol. Metab.*, 42.

The EU-ToxRisk method documentation, data processing and chemical testing pipeline for the regulatory use of new approach methods. Krebs A. , van Vugt-Lussenburg B.M.A. , Waldmann T. , Albrecht W. , Boei J. , ter Braak B. , Brajnik M. , Braunbeck T. , **Brecklinghaus T.** , Busquet F. , Dinnyes A. , Dokler J. , Dolde X. , Exner T.E. , Fisher C. , Fluri D. , Forsby A. , Hengstler J.G. , Holzer A.K. , Janstova Z. , Jennings P. , Kisitu J. , Kobolak J. , Kumar M. , Limonciel A. , Lundqvist J. , Mihalik B. , Moritz W. , Pallocca G. , Ulloa A.P.C. , Pastor M. , Rovida C. , Sarkans U. , Schimming J.P. , Schmidt B.Z. , Stöber R. , Strassfeld T. , van de Water B. , Wilmes A. , van der Burg B. , Verfaillie C.M. , von Hellfeld R. , Vrieling H. , Vrijenhoek N.G. , Leist M. , (2020). *Arch. Toxicol.*, 94, 2435–2461.

Stimulation of de novo glutathione synthesis by nitrofurantoin for enhanced resilience of hepatocytes. Wijaya L.S. , Rau C. , Braun T.S. , Marangoz S. , Spegg V. , Vlasveld M. , Albrecht W. , **Brecklinghaus T.** , Kamp H. , Beltman J.B. , Hengstler J.G. , van de Water B. , Leist M. , Schildknecht S. , (2021). *Cell Biol. Toxicol.*

11 Acknowledgement

First of all, I would like to thank Prof. Dr. Jan G. Hengstler for the opportunity to work at the IfADo and for the outstanding supervision during the last years. In addition to an interesting project, I was offered an excellent research environment, both materially and intellectually for my work. You always motivated me, gave constructive criticism and despite numerous other projects you always had time for a meeting.

I would also like to thank all colleagues from the department of toxicology for the friendly working environment and the willingness to help with any issues. A special thank goes to my project partner Dr. Wiebke Albrecht. Thank you for the open acceptance into the team, your constant support in and outside of the lab and many humorous moments. Furthermore, I would like to thank my office colleague Dr. Florian Seidel, who not only gave me many helpful tips, but was always available for discussions, both scientifically and more generally. I appreciate your honest, open and humorous manner, which has facilitated the office partnership.

Without the valuable support of our cooperation partners, the project would not have been possible. My thanks go to Dr. Franziska Kappenberg, Julia Duda and Prof. Dr. Jörg Rahnenführer from the statistics department of the TU Dortmund University. Thank you very much for the excellent cooperation and constant support. Likewise, I would like to thank Dr. Iain Gardner (Certara) for continuously creating, reviewing, and improving the PBPK models.

Last but not least, I would like to thank my family, my girlfriend Irina and my friends who have supported and accompanied me over the past years.